UNIVERSITY OF NIŠ

ISSN 0354-804X (Print)
ISSN 2406-0534 (Online)
COBISS.SR-ID 72210956
UDC 502/504

FACTA UNIVERSITATIS

Series
WORKING AND LIVING ENVIRONMENTAL PROTECTION

Vol. 21, Nº 1, 2024

Scientific Journal **FACTA UNIVERSITATIS**
UNIVERSITY OF NIŠ
Univerzitetski trg 2, 18000 Niš, Republic of Serbia
Phone: +381 18 257 095 Telefax: +381 18 257 950
e-mail: facta@ni.ac.rs http://casopisi.junis.ni.ac.rs/

Scientific Journal FACTA UNIVERSITATIS publishes original high scientific level works in the fields classified accordingly into the following periodical and independent series:

Architecture and Civil Engineering
Automatic Control and Robotics
Economics and Organization
Electronics and Energetics
Law and Politics
Linguistics and Literature
Mathematics and Informatics
Mechanical Engineering
Medicine and Biology
Philosophy, Sociology, Psychology and History
Physical Education and Sport
Physics, Chemistry and Technology
Teaching, Learning and Teacher Education
Visual Arts and Music
Working and Living Environmental Protection

SERIES **WORKING AND LIVING ENVIRONMENTAL PROTECTION**

Publication frequency – one volume, three issues per year.
Published by the University of Niš, Republic of Serbia

Printed by ATLANTIS DOO, Niš, Republic of Serbia
Circulation 50

ISSN 0354 – 804X (Print)
ISSN 2406 – 0534 (Online)
COBISS.SR-ID 72210956
UDC 502/504

FACTA UNIVERSITATIS

SERIES **WORKING AND LIVING ENVIRONMENTAL PROTECTION**
Vol. 21, Nº 1, 2024

UNIVERSITY OF NIŠ

INSTRUCTIONS FOR CONTRIBUTORS

Contributions should be (preferably) in English, French or German.

Under the paper title, the name(s) of the author(s) should be given while the full name, official title, institute or company affiliation and the like should be placed at the end of the paper together with the exact mail and e-mail address, as well as short (running) title of paper.

Manuscript format. A brief abstract of approximately 100 to 150 words in the same language and a list of up to six key words should precede the text body of the manuscript. All the authors apart from foreign ones should also submit a complete manuscript in Serbian. Manuscript should be prepared using a Word template, downloaded from web address:
http://casopisi.junis.ni.ac.rs/index.php/FUWorkLivEnvProt/about/submissions#authorGuidelines

Manuscript length. Brief articles and discussions (10 pages or less) are encouraged. Otherwise, papers should present well-focused arguments of approximately 16 pages.

Style requirements. **Letters, figures and symbols** should be clearly denoted.

Equations should be typewritten and, with the number, placed in parentheses at the right margin. References to equations should be in the form "Eq. (2)" or simply (2). For equations that cannot be entered in a single line, use the Equation Editor in MS Word. In equations and in the text, *italicize* symbols that are used to represent variables or parameters, including subscripts and superscripts. Only use characters and symbols that are available in the Equation Editor, in the *Symbol font* or in *Times New Roman*.

All illustrations (figures, photographs, line drawings, graphs) should be numbered in series and all legends should be included at the bottom of each illustration. All figures, photographs, line drawings and graphs, should be prepared in electronic form and converted in TIFF or JPG (max quality) file types, in 300 dpi resolution, for superior reproduction. Figures, line drawings and graphs prepared using elements of MS Drawing or MS Graph must be converted in form of pictures and unchangeable. All illustrations should be planned in advance so as to allow reduction to 12.75 cm in column width. Please review all illustrations to ensure that they are readable.

All **tables** should be numbered with consecutive Arabic numbers. They should have descriptive captions at the top of each table and should be mentioned in the text.

References should be listed alphabetically at the end of the manuscript, in the same way as the following examples (for a paper in a journal, a book, paper in a contributed volume and for an unpublished paper):

1. Connor, J. J., Logcher, R. D. and Shing-Ching, C.: *Nonlinear Analysis of Elastic Framed Structures*, J. Struct. Div., ASCE Vol. **ST** 6, pp. 1525-1547, 1968.
2. Arriaga F. and others: *Grading and load carrying capacity determination of old timber beams*, American Society for Agricultural Engineers, paper No 92-4068, 1992.
3. J. N. Reddy: *A refined nonlinear theory of plates with transverse shear deformation*, J. Solids and Struct., Vol bf 20, pp. 881-896, 1984, Comput. Struct., Vol. **5**, pp. 257-260, 1975.

References should be quoted in the text by the corresponding number in square brackets.

Electronic submission. Papers for consideration should be submitted to the Series Editor in electronic form via the Journal's home page: http://casopisi.junis.ni.ac.rs/index.php/FUWorkLivEnvProt.

FACTA UNIVERSITATIS

Series

Working and Living Environmental Protection

Vol. 21, Nº 1, 2024

Contents

FACTA UNIVERSITATIS
Series: **Working and Living Environmental Protection** Vol. 21, Nº 1, 2024, pp. 1 - 17
https://doi.org/10.22190/FUWLEP240314001M

Original Scientific Paper

SOUND ABSORPTION COEFFICIENT MEASUREMENT METHODS IN REVERBERATION ROOM AND IMPEDANCE TUBE

UDC 535.341.534.843.2

Darko Mihajlov[1], Momir Praščević[1], Petar Jovanović[1], Roumen Iankov[2], Nodira Abed[3]

[1]University of Nis, Faculty of Occupational Safety of Nis, Niš, Republic of Serbia
[2]Institute of Mechanics, Bulgarian Academy of Sciences, Sofia, Republic of Bulgaria
[3]State Unitary Enterprise "Fan va tarakkiyot", Tashkent State Technical University, Tashkent, Uzbekistan

ORCID iDs:	Darko Mihajlov	https://orcid.org/0000-0003-4528-170X
	Momir Praščević	https://orcid.org/0000-0002-7017-1038
	Petar Jovanović	https://orcid.org/0009-0007-1706-4456
	Roumen Iankov	https://orcid.org/0000-0003-1621-9325
	Nodira Abed	https://orcid.org/0000-0002-5020-0903

Abstract. *Sound absorption materials are very often used for space design in order to reduce the noise level and adjust the acoustic characteristics of the space depending on its purpose. Therefore, knowledge of the acoustic quantities that characterize sound absorption materials is of crucial importance. The most commonly used acoustic quantity is the sound absorption coefficient, which can be determined using standardized methods and methods used only for research purposes. This paper will provide an overview of the most commonly used standardized methods for determining the sound absorption coefficient: the reverberation room method and the impedance tube method. Since the impedance tube method, which provides the normal incidence sound absorption coefficient, is more suitable when developing new absorption materials, and in practical applications, it is desirable to know the random incidence sound absorption coefficient, this paper discusses approaches for predicting the random incidence sound absorption coefficient based on the acoustic parameters of the sound absorption materials measured in an impedance tube.*

Key words: *normal incidence sound absorption coefficient, random incidence sound absorption coefficient, reverberation room method, incidence tube method*.

Received March 14, 2024 / Accepted April 9, 2024
Corresponding author: Momir Praščević
University of Niš, Faculty of Occupational Safety, Čarnojevića 10a, 18000 Niš, Serbia
E-mail: momir.prascevic@znrfak.ni.ac.rs

1. INTRODUCTION

There are many unwanted noise sources in our working and living environment that create an undesirable environment and have harmful effects on human health. Noise sources in both the working and the living environment are very diverse in terms of their physical forms, mechanisms, and characteristics of noise generation, so emitted noise in the time and frequency domain can be steady, fluctuating, intermittent, impulse, wideband, narrowband, tonal noise, etc.

Noise sources, acoustically defined by their sound power (or the sound pressure emission) and the radiation directivity, emit sound into the environment in which they are located. The sound heard is a combination of direct sound emitted by the sources and indirect reflections from adjacent surfaces and objects. Acoustic noise pollution resulting from the operation of these noise sources can be reduced by lowering the radiation of the noise source itself, by reflecting the sound in different directions, by dispersing it or by absorbing the sound energy. Sometimes it is impossible to reduce the radiation of the noise source itself, so in many cases, sound absorption materials are used to mitigate the acoustic pollution. Sound absorption materials are widely employed to solve noise problems: inside machine enclosures, on the side of barriers facing the road, inside ventilation ducts and pipelines, for acoustic treatment of rooms, within hearing protection cups, etc. Considering that the emitted noise can have different characters in the time and frequency domain, there are no universal sound absorption materials that would be used for all types of emitted noise. That is why knowledge of their acoustic characteristics is important for the application of sound absorption materials.

Sound striking a surface of sound absorption materials can be transmitted, absorbed or reflected. The amount of transmitted, absorbed and reflected energy depends on the acoustic properties of the sound absorption materials. The effect of the sound absorption material on the propagation of a sound wave can be characterized by four interrelated acoustic quantities: surface impedance, surface admittance, sound reflection coefficient and sound absorption coefficient [1]. Knowledge of these four acoustic quantities is fundamental to calculating noise reduction when applying sound absorption materials. In addition, the well-known Delaney and Beazley empirical model [1, 2] requires knowledge of the flow resistance and porosity of the acoustical material.

Over the years, sound absorption materials have constantly evolved and improved. New materials have become safer, lighter and technologically optimized. Furthermore, ecological concepts, sustainable development and the use of recycled and green building materials will soon play an important role in the application of sound absorption materials. These new directions encourage the development of new materials and/or the improvement of existing ones. Also, the main goal of the project [3] is to develop an advanced environmentally friendly technology for producing new biodegradable composite materials with improved sound insulating and sound absorbing properties. An increase in the insulating and absorbing ability of composites in the audio range will be achieved by using viscoelastic polymer components modified with nanosized carbon and silicate particles as the matrix phase [3].

Although there are well-known theoretical models for characterizing sound absorption materials used during the development of new materials [1], many methods have been developed over the years to measure acoustic quantities that characterize the sound absorption materials. Some of these methods are standardized (impedance tube and reverberation room method) and some are only used for research purposes. A review of methods for measuring the sound absorption coefficient of sound absorption materials in a reverberation room and impedance tube will be presented in this paper. Also, the approaches used for establishing the relationship between the random incidence sound absorption coefficient and normal incidence sound absorption coefficient will be presented.

2. Reverberation Room Method

The reverberation room method is used for determining the random incidence sound absorption coefficient, a parameter that is most often used in space design to specify the absorption performance of materials. The reverberant room method is standardized in ISO 354 [4] and ASTM C423 [5]. There are differences between these standards in terms of required sample size and room volumes, differences in sample mounting, and calculation methods [6].

The principle applied in the mentioned standards is based on the determination of the equivalent sound absorption of reverberation room with and without a mounted test sample. ASTM C423 uses only the interrupted noise method for the sound pressure decay rate measurement, while ISO 354 on the other hand uses the interrupted noise method and integrated impulse response method for the reverberation time measurement.

To apply the reverberation room method, it is necessary to have a diffuse sound field in the room, where the sound level has minimal changes throughout the room. For this purpose, diffusers are often used and the shape of the reverberation room shall be such that the following condition is fulfilled [4]:

$$l_{max} < 1.9V^{1/3}, \tag{1}$$

where

l_{max} is the length of the longest straight line which fits within the boundary of the room, in [m];

V is the volume of the room, in [m^3].

Very often it can be expected that the sound field in the room is not completely diffused, so it is recommended to use multiple source and receiver positions and to average the results to reduce the effect of non-diffuseness.

Based on the measured sound pressure decay rate and reverberation time, the equivalent sound absorption area (in square meters) of the reverberation room for the empty reverberation room ($A_{ASTM,0}$, $A_{ISO,0}$) and reverberation room with a sample ($A_{ASTM,1}$, $A_{ISO,1}$) is determined using the following equations [7]:

$$A_{ASTM} = 0.921\frac{Vd}{c}, \tag{2}$$

$$A_{ISO} = \frac{55.3V}{cT_R} - 4Vm, \tag{3}$$

where

c is the speed of sound, in [m/s];

d is the sound pressure decay rate, in [dB/s];

T_R is the reverberation time, in [s];

m is the power attenuation coefficient calculated according to ISO 9613-1 [8], in [m^{-1}].

The random incidence (or diffuse field) sound absorption coefficient of the sample can be calculated as:

$$\alpha_r = \frac{A_1 - A_0}{S} + \frac{A_1}{S_0}, \tag{4}$$

where

S is the area of the sample, in [m^2];

S_0 is the area of the reverberation room boundary surfaces, in [m^2].

In ISO 354 and in reference [2], the second term in equation (4) is omitted, because the term [$S_0 - S$] is approximated to S_0, which simplifies the end formulation for the absorption coefficient of the sample [4].

In addition to the fact that the reverberation room method gives the random incidence sound absorption coefficient, most often used, this method also has certain disadvantages:

- the other acoustic characteristics of the sound absorption material, except the sound absorption coefficient, cannot be determined;
- large and expensive facilities are required;
- large samples are required which are not always available, especially in the developing material phase;
- position and size of the sample can influence the results [9];
- sound absorption coefficient values are often overestimated and higher than 1 (Fig.1), because of edge diffraction, non-diffuseness, and/or Sabine formulation [10];
- significant differences in results may occur for different reverberation rooms (Fig.1), also see [11].

The mean sound absorption coefficient for 13 different laboratories is shown for each sample in Fig.1, along with error bars indicating the 95% confidence limit. The left graph is for a 100 mm mineral wool absorber in a wooden casing covered with nonwoven fleece and the right is for a 25-mm-thick foam absorber [1].

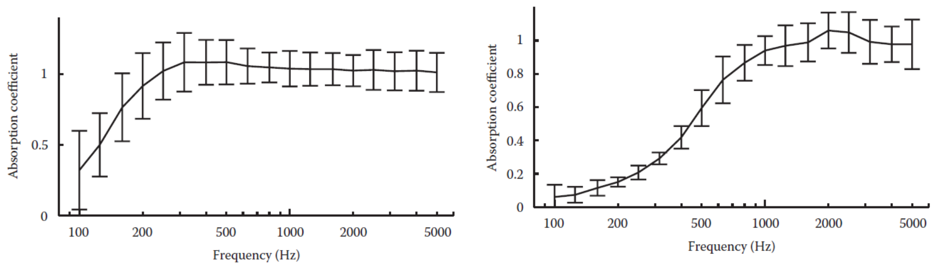

Fig. 1 Comparison of sound absorption coefficients for two different samples [1]

3. IMPEDANCE (KUNDT`S) TUBE METHOD

The impedance tube method, very often called a Kundt`s tube method, enables both the normal incidence sound absorption coefficient and surface impedance measurement. The measurement is carried out under well-defined and controlled conditions and is very often used in developing new sound absorption materials and validation of prediction methods. The advantage of this method is that it requires only small samples and relatively simple instrumentation that can be placed in a normal room. The time and costs of testing are far less compared to the reverberation room method. The problem in applying this method arises when small samples are not representative of the behavior of large samples, so it is most often used with porous absorbers.

There are different types of measuring the acoustic properties of materials using an impedance tube:

- Standing wave ratio method with one microphone
- Transfer function method with two/three microphones
- Transfer function matrix method with four microphones
- Transfer function method with two microflows
- P-U method.

3.1. Standing wave method with one microphone

ISO 10534-1 [12] and ASTM C-384-04 [13] specify a method for determination of the normal incidence sound absorption coefficient. In addition, it is possible to determine the normal incidence sound reflection coefficient, the surface impedance and surface admittance of the materials. The standing wave ratio method is the oldest and simplest direct method for measuring the acoustic properties of materials using the impedance tube with one microphone.

The material sample, whose acoustic characteristics are to be determined is mounted on one end of the impedance tube. At the other end, a loudspeaker is mounted to generate an incident plane sinusoidal sound wave. The generated sound wave is reflected from the material sample and the superposition of incident and reflected waves creates a standing wave in the impedance tube (Fig. 2). The standing wave created inside the tube contains a number of nodes and anti-nodes, with the minimum sound pressure level and maximum sound pressure level, respectively. The standing wave ratio, i.e. the ratio of the maximum sound pressure to the minimum sound pressure, is used to determine the normal incidence sound absorption coefficient. The maximum and minimum sound pressure is measured by moving the microphone (Fig. 3). The microphone is moved from the sample towards the loudspeaker, and the first sound pressure level minimum is detected, then the following maximum is detected. Normally the sound pressure level will first experience a maximum when moving the microphone from the sample towards the loudspeaker, as illustrated in Fig. 2, but the second maximum is used for determining the standing wave ratio [14]. This procedure is repeated for all frequencies of interest.

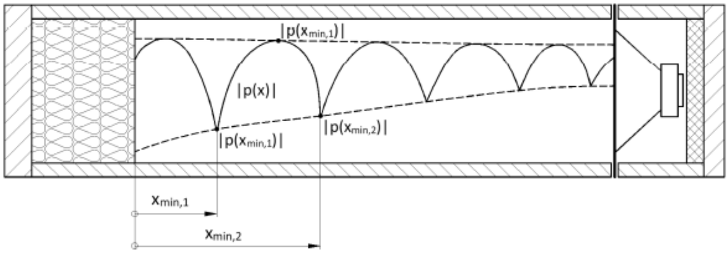

Fig. 2 Schematic view of the standing wave ratio method [2]

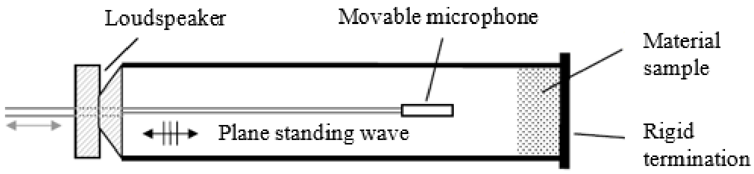

Fig. 3 Measurement setup for the standing wave ratio method with one microphone (adopted from [7])

If the difference between the maximum sound pressure level and the minimum sound pressure level is ΔL [dB], then the normal incidence sound absorption coefficient follows [12]:

$$\alpha_{\mathrm{n}} = \frac{4 \cdot 10^{\Delta L/20}}{(10^{\Delta L/20} + 1)} . \tag{5}$$

The results of the investigation of the sound absorption characteristics of single and multi-layered porous materials presented in the paper [15] show that the standing wave method is simpler but the transfer function method is a more accurate approach.

3.2. Transfer function method with two/three microphones

ISO 10534-2:2008 [16] describes the method for determining the normal incidence sound absorption coefficient of sound absorbers using the transfer function between two microphone locations. The American standard ASTM E1050-19:2019 [17] describes this procedure in an almost identical way to the mentioned ISO standard. The method uses an impedance tube with a sound source connected to one end and the test sample mounted at the other end (as in ISO 10534-1), with two microphone locations and a digital frequency analysis system (Fig. 4). It can also be applied for determining the acoustical surface impedance or surface admittance of sound absorbing materials. In this method, the

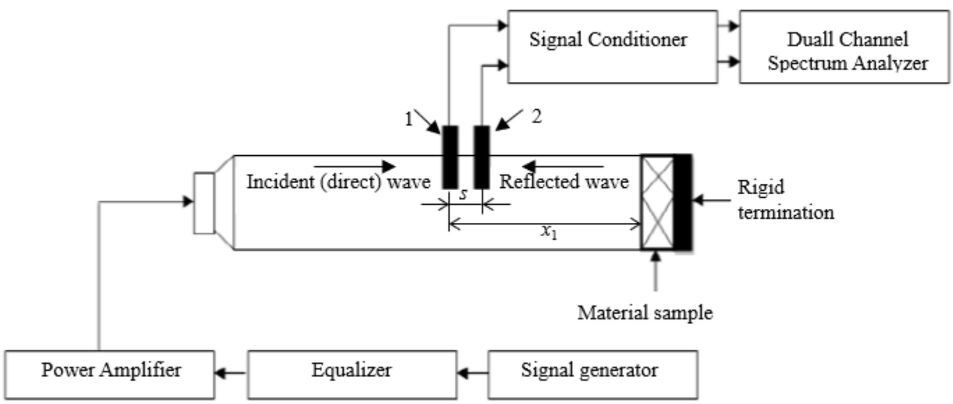

Fig. 4 Measurement setup for the transfer function method with two microphones (adopted from [18])

broadband excitation signal forms a standing plane wave in the tube, comprising two components: the direct waves moving from the sound source to the sample and the reflected waves moving from the sample surface to the other end of the tube where the sound source is located. Decomposition of the standing wave is achieved by simultaneously measuring the sound pressure at two spatially separated positions on the tube surface using two wall-mounted microphones and then calculating the complex acoustic transfer function, the normal incidence sound absorption coefficient and the impedance ratios of the acoustic material.

The complex sound pressure levels, $\underline{p}_1$ and $\underline{p}_2$, are measured at the microphone position 1 and 2, and the normal incidence sound absorption coefficient is determined as [16]:

$$\alpha_{\mathrm{n}} = 1 - |\underline{r}|^2 . \tag{6}$$

The complex normal incidence sound reflection coefficient, $\underline{r}$, is determined as:

$$\underline{r} = |\underline{r}| e^{j\phi_r} = \frac{\underline{H}_{12} - e^{-jks}}{e^{jks} - \underline{H}_{12}} e^{2jkx_1} . \tag{7}$$

where

x_1 is the distance between the material sample and the microphone position 1, in [m];

k is the wave number, $k = 2\pi f / c$ (f is the frequency, c is the speed of sound);

$\underline{H}_{12}$ is the transfer function between two microphone positions 1 and 2:

$$\underline{H}_{12} = \frac{\underline{p}_2}{\underline{p}_1} = \frac{\underline{S}_{12}}{\underline{S}_{11}} = \frac{\underline{S}_{22}}{\underline{S}_{21}} = \sqrt{\frac{\underline{S}_{12}}{\underline{S}_{11}} \cdot \frac{\underline{S}_{22}}{\underline{S}_{21}}} . \tag{8}$$

In eq. (8), $\underline{S}$ represents the auto/cross spectrum determined as the product of complex sound pressures at corresponding microphone positions, for example $\underline{S}_{12} = \underline{p}_2 \cdot \underline{p}_1^*$. The transfer function must be compensated for phase and amplitude mismatch of the microphones by the procedure described in [16, 17].

The slightly modified method is described in the paper [18]. The same measurement setup is used, but instead of the transfer function, the auto spectra of the incident and reflected waves are determined. The two microphones placed in two locations measure the auto spectrum S_{11} and S_{22} and the cross spectrum $\underline{S}_{12} = X_{12} + jY_{12}$. The auto spectrum of the incident and reflected waves, $\underline{S}_{\mathrm{AA}}$ and $\underline{S}_{\mathrm{BB}}$, are determined as [17]:

$$\begin{bmatrix} \underline{S}_{\mathrm{AA}} \\ \underline{S}_{\mathrm{BB}} \\ X_{\mathrm{AB}} \\ Y_{\mathrm{AB}} \end{bmatrix} = \begin{bmatrix} 1 & 1 & 2\cos(2kx_1) & 2\sin(2kx_1) \\ 1 & 1 & 2\cos(2kx_2) & 2\sin(2kx_2) \\ \cos(kn) & \cos(kn) & 2\cos(km) & 2\sin(km) \\ -\sin(kn) & \sin(kn) & 0 & 0 \end{bmatrix}^T \cdot \begin{bmatrix} \underline{S}_{11} \\ \underline{S}_{22} \\ X_{12} \\ Y_{12} \end{bmatrix}, \tag{9}$$

where $\underline{S}_{\mathrm{AB}} = X_{\mathrm{AB}} + jY_{\mathrm{AB}}$ is the cross spectrum between the incident and reflected waves, $m = x_1 + x_2$ and $n = x_1 - x_2$. The distance x_1 and x_2 are illustrated in Fig. 5.

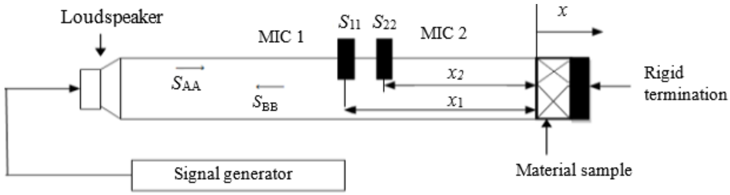

Fig. 5 Measurement setup for the transfer function method with two microphones (adopted from [18])

The normal incidence sound absorption coefficient is calculated from:

$$\alpha_n = 1 - \left| \frac{\underline{S}_{BB}}{\underline{S}_{AA}} \right|^2 , \tag{10}$$

where $\underline{S}_{AA} = X_{AA} + jY_{AA}$ and $\underline{S}_{BB} = X_{BB} + jY_{BB}$.

The two-microphone transfer function method can be enhanced to determine additional material characteristics by incorporating an extra microphone mounted flush with the inner wall of the rigid termination of the impedance tube. The characteristic impedance, wave number, equivalent bulk modulus and equivalent density of the material sample can be calculated based on the measurement results [19, 20]. An impedance tube configuration with three microphones is illustrated in Fig. 6.

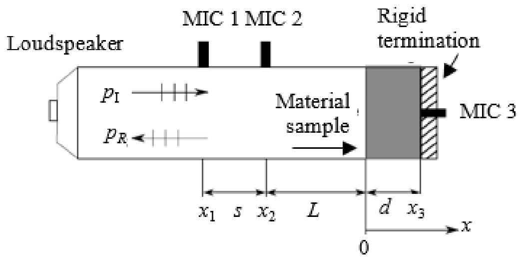

Fig. 6 Impedance tube configuration with three microphones (adopted from [21])

For testing the acoustic characteristics of the material, a standardized impedance tube described in ISO 10534-2:2008 and ASTM E1050-19:2019 is used [10, 22]. Due to the high cost of commercially available impedance tubes and the associated measurement software, the impedance tubes were designed and constructed using low-cost materials, but without reducing the accuracy and reliability of the measurement results [23, 24].

The investigation results obtained by applying the two-microphone transfer function method [25-27] indicate that this method can also be used to determine the absorption characteristics of the new composite materials [23].

3.3. Transfer function matrix method with four microphones

The standard test method for determining the acoustic properties of porous materials at normal incidence based on the transfer function matrix method described in the American standard ASTM E2611-19 [28] is primarily intended for determining normal incident sound transmission loss, but it can also be used to determine other acoustic properties of materials, such as the normal incidence sound absorption coefficient.

The transfer function matrix method is similar to the method described in ASTM E1050-19 and ISO 10534-2, where an impedance tube is used with a broadband sound source connected to one end of the tube and the material sample mounted in the middle part of the tube. The difference is that the transfer function matrix method uses four microphones, two on each side of the material sample with diaphragms flushed to the inside surface of the impedance tube (Fig. 7). These microphones simultaneously measure the sound pressure levels at all four locations including their relative amplitudes and phases. The method requires at least one microphone and a two-channel analyzer, but employing more microphones and channels speeds up the measurement procedure. Allowable measurement configurations and procedures are shown in Table 1.

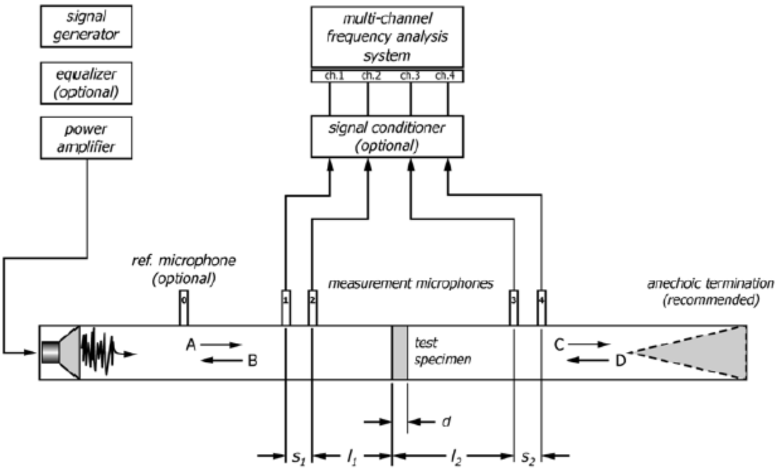

Legend: A, B, C and D are the forward and backward components of the standing wave

Fig. 7 Measurement setup for transfer function matrix method [28]

Table 1 Measurement configurations and procedures [28]

Number of channels	Number of microphones	Transfer function reference	Measured transfer function	Procedure
2	1	source signal	$\underline{H}_{1s}, \underline{H}_{2s}, \underline{H}_{3s}, \underline{H}_{4s}$	single microphone moves to locations 1–4
2	2	mic. 1 at location 0	$\underline{H}_{10}, \underline{H}_{20}, \underline{H}_{30}, \underline{H}_{40}$	microphone 2 moves to locations 1–4
2	2	mic. 1 at location 1	$\underline{H}_{11} = 1, \underline{H}_{21}, \underline{H}_{31}, \underline{H}_{41}$	microphone 2 moves to locations 2–4
4	4	mic. 1 at location 1	$\underline{H}_{11} = 1, \underline{H}_{21}, \underline{H}_{31}, \underline{H}_{41}$	fixed microphones in locations 1–4
5	4	source signal	$\underline{H}_{1s}, \underline{H}_{2s}, \underline{H}_{3s}, \underline{H}_{4s}$	fixed microphones in locations 1–4
5	5	mic. 1 at location 5	$\underline{H}_{10}, \underline{H}_{20}, \underline{H}_{30}, \underline{H}_{40}$	fixed microphones in locations 1–4

The acoustic properties of the material are determined based on the transfer function matrix formed from the measurements of complex sound pressures at the microphone positions. Practically, the transfer function between the reference position and other microphone positions is determined based on the corresponding auto spectra and cross spectra (see Eq. (8)). The transfer function matrix relates the sound pressure and the particle velocity on the front and back surface of the test material sample:

$$\begin{bmatrix} \underline{p} \\ \underline{u} \end{bmatrix}_{x=0} = \begin{bmatrix} \underline{T}_{11} & \underline{T}_{12} \\ \underline{T}_{21} & \underline{T}_{23} \end{bmatrix} \begin{bmatrix} \underline{p} \\ \underline{u} \end{bmatrix}_{x=d} . \tag{11}$$

The acoustic standing wave formed on both sides of the test material sample is decomposed into components A, B, C and D, as indicated in Fig. 7, based on the following equations [28]:

$$\underline{A} = j\,\frac{\underline{H}_{1,\mathrm{ref}}\, e^{-jkl_1} - \underline{H}_{2,\mathrm{ref}}\, e^{-jk(l_1 - s_1)}}{2\sin(ks_1)} , \tag{12}$$

$$\underline{B} = j\,\frac{\underline{H}_{2,\mathrm{ref}}\, e^{jk(l_1 + s_1)} - \underline{H}_{1,\mathrm{ref}}\, e^{jkl_1}}{2\sin(ks_1)} , \tag{13}$$

$$\underline{C} = j\,\frac{\underline{H}_{3,\mathrm{ref}}\, e^{jk(l_2 + s_2)} - \underline{H}_{4,\mathrm{ref}}\, e^{jkl_2}}{2\sin(ks_2)} , \tag{14}$$

$$\underline{D} = j\,\frac{\underline{H}_{4,\mathrm{ref}}\, e^{-jkl_2} - \underline{H}_{3,\mathrm{ref}}\, e^{-jk(l_2 - s_2)}}{2\sin(ks_2)} . \tag{15}$$

The sound pressure and the particle velocity on both faces of the test material sample are determined as [28]:

$$\begin{aligned} \underline{p}_{x=0} &= \underline{p}_0 = \underline{A} + \underline{B}, & \underline{p}_{x=d} &= \underline{p}_d = \underline{C}e^{-jkd} + \underline{D}e^{jkd}, \\ \underline{u}_{x=0} &= \underline{u}_0 = \frac{\underline{A} - \underline{B}}{\rho c}, & \underline{v}_{x=d} &= \underline{v}_d = \frac{\underline{C}e^{-jkd} - \underline{D}e^{jkd}}{\rho c}. \end{aligned} \tag{16}$$

Distances l_1, l_2, s_1, s_2 and d in eq. (12-16) are indicated in Fig. 7.

The elements of the transfer function matrix are determined from two measurements with two different terminations: the recommended anechoic termination or termination with minimum reflection (termination "a"), and the rigid (blocked) or open termination, reflecting part of the incident wave (termination "b").

Then, the transfer function matrix is [28]:

$$T = \begin{bmatrix} \dfrac{\underline{p}_{0\mathrm{a}}\underline{u}_{d\mathrm{b}} - \underline{p}_{0\mathrm{b}}\underline{u}_{d\mathrm{a}}}{\underline{p}_{d\mathrm{a}}\underline{u}_{d\mathrm{b}} - \underline{p}_{d\mathrm{b}}\underline{u}_{d\mathrm{a}}} & \dfrac{\underline{p}_{0\mathrm{b}}\underline{p}_{d\mathrm{a}} - \underline{p}_{0\mathrm{a}}\underline{p}_{d\mathrm{b}}}{\underline{p}_{d\mathrm{a}}\underline{u}_{d\mathrm{b}} - \underline{p}_{d\mathrm{b}}\underline{u}_{d\mathrm{a}}} \\ \dfrac{\underline{u}_{0\mathrm{a}}\underline{u}_{d\mathrm{b}} - \underline{u}_{0\mathrm{b}}\underline{u}_{d\mathrm{a}}}{\underline{p}_{d\mathrm{a}}\underline{u}_{d\mathrm{b}} - \underline{p}_{d\mathrm{b}}\underline{u}_{d\mathrm{a}}} & \dfrac{\underline{p}_{d\mathrm{a}}\underline{u}_{0\mathrm{b}} - \underline{p}_{d\mathrm{b}}\underline{u}_{0\mathrm{a}}}{\underline{p}_{d\mathrm{a}}\underline{u}_{d\mathrm{b}} - \underline{p}_{d\mathrm{b}}\underline{u}_{d\mathrm{a}}} \end{bmatrix} . \tag{17}$$

If the material sample is geometrically symmetrical, the measurement procedure can be simplified with only one termination, preferably anechoic (often called the two-cavity method). In this case, the transfer function matrix is [28]:

$$T = \begin{bmatrix} \dfrac{\underline{p}_d \underline{u}_d + \underline{p}_0 \underline{u}_0}{\underline{p}_0 \underline{u}_d + \underline{p}_d \underline{u}_0} & \dfrac{\underline{p}_0^2 - \underline{p}_d^2}{\underline{p}_0 \underline{u}_d + \underline{p}_d \underline{u}_0} \\ \dfrac{\underline{u}_0^2 - \underline{u}_d^2}{\underline{p}_0 \underline{u}_d + \underline{p}_d \underline{u}_0} & \dfrac{\underline{p}_d \underline{u}_d + \underline{p}_0 \underline{u}_0}{\underline{p}_0 \underline{u}_d + \underline{p}_d \underline{u}_0} \end{bmatrix}. \tag{18}$$

Finally, the normal incidence sound absorption coefficient is determined as:

$$\alpha_{\mathrm{n}} = 1 - \left| \frac{\underline{T}_{11} - \rho c \underline{T}_{21}}{\underline{T}_{11} + \rho c \underline{T}_{21}} \right|^2 . \tag{19}$$

The transfer function matrix method with four microphones is more suitable for materials with low flow resistivity [29]:

The usable frequency range of the standard impedance tube is limited to 6.4 kHz based on the microphone spacing and impedance tube diameter. However, a newly developed high-frequency impedance tube can measure the acoustic characteristics of materials up to 12.8 kHz [30]. In the paper [30], this impedance tube was verified and the obtained results were compared with those from conventional impedance tubes.

3.4. Transfer function method with two microflowns

The development of a novel particle velocity sensor, the microflown, enabled the application of the transfer function method using two microflowns and a measurement setup similar to the one shown in Fig. 4. The positions for microphones in Fig. 4 are used for the microflowns. In order to determine the normal incidence sound absorption coefficient, the transfer function between the two microflowns must be determined:

$$\alpha_{\mathrm{n}} = 1 - \left| \frac{e^{jk(x_1 - s)} - \underline{H}_{12} e^{jkx_1}}{e^{-jk(x_1 - s)} - \underline{H}_{12} e^{-jkx_1}} \right|^2 , \tag{20}$$

where $\underline{H}_{12}$ is the transfer function between two microflowns position 1 and 2:

$$\underline{H}_{12} = \frac{\underline{u}_2}{\underline{u}_1} = \frac{\underline{S}_{12}}{\underline{S}_{11}} = \frac{\underline{S}_{22}}{\underline{S}_{21}} = \sqrt{\frac{\underline{S}_{12}}{\underline{S}_{11}} \cdot \frac{\underline{S}_{22}}{\underline{S}_{21}}} . \tag{21}$$

The method is described in [31, 32].

3.5. P-U method

The combination of a microphone and a microflown provides information about the sound intensity and sound energy density. Fahy [33] showed that the ratio between the mean sound intensity and the mean sound energy density is related to the amplitude reflection coefficient:

$$\frac{\bar{I}}{\bar{E}} = c\frac{1-|\underline{r}|^2}{1+|\underline{r}|^2} \ . \tag{22}$$

The normal incidence sound absorption coefficient of the material sample can be calculated as:

$$\alpha_{\mathrm{n}} = \frac{\bar{E}c-\bar{I}}{\bar{E}c+\bar{I}}\cos(2kL) \ . \tag{23}$$

The impedance tube configuration for p-u method is shown in Fig. 8, where the microphone and the microflown positions are indicated by *p* and *v*.

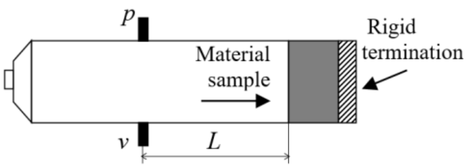

Fig. 8 Impedance tube configuration for p-u method

Using two channel FFT analyzer, the mean sound intensity and the mean sound energy density can be calculated by measuring auto spectra and cross spectra as [31]:

$$\bar{E} = \frac{1}{2}\rho_0 S_{uu} + \frac{1}{2\rho_0 c^2} S_{pp} \ . \tag{24}$$

$$\bar{I} = \mathrm{Re}\{\underline{S}_{pu}\} \ . \tag{25}$$

Replacing eq. (24) and eq. (25) in eq. (23), the normal incidence sound absorption coefficient of material sample can be calculated based on auto spectra and cross spectra measurement.

4. Relationship between Impedance Tube and Reverberation Room Methods

In chapters 2 and 3, different methods for measuring sound absorption coefficient were outlined. The methods discussed in chapter 2 provide the random incidence sound absorption coefficient, while those in chapter 3 provide the normal incidence sound absorption coefficients. Converting sound absorption coefficients is not easy but is very useful. The impedance tube methods are conducted in a controlled environment on small samples, which is ideal when developing new absorption materials and validating prediction models. On the other hand, the random incidence sound absorption coefficient is the parameter most used in the design of spaces to specify the absorption performance of materials [1].

There are different approaches to solving this problem: a theoretical approach and an empirical approach and combination of both.

In the theoretical approach [34, 35], the random incidence sound absorption coefficient is determined based on the characteristic impedance measurement in the impedance tube.

All methods outlined in chapter 3 provide determining the characteristic impedance of the test material. The random incidence sound absorption coefficient is determined using the following equations [34]:

$$\alpha_{\mathrm{r}} = 2\int_{o}^{\pi} \alpha(\theta)\sin\theta\cos\theta \,, \tag{26}$$

$$\alpha(\theta) = \frac{4R_{\mathrm{n}}\cos\theta}{(1+R_{\mathrm{n}}\cos\theta)^2 + (X_{\mathrm{n}}\cos\theta)^2} \,, \tag{27}$$

where

- θ is the sound incidence angle, in [rad];
- R_{n} is the real part of the normal sound incidence normalized characteristic impedance;
- X_{n} is the imaginary part of the normal sound incidence normalized characteristic impedance.

Solving eq (26), an expression to estimate the random sound incidence absorption coefficient is obtained [36]:

$$\alpha_{\mathrm{r}} = 8\frac{R_{\mathrm{n}}}{R_{\mathrm{n}}^2 + X_{\mathrm{n}}^2}\left[1 - \frac{R_{\mathrm{n}}}{R_{\mathrm{n}}^2 + X_{\mathrm{n}}^2}\ln(1+2R_{\mathrm{n}} + R_{\mathrm{n}}^2 + X_{\mathrm{n}}^2) + \frac{1}{X_{\mathrm{n}}}\frac{R_{\mathrm{n}}^2 - X_{\mathrm{n}}^2}{R_{\mathrm{n}}^2 + X_{\mathrm{n}}^2}\arctan\frac{X_{\mathrm{n}}}{1+R_{\mathrm{n}}}\right]. \tag{28}$$

Fig. 9 shows the comparison between the random incidence sound absorption coefficients obtained in a reverberation room and those estimated from eq. (28) for recycled foam with a density of 150 kg/m^3 and thickness of 40 mm.

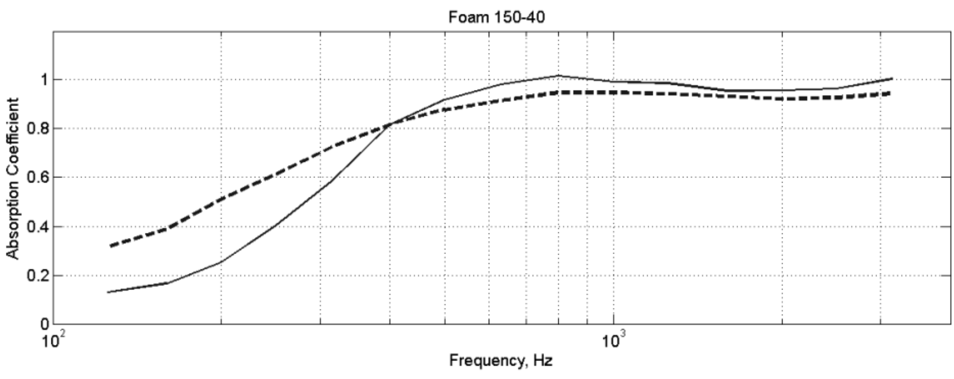

Fig. 9 Comparison between measured (continuous line) and estimated (dotted line) random incidence sound absorption coefficient [35]

In the experimental approach [10], the relationship between the random incidence absorption coefficient and the normal incidence absorption coefficient is established based on measurement results for 28 polyester samples tested using the reverberation room interrupt method and the transfer function impedance tube method. The predicted random incidence sound absorption coefficient can be calculated based on the measured normal incidence sound absorption coefficient using the equation [10]:

$$\alpha_{\mathrm{r}}(f) = 0.945 + 0.245\ \ln\alpha_{\mathrm{n}} + \phi(f) - 0.002\rho + 0.0015d + 7.52e^{-6}R\ . \qquad (29)$$

where

- ρ is the density of the material sample, in [kg/m^3];
- d is the thickness of the material sample, in [m];
- X_{n} is the flow resistivity of the material sample, in [Pa·s/m^3];
- $\phi(f)$ are the frequency factor coefficients shown in Table 2 [10].

Fig. 10 shows the comparison between the random incidence sound absorption coefficients obtained in a reverberation room and those estimated from eq. (29) for two polyester samples.

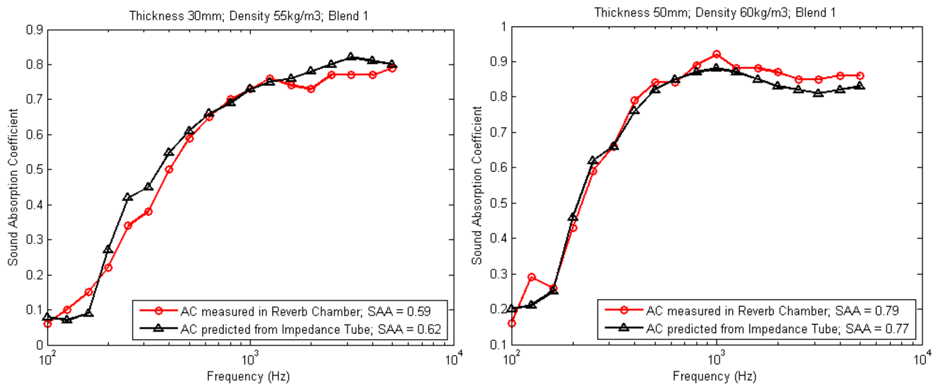

Fig. 10 Comparison between measured and estimated random incidence sound absorption coefficient (adopted from [10])

5. CONCLUSIONS

The absorption performances of acoustic materials can be characterized by four interrelated acoustic quantities: surface impedance, surface admittance, sound reflection coefficient and sound absorption coefficient. Knowledge of these four acoustic quantities is fundamental for calculating noise reduction using sound absorption materials and for the acoustic design of spaces depending on their purpose.

While there are well-known theoretical models for characterizing sound absorption materials, numerous methods have been developed over the years to measure acoustic quantities that define sound absorption materials. The most commonly used methods are two standardized approaches: the reverberation room method and the incidence tube method.

The reverberation room method is exclusively used for determining the random incidence sound absorption coefficient, an acoustic quantity frequently employed in design to specify the absorption performance of materials. To apply the reverberation room method, it is necessary to have a diffuse sound field in the room, where the interrupt noise method and integrated impulse response method can be used.

Despite its popularity in determining the random incidence sound absorption coefficient, the reverberation room method has certain disadvantages:

- other acoustic characteristics of the sound absorption material, except the sound absorption coefficient, cannot be determined;
- large and expensive facilities are required;
- large samples are required which are not always available, especially in the material development phase;
- the position and size of the sample can influence the results;
- sound absorption coefficient values are often overestimated and higher than 1, due to edge diffraction, non-diffuseness, and/or Sabine formulation;
- significant differences in results may occur for different reverberation rooms.

The impedance tube method provides the surface impedance, the surface admittance, the sound reflection coefficient and the sound absorption coefficient. The measurement is carried out under well-defined and controlled conditions and can be frequently used in the development of new sound absorption materials and validation of prediction methods. The advantage of this method is that it requires only small samples and relatively simple instrumentation that can be placed in a normal room. The time and costs of testing are far less compared to the reverberation room method. The problem in applying this method arises when small samples are not representative of the behavior of large samples, so it is most often used with porous absorbers. Different types of measuring the acoustic properties of materials using an impedance tube are outlined in this paper. The transfer function matrix method is primarily intended for determining normal incident sound transmission loss, but it can also be used to determine other acoustic properties of materials such as the normal incidence sound absorption coefficient.

The investigation results of the sound absorption characteristics of single and multi-layered porous materials show that the standing wave method is simpler, but the transfer function method and the transfer function matrix method are more accurate.

The investigation results obtained applying the two-microphone transfer function method show that this method can also be used for determining the absorption characteristics of the new composite materials [3].

The reverberation method provides the random incidence sound absorption coefficient, while the impedance tube method provides the normal incidence sound absorption coefficient. Although converting sound absorption coefficients is not easy, it can be very useful. Applying the available theoretical and empirical approaches for converting the measurement results obtained in the impedance tube into the random incidence sound absorption coefficient, good agreement between the predicted and measured random incidence sound absorption coefficient can be obtained.

Acknowledgement: *This research was sponsored by the NATO Science for Peace and Security Programme under grant SPS MYP G6006 "Acoustic Multi-Functional Composites for Environmental Risks and Health Hazards Reduction" and by the Ministry of Science, Technological Development and Innovation of the Republic of Serbia under the contract no. 451-03-66/2024-03/200148.*

REFERENCES

1. Cox T., D`Antonio P., (2017), *Acoustic Absorbers and diffusers*, CRC Press, 978-1-4987-4099-9 (Hardback), p. 502
2. Radicevic B., (2016), *Development of a decision-making model for the selection of the optimal mixture of sound absorbing materials*, PhD thesis, University of Kragujevac, Faculty of Mechanical and Civil Engineering in Kraljevo, p. 275
3. NATO SPS MYP G6006 project website https://3dlab.iict.bas.bg/g6006/
4. ISO 354, (2003), *Acoustics - Measurement of sound absorption in a reverberation room*
5. ASTM C423, (2023), *Standard Test Method for Sound Absorption and Sound Absorption Coefficients by the Reverberation Room Method*
6. Bischel, M. Roy, K. and Greenslade, J., (2008), Comparison of ASTM and ISO sound absorption test methods, *The Journal of the Acoustical Society of America*, Acoustical Society of America, 123 (5), DOI: 10.1121/1.2933311, pp. 1669- 1674,
7. Tijs E.H.G., (2013), *Study and development of an in situ acoustic absorption measurement method*, PhD thesis, University of Twente, Enschede, The Netherlands
8. ISO 9613-1, (1993), *Acoustics - Attenuation of sound during propagation outdoors - Part 1: Calculation of the absorption of sound by the atmosphere*
9. Carvalho A., Sousa M., (2016), Effect of sample area in reverberant chamber measurements of sound absorption coefficients, *Proceedings of the 22nd International Congress on Acoustics*, Buenos Aires, Argentina,5-9 September 2016, p. 10
10. McGrory M., Cirac C. D., Gaussen O. and Cabrera D., (2012), Sound absorption coefficient measurement: Re-examining the relationship between impedance tube and reverberant room methods, *Proceedings of Acoustics 2012*, Fremantle, Australia, 21-23 November 2012, p. 8
11. Scrosati C, at all, (2020) Towards more reliable measurements of sound absorption coefficient in reverberation rooms: An Inter-Laboratory Test, *Applied Acoustics*, Elsevier, 165, DOI: 10.1016/j.apacoust.2020.107298, p. 19
12. ISO 10534-1, (1996), *Acoustics - Determination of sound absorption coefficient and impedance in impedance tubes - Part 1: Method using standing wave ratio*
13. ASTM C384-04, (2022), *Standard Test Method for Impedance and Absorption of Acoustical Materials by Impedance Tube Method*
14. Heed C., (1998), *Sound absorption and acoustic surface impedance,* KTH, Marcus Wallenberg Laboratory, Stockholm, Sweeden
15. Niresh J., Neelakrishnan S., Subharani, S. and Prabhakaran R., (2015), Performance Testing for Sound Absorption Coefficient by Using Impedance Tube, *Research Journal of Applied Sciences, Engineering and Technology*, Maxwell Scientific Publication Corp., 1 (2), DOI: 10.19026/rjaset.11.1706, pp. 185-189
16. ISO 10534-2, (1998), *Acoustics - Determination of sound absorption coefficient and impedance in impedance tubes - Part 2: Transfer-function method*
17. ASTM E1050-19, (2019), *Standard Test Method for Impedance and Absorption of Acoustical Materials Using a Tube, Two Microphones and a Digital Frequency Analysis System*
18. Niresh J., et all, (2015), Review of acoustic characteristics of materials using impedance tube, *ARPN Journal of Engineering and Applied Sciences*, Asian Research Publishing Network, 10 (8), pp. 3319-3326
19. Izumi Y., Iwase, T. and Kawabata, R., (1998), A new measuring method for sound propagation constant by using sound tube without any air spaces back of a test material. Proceedings of Inter-noise Congress, Institute of Noise Control Engineering, Christchurch, New Zealand, pp.1265-1268
20. Yacoubou S., and Panneton, R., (2010), Wideband characterization of the complex wave number and characteristic impedance of sound absorbers, *The Journal of the Acoustical Society of America*, Acoustical Society of America, 128(5), DOI:10.1121/1.3488307, pp. 2868–2876
21. Wolkesson M., (2013), *Evaluation of impedance tube methods - A two microphone in-situ method for road surfaces and the three microphone transfer function method for porous materials*, master thesis, Chalmers University of Technology, Goteborg, Sweden, p. 69
22. Niresh J., Neelakrishnan S., Subharani S. and Shylendran R., (2015), Characterization of sound absorption co-efficient of PUF and cotton felt material by impedance tube method, *International Journal of Scientific Engineering and Applied Science (IJSEAS)*, 1(9), pp. 229-233
23. Arunkumar B., Jeyanthi S., (2017), Design and analysis of impedance tube for sound absorption measurement, *ARPN Journal of Engineering and Applied Sciences*, Asian Research Publishing Network, 12(5), pp. 1400-1405

24. Bhattacharya S. S., Bihola D. V., (2019), Design and Construction of Impedance Tube for Sound Absorption Coefficients Measurements, *International Journal of Advance Research in Science and Engineering*, A R Research publication, 8(9), pp. 93-104
25. Kumar K.S., Reddy S. P, Murthy G. N., Babji M., (2018), Characterization of Epoxy Composites Reinforced with Short Palmyra Fibers, *International Journal of Science Engineering and Advance Technology*, 6 (5), pp. 221-225
26. Mazrouei-Sebdani Z., et. all, (2021), A review on silica aerogel-based materials for acoustic applications, *Journal of Non-Crystalline Solids*, Elsevier, 562, DOI: 10.1016/j.jnoncrysol.2021.120770, p. 17
27. Cops M.J., et. all, (2020), Measurement and analysis of sound absorption by a composite foam, *Applied Acoustics*, Elsevier, 160, DOI: 10.1016/j.apacoust.2019.107138, p. 10
28. ASTM E2611-19, (2019), *Standard Test Method for Normal Incidence Determination of Porous Material Acoustical Properties Based on the Transfer Matrix Method*
29. Muehleisen, R.T. and Beamer, C.W., (2002) Comparison of errors in three- and four-microphone methods used in the measurement of the acoustic properties of porous materials, *Acoustics Research Letters Online, 3(4), Acoustical Society of America*, DOI: 10.1121/1.1498175, pp. 112-117.
30. Kimurakimura M., Kunio I. J., Schuhmacher A., and Ryu Y., (2014), A new high frequency impedance tube for measuring sound absorption coefficient and sound transmission loss, *Proceedings of Inter-noise 2014*, Melbourne, Australia, 16-19 November 2014, p. 10
31. Bree H-E., Rerden F.J.M., Honschten J.W., A novel technique for measuring the reflection coefficient of sound absorbing materials, University Twente Repository, available at: https://ris.utwente.nl/ws/portalfiles/portal/5483529/Bree00novel.pdf, accessed 1 March 2024
32. Hiremath N., Kumar V., Motahari N., and Shukla D., (2021), An Overview of Acoustic Impedance Measurement Techniques and Future Prospects, *Metrology*, MDPI AG, 1, DOI: 10.3390/metrology1010002, pp. 17–38.
33. Fahy F.J., *Sound Intensity*, E&FN Spon, London, p. 291
34. Herrin D., Determination of Diffuse Field Sound Absorption from a Normal Incidence Impedance Measurement (presentation), University of Kentucky, available at https://vac.engr.uky.edu/sites/vac/files/Webinars/32_VAC_Web_Meeting_Diffuse_Field_Absorption.pdf, accessed 3 March 2024
35. Del Ray, R. et all, Determination of the statistical sound absorption coefficient of porous materials from normal-incidence measurements, Proceedings of the 21st International Congress on Sound and vibration, Beijing/China, 13-17 July 2014, p. 8

METODE ZA MERENJE KOEFICIJENTA APSORPCIJE ZVUKA U REVERBERACIONOJ PROSTORJI I IMPEDANSNOJ CEVI

Zvučno-apsorpcioni materijali se veoma često koriste za projektovanje prostora u cilju smanjenja nivoa buke i podešavanja akustičkih karakteristika prostora u zavisnosti od njegove namene. Stoga je poznavanje akustičkih veličina koje karakterišu zvučno-apsorpcione materijale od ključnog značaja. Najčešće korišćena akustička veličina je koeficijent apsorpcije zvuka koja se može odrediti primenim standardizovanih metoda i metoda koje se koriste samo za istraživačke svrhe. U ovom radu će biti dat pregled najčešće korišćenih standardizovanih metoda za određivanje koeficijenta apsorpcije zvuka: metod reverberacione prostorije i metod impedansne cevi. Kako je u fazi razvoja novih materijala pogodnija primena metode impedansne cevi koja daje koeficijent apsorpcije zvuka pri normalnoj incidenciji, a u praktičnoj primeni je poželjno poznavanje koeficijenta apsorpcije zvuka pri slučajnoj incidenciji, u ovom radu će biti prikazani pristupi za predikciju koeficijenta apsorpcije zvuka pri slučajnoj incidenciji na osnovu merenja akustičkih parametara zvučno-apsorpcionih materijala u impedansnoj cevi.

Ključne reči: *koeficijent apsorpcije zvuka pri slučajnoj incidenciji, koeficijent apsorpcije zvuka pri normalnoj incidenciji, metod reverberacione prostorije, metod impedansne cevi*.

FACTA UNIVERSITATIS
Series: **Working and Living Environmental Protection** Vol. 21, Nº 1, 2024, pp. 19 - 35
https://doi.org/10.22190/FUWLEP240414002P

Review Paper

OVERVIEW OF COMMON METHODS FOR FIRE TESTING

UDC 614.842

Milan Protić[1], Nikola Mišić[1], Miomir Raos[1], Milena Mančić[1], Marjan Popović[2]

[1]University of Niš, Faculty of Occupational Safety, Niš, Republic of Serbia
[2]Miphem, Belgrade, Republic of Serbia

ORCID iDs:	Milan Protić	https://orcid.org/0000-0003-4957-7882
	Nikola Mišić	https://orcid.org/0000-0003-2314-4851
	Miomir Raos	https://orcid.org/0000-0001-5586-0276
	Milena Mančić	https://orcid.org/0000-0002-6181-2286
	Marjan Popović	N/A

Abstract. *Fire testing is critical for assessing the behavior of building materials under fire conditions, providing indispensable insights into important variables such as flammability, heat release rate, and smoke production. This paper provides an overview of common fire testing methods, including the procedures for test selection, sample preparation, data collection, and analysis. These fire testing methods are outlined in standards issued by world-respected standardization bodies such as ISO, EN, ASTM, and UL. These standards guarantee and ensure the consistency and reliability of prescribed methods. Moreover, this paper presents a detailed description of a custom-made installation hosted at the Fire Protection Laboratory at the Faculty of Occupational Safety, University of Niš, used for evaluating the flammability parameters of a broad spectrum of materials. This hyphenated installation, comprising a mass loss calorimeter and an FTIR gas analyzer, can be used for comprehensive and simultaneous real-time measurement of flammability parameters and fire effluent analysis.*

Key words: *fire testing, ignitability, flame spread, fire effluents, heat release rate, mass loss calorimeter, gas analyzer.*

1. INTRODUCTION

Fire testing is crucial for ensuring building and occupant safety by assessing how building materials respond to fire, considering factors like flammability, smoke production, and structural integrity. Understanding common fire testing methods helps in selecting materials that mitigate fire hazards and enhance life safety. Typically, fire testing procedures

Received April 14, 2024 / Accepted June 27, 2024
Corresponding author: Nikola Mišić
University of Niš, Faculty of Occupational Safety, Čarnojevića 10a, 18000 Niš, Serbia
E-mail: nikola.misic@znrfak.ni.ac.rs

involve the following steps: Test selection, Sample preparation, Testing procedure, Data collection and Analysis and classification and reporting.

Selecting the correct fire test is essential to guarantee the safety and effectiveness of building materials. Before performing any specific tests, it's critical to understand the fire properties being evaluated. The most important properties are: flammability, fire resistance, smoke production, and heat release. Several factors influence which fire test is most appropriate for a particular need. However, two are the most important: prospective material use and building code requirements. The intended use of the material plays a significant role. Fire resistance testing is crucial for structural elements, while flammability is the primary concern for building products. Local building codes typically include specific fire testing requirements suited to various building materials and their intended uses.

ISO, ASTM, and EN standards provide guidelines for gathering material samples that accurately represent the bulk material. This process may include sampling from multiple locations within a batch or using specific extraction tools. Certain materials may require conditioning before testing to achieve the desired moisture content, which ensures consistent results since moisture has a significant influence on fire behavior. Conditioning is frequently performed using ovens or desiccators. Tests frequently require that samples are cut or shaped to precise dimensions based on the test method. This ensures proper placement within the testing apparatus and uniform heat exposure throughout the test. Sample preparation for composite materials with multiple layers may include separating the layers or testing them individually, depending on the test requirements. For materials with coatings or finishes, tests may require preparing samples with and without the treatment to assess its effect on fire performance. Depending on the material, specific safety precautions such as wearing appropriate personal protective equipment (PPE) or providing adequate ventilation for dust control may be required during sample preparation. A thorough sample preparation is vital to achieve reliable fire test results. Poorly prepared samples can produce inaccurate data, jeopardizing the overall validity of the test. Standardized sample preparation procedures ensure consistency and repeatability, allowing for meaningful comparisons of different materials.

To obtain consistent and repeatable results, specialized equipment and controlled laboratory environments are used. Usually, in order to guarantee adherence to relevant testing requirements, these facilities follow particular accreditations. The tested sample is inserted into the testing apparatus in line with the chosen methodology, which frequently requires the use of special fixtures or configurations to replicate real-world situations. The sample may need to be positioned horizontally for a floor application or vertically to replicate a wall in some tests. A standardized ignition source, such as an electrical radiant panel or pilot flame, is introduced to initiate combustion, depending on the type of test. The requirements specified in the test standard regulate the choice and positioning of the ignition source.

The data acquisition system is used to systematically document key data throughout the test procedure. Usually, the following parameters are documented: Temperature (in almost all cases K- type thermocouples are used), Time to ignition (the time it takes for the sample to achieve a specific ignition criterion, such as flaming combustion), Heat flux (the rate of heat transfer through a surface per unit area i.e. the amount of heat energy that flows through a specific area over a given period of time), Heat release rate (defines the rate of heat transfer through a surface per unit area), Smoke density (the concentration of smoke particles generated during combustion), Gas/Vapor emission (structure of fire effluents - gases released during combustion, which can be important for assessing toxicity hazards) and Fire spread (rate of flames spread across the sample's surface).

The material is classified or given a fire rating in accordance with applicable standards based on the test results. These classifications or ratings show how well a material performs in terms of smoke production, flame spread, fire effluent toxicity, and fire resistance.

Because fire testing involves inherent risks, strict adherence to safety precautions is required. Thorough safety protocols are essential during the testing process to protect people and the surrounding environment. This includes adhering to hazard management procedures, using efficient ventilation systems, fire suppression equipment, and flame-resistant clothing. Additionally, testing facilities need to maintain strict quality control procedures to ensure the accuracy and consistency of their test results. This entails following established testing procedures, regularly calibrating equipment, and participating in proficiency testing programs.

2. Classes of Fire Tests

Fire tests have been developed to address nearly every aspect of fire behavior. Leading organizations such as the Society of Fire Protection Engineers (SFPE) [1], the National Fire Protection Association (NFPA) [2], ASTM International (formerly the American Society for Testing and Materials) [3], the International Organization for Standardization (ISO) [4], European Norms (EN) [5], and Underwriters Laboratories (UL) [6] are responsible for developing fire-related tests and standards in the USA, EU, and internationally. Their mandate covers two key categories for fire testing: fire resistance and reaction to fire.

Fire resistance tests are designed to check whether building construction assemblies prevent fires from spreading from the point of origin through the assembly and into adjacent compartments. These kinds of tests are usually performed on building structural elements and fire-resistant barriers (walls, floors, columns, doors, and windows). Also, these tests assess the duration for which a structural element of a building can endure exposure to a standardized fire without collapsing or impairing its intended functionality.

Reaction to fire tests evaluates how materials behave when exposed to a fire source, focusing on their immediate response. Unlike fire resistance tests, they do not measure the duration a material can endure fire exposure. Understanding how materials react to fire allows building designers, architects, and fire safety professionals to make informed material selection decisions and implement fire risk reduction strategies within buildings.

3. Fire Resistance Test Standards

Fire resistance test standards ensure that structures meet the fire protection and separation standards outlined in building codes. These kinds of standards are crucial for ensuring safe construction by evaluating the performance of building elements under fire conditions. In these tests, the "fire resistance rating" indicates the duration the assembly can withstand standard exposure before reaching a "critical endpoint". For example, in the case of walls and partitions, the "critical endpoint" is reached when a specific temperature rise (the value of which depends on the standard) above the initial temperature of the test specimen on the unexposed side is attained. The construction element undergoes exposure to a progressively intense fire, following a standard time-temperature curve. The standard time-temperature curve is a key component of fire resistance testing. It essentially depicts a controlled temperature increase over time, simulating a specific fire scenario within a testing furnace. It's noteworthy that the fire resistance rating pertains to the entire tested assembly rather than its individual components. Tests are performed in Fire Resistance Test Furnaces.

Internationally, ISO 834 Fire-resistance tests — Elements of building construction comprise a series of standards covering various aspects of fire resistance testing. This battery of standards, consisting of 14 individual standards, focuses on both loadbearing and non-loadbearing vertical and horizontal separating elements, as well as beams, columns, ceiling elements, structural steel elements, beams, and bars.

Fire resistance tests for load-bearing structural elements also assess the specimen's ability to carry loads under test conditions. In the USA for fire resistance testing following standards apply: ASTM E119 Standard Test Methods for Fire Tests of Building Construction and Materials [7]. Requirements for ISO, ASTM, and NFPA standards are very similar, with minor differences arising primarily in the standard time-temperature curves.

Few studies have explored the precision of fire resistance testing due to its complex and costly nature [8]. This creates a discrepancy between code requirements and actual test results, where even slight differences are expected. Variability in test results can stem from the precision of the fire test, execution variability in the laboratory, and differences in the test specimen. This also implies that manufacturers may use "selective testing" by running multiple tests, possibly in different laboratories, until they achieve the desired result, thereby avoiding the need for additional testing. The reproducibility and consistency of test results is an ongoing topic of discussion and debate.

The standard time-temperature curves often don't capture the real-world complexities of fires with varying fuels, ventilation, and growth patterns. Their simplified assumptions and one-size-fits-all approach might miss crucial details in specific building configurations or fire safety concerns. Additionally, the lack of customization hinders them from reflecting unique situations or fire protection objectives. Ariyanayagam [9] highlights the limitations of standard time-temperature curves in fire resistance testing. He pointed out that the ISO 834 curve was developed in the early 1900s when wood was the primary fuel source, and emphasized that current standard time-temperature curves do not accurately represent modern building materials, which include thermoplastic materials, synthetic foams, and fabrics, among others. Therefore, standard curves should be used cautiously and complemented by further analysis for a more complete understanding of fire safety performance.

4. Reaction to Fire Test Standards

Most of the ongoing fire testing primarily focuses on examining reaction-to-fire characteristics. These tests typically evaluate properties such as ignition capacity, ease of extinction, flame propagation, smoke and release of toxic gases and heat release rate [10].

4.1. Ignitibility

Ignitability refers to a material's tendency to ignite and sustain combustion [10]. Key properties that characterize the ignition are minimum ignition temperature, critical/minimal heat flux required to initiate the ignition and time to ignition under the specified incident heat flux. The ignitibility of materials has been extensively studied by Babrauskas, who condensed a significant body of knowledge on the subject in the seminal Ignition Handbook [11].

While ignition temperature is crucial, only a few standards specifically address the procedures for determining it. The standards mainly refer to plastic materials. These are the following standards ASTM D1929-23 Standard Test Method for Determining Ignition Temperature of Plastics [12] and ISO 871:2022 Plastics - Determination of ignition temperature using a hot-air furnace [13]. Although these standards provide valuable information regarding the ignition temperatures of plastics, their applicability to other materials may be limited [14]. They are primarily designed for plastics and might not work well for other materials. The controlled lab environment may not perfectly reflect real fires, and the single ignition source used in the test might not represent all fire scenarios. Additionally, the test only provides one data point (ignition temperature) and doesn't consider factors like airflow, which can significantly impact ignition behavior in real-world fires. Therefore, while these standards are very useful, they should be used alongside other tests and considerations to provide a more complete overview of a material's fire safety characteristics.

It is important to note that the minimum ignition temperature is measured as an additional parameter during heat and smoke release tests. Some of the most commonly used standards for determining heat and smoke release are: ISO 5660 - Reaction-to-fire tests — Heat release, smoke production and mass loss rate — Part 1: Heat release rate (cone calorimeter method) and smoke production rate (dynamic measurement) [15]; ASTM E2058 - Standard Test Methods for Measurement of Material Flammability Using a Fire Propagation Apparatus (FPA) [16]; ASTM E1354 - Standard Test Method for Heat and Visible Smoke Release Rates for Materials and Products Using an Oxygen Consumption Calorimeter [17]; ASTM E1321 - Standard Test Method for Determining Material Ignition and Flame Spread Properties [18] and ISO 5657 - Fire tests — Reaction to fire — Ignitability of building products subjected to direct impingement of flame [19]. These standards are reviewed in the heat release rate section.

4.2. Ease of extinction

ASTM D2863 Standard Test Method for Measuring the Minimum Oxygen Concentration to Support Candle-Like Combustion of Plastics (Oxygen Index) [20] and ISO 4589-2 Plastics Determination of burning behaviour by oxygen index Part 2: Ambient-temperature test are two similar standards used for measuring materials ease of extinction [21]. They describe a method for determining the combustion behavior of plastics by measuring the oxygen index at ambient temperature. The oxygen index indicates the lowest concentration of oxygen in an oxygen-nitrogen mixture that supports material combustion. This test provides critical information about the flammability of plastics in normal environmental conditions. The method requires just a small sample of material to be tested and has excellent reproducibility and repeatability. Because of this, these standards stand out as cost-effective and highly accurate quality control tests for combustible materials.

The limitations of the quoted testing methods include their focus on ambient temperature testing, which may not fully represent real-world fire conditions with elevated temperatures. They primarily assess burning behavior using the oxygen index method, limiting their scope to plastics and potentially excluding other materials. Environmental factors such as humidity and airflow are not always considered, and test result interpretation may vary due to factors such as sample preparation and testing conditions. Despite providing valuable insights, these standards/methods of testing have limitations that should be acknowledged when assessing fire safety.

4.3. Flame spread

Understanding flame spread is crucial for predicting fire growth and flashover. Flame spread tests are widely used to gauge material performance in fire situations. The angle formed between the exposed side and the horizontal reference plane can be used to categorize flame spread tests. [22]. This angle largely influences the rate at which gaseous combustion products heat the surface of the tested material [23].

The ASTM E84 Standard Test Method for Surface Burning Characteristics of Building Materials [24], commonly known as the Steiner Tunnel Test, is widely used in the USA for assessing the surface flammability of building materials. The Steiner test is widely used in North America to determine if building materials meet the requirements set forth by building codes. The method of preparing samples for this test is defined by the accompanying ASTM standards.

As a result of testing according to ASTM E84, the dimensionless flame spread index (FSI) is obtained. The FSI is calculated based on the distance and time it takes for flames to spread along the surface of a specimen compared to a reference material under controlled conditions. A lower FSI indicates slower flame spread and better fire resistance of the material. The problem with this test is that FSI is a relative quantity and as such cannot be used in any way in fire modeling.

In North America, a number of standards and tests have been developed for testing the flame spread of pipes and cables based on ASTM E84 such as NFPA 262 Standard Method of Test for Flame Travel and Smoke of Wires and Cables for Use in Air-Handling Spaces [24]. There is no ISO standard corresponding to the Steiner Tunnel Surface Flame spread test.

In addition to the Steiner test, the Lateral Ignition and Flame Spread Test (LIFT) ASTM E1321 Standard Test Method for Determining Material Ignition and Flame Spread Properties [18] and ISO 5658 Reaction to fire tests Spread of flame Part 2: Lateral spread on building and transport products in vertical configuration [26], along with ASTM E162 Standard Test Method for Surface Flammability of Materials Using a Radiant Heat Energy Source [27], are utilized to assess flame spread. The LIFT test was developed to improve the ASTM E162 standard by providing engineering variables derived from the test, which can be utilized in fire safety calculations and predicting full-scale flame spread performance [28]. LIFT is used to determine the value of critical heat flux, surface temperature required for flame spread and thermal inertia of tested material. Additionally, a flame spread parameter is obtained as an output, which can be used to compare fire responses of different materials.

While ISO 5658 provides a number of useful variables for fire safety calculations, according to ISO, it would be insufficient to rely solely on this standard for describing or evaluating the fire hazard of materials, products, or assemblies in actual fire situations.

4.4. Smoke and toxic gas release

Smoke from fires poses several significant problems. Two are the most important: reduced visibility and toxicity.

Smoke clouds can severely limit visibility, making it difficult to escape a burning building. ASTM E662 Standard Test Method for Specific Optical Density of Smoke Generated by Solid Materials [29] and ISO 5659 Plastics - Smoke generation Part 2: Determination of optical density by a single-chamber test [30] standards are used for testing the potency of certain materials to emit smoke. In ASTM E662 a material sample measuring 7.5 x 7.5 mm is placed vertically and exposed to a heat flux of 25 kW/m^2 inside the specially designed chamber. The amount of smoke emitted by materials during combustion is measured indirectly by measuring the light transmitted.

The test has faced significant criticism due to its static nature, as it does not yield reliable values that accurately reflect real fire conditions. Despite these limitations, the test continues to be widely utilized for evaluating both existing materials and the development of new ones. ISO 5659 provides significant improvements over ASTM E662 by allowing testing up to a heat flux of 50 kW/m^2, horizontal sample orientation and real-time mass loss measurement. However, the most reliable data is obtained in full-scale tests, which involve testing the material on a full scale.

Although surprising at first glance, statistical data show that smoke toxicity is not the most significant fire hazard. It has been found that there is a strong correlation between fire fatalities and the amount of CO released during a fire [31,31,32]. Since CO is always produced during a fire due to incomplete combustion, the amount of CO generated will depend on the size of the fire. Therefore, objects and materials that release a smaller amount of heat per unit of time by burning carry a smaller fire hazard, regardless of the toxicity of the compounds released by burning them.

Through the working group ISO/TC92/SC3 - "Fire threat to people and environment", ISO has defined a number of standards related to fire chemistry [33]. Among these, ISO 19702 [33] provides guidance for sampling and analyzing toxic gases and vapors in fire effluents using Fourier Transform Infrared (FTIR) spectroscopy. Additionally, ISO/TS 21397 [35] addresses FTIR analysis of fire effluents in cone calorimeter tests, while ISO 13344 [36] focuses on estimating the lethal toxic potency of fire effluents. For calculating pollutant emissions, ISO 19703 [37] is recommended including calculating species yields, equivalence ratios, and combustion efficiency in experimental fires.

4.5. Heat release rate

Heat release rate (HRR) stands out as the most crucial parameter in assessing the size of a fire and its associated hazard [32]. HRR is significantly more important in assessing fire hazard than factors such as ignitability, fire spread, and toxic effluent emissions.

The first instrument for measuring HRR was developed in the late 1960s at Ohio State University (OSU) in the USA [38]. This instrument is now standardized through the ASTM E906 Standard Test Method for Heat and Visible Smoke Release Rates for Materials and Products Using a Thermopile Method [39]. It became the first method for determining HRR to be regulated after the Federal Aviation Administration (FAA) established a clear correlation between HRR size and the time needed to rescue passengers from a burning aircraft under real-scale conditions [40]. Around the same time, Tewerson from FM Global began developing a fire propagation apparatus, a device designed for measuring HRR and fire release. Unlike OSU devices that rely on temperature measurement, this apparatus calculates HRR by measuring the concentration of CO2 in combustion products, providing a more reliable method.

Today, the most widely used instrument for determining heat release rate is the bench-scale cone calorimeter, designed by Babrauskas from NIST in the early 1980s. This device exposes a sample measuring 10 x 10 cm to a uniform incident heat flux of up to 100 kW/m^2 using a truncated cone heater. Combustion products are conveyed through a duct where oxygen content, and optionally the concentration of CO, CO2, and H2O, are precisely measured in real time. The HRR is calculated based on the oxygen depletion principle. Additionally, the device is utilized to determine the flammability characteristics of materials, mass loss over time, and smoke release. The device gained popularity after establishing a correlation between the results obtained on the cone calorimeter and full-scale tests [41]. It's considered one of the most widely used devices in fire research and fire hazard assessment.

Although small-scale testing is practical, it may not provide insight into the flammability characteristics of whole products, especially if they are highly heterogeneous or contain multiple layers. For such cases, medium and large-scale tests based on the oxygen depletion principle are utilized.

The Intermediate Scale Calorimeter (ICAL) is a device used in North America for medium-scale fire tests. The test method is standardized through ASTM E1623 Standard Test Method for Determination of Fire and Thermal Parameters of Materials, Products, and Systems Using an Intermediate Scale Calorimeter (ICAL) [42]. A flat sample measuring 1 x 1m is exposed to a radiant heater source (gas-fired radiant panel) with a range of heat fluxes up to 50 kW/m^2. This test has very good correlations with full-scale tests, but it is still not included in the regulatory framework.

On the other hand, in the EU, the Single Burning Item (SBI) test EN 13823 Reaction to fire tests for building products - Building products excluding floorings exposed to the thermal attack by a single burning item [43] is a regulatory intermediate-scale test that is used to regulate building products. In the SBI test, two samples measuring 1.5 x 1.5 m and 1.5 x 0.5 m are exposed to a 30 kW radiation source (propane gas burner). During the test, heat release rate, smoke release, flame spread, ignitability and flaming droplets are determined. FIGRA (fire growth rate) and SMOGRA (smoke growth rate) are two condensed variables that are used for regulatory and classification purposes.

However, the most reliable method to evaluate the fire performance of materials and products is through full-scale testing. ASTM and ISO organizations have developed several full-scale tests, with the room-corner test being the most widely used. ASTM E2257 Standard Test Method For Room Fire Test Of Wall And Ceiling Materials And Assemblies [44] test serves as an alternative to Steiner testing, offering various engineering quantities useful for fire calculations and material/product comparisons.

5. DESCRIPTION OF CUSTOM-MADE INSTALLATION FOR EVALUATION OF FLAMMABILITY PARAMETERS

Unlike the oxygen bomb calorimeter, which undergoes combustion with complete oxidation, small bench-scale devices such as the fire propagation apparatus, cone calorimeter, and mass loss calorimeter analyze flammability parameters as they manifest in real fires, under specific heat flux conditions and constant ventilation.

Despite the simplicity of measuring the flammability parameters of materials in fire conditions with a mass loss calorimeter, a limitation of this instrument is the lack of analysis of evolved gases and soot smoke particles. Using the mass loss calorimeter with an appropriate hood enables users to conduct thermal exposure studies under nearly identical conditions to those employed in the cone calorimeter. This setup enables the visual observation of specimen reactions and the measurement of flammability parameters. The fire model incorporated in the mass loss calorimeter complies with the specifications of the ISO 5660 Cone Calorimeter, which ensures that equivalent results are achieved compared to the cone calorimeter for various materials [45].

The primary objective of coupling the mass loss calorimeter and FTIR gas analyzer is to conduct more detailed analyses of the toxic gases emitted during specific stages of thermal decomposition and flame combustion of the samples tested in the cone calorimeter.

The parameters measured with the mass loss calorimeter are: heat release rate (HHR), time to ignition (tig), and mass loss rate (MLR), Total Heat release (THR), and Effective Heat of Combustion (EHC) of materials. While measuring the flammability parameters of materials in fire conditions with mass loss calorimeter is straightforward, a limitation of this device is its inability to analyze evolved gases.

In this regard, at the Faculty of Occupational Safety in Niš, University of Niš, Serbia, within the Fire Protection Laboratory (https://www.znrfak.ni.ac.rs/fpl/), a custom-made hood was developed for simultaneous determination of the flammability characteristics of materials of various structures and types, and fire effluents resulting from the combustion process in real-time (see Fig 1). To perform this kind of experiment, the laboratory is equipped with the following equipment:

- Bench scale device, mass loss calorimeter (Fire Testing Technology (FTT), UK)
- FTIR gas analyzer, GASMET DX4000 (Gasmet, Finland)

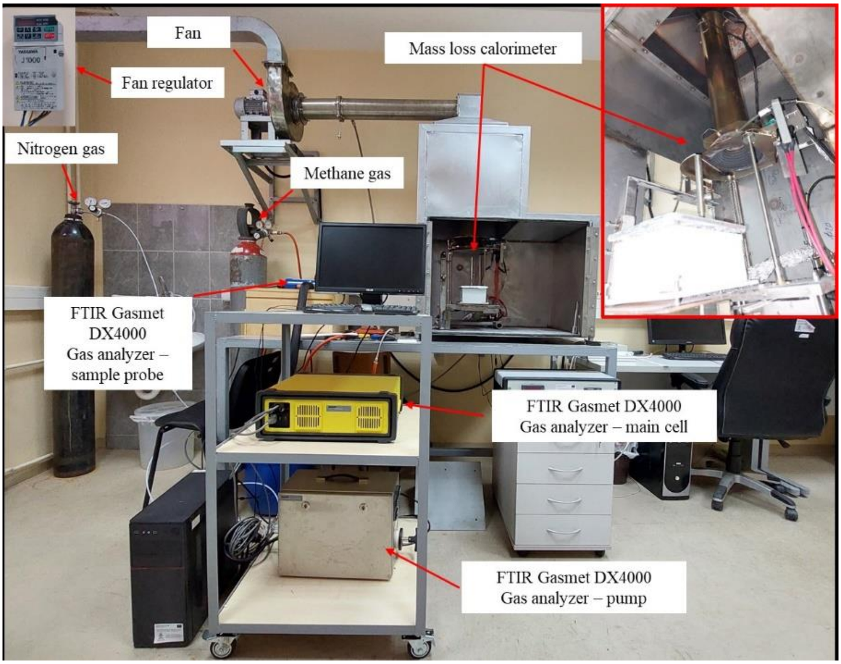

Fig. 1 Experimental installation with the adapted mass loss calorimeter [46]

5.1. Mass loss calorimeter

Heat release rate, as the single most important variable in determining the hazard from a fire, can be calculated by measuring the depletion of oxygen in the fire atmosphere. Devices for measuring oxygen concentration, particularly those of the paramagnetic type, have now reached a level of precision capable of detecting the subtle variations in oxygen levels necessary for determining heat release rates. Given that heat release apparatuses based on oxygen consumption principles tend to be quite expensive, an alternative solution may lie in devices utilizing the thermopile technique, such as those found in mass loss calorimeters.

The mass loss calorimeter features a thermopile consisting of four thermocouples positioned at the top of a chimney, directly connected to the conical heater. This chimney collects all the smoke released during the fire test emitted during the fire test, while the thermopile assesses the heat release rate.

Common characteristics that describe the utility of the mass loss calorimeter include:

- validity and accuracy;
- precision, repeatability, and reproducibility;
- ease of calibration;
- simplified specimen preparation to minimize uncertainties in starting time;
- specimen size can reach up to 100 mm by 100 mm, with variable thickness up to 50 mm;
- ease of data analysis and interpretation;
- simple and affordable enough to be useful for testing laboratories;
- short preparation and testing time;
- ruggedness of apparatus;
- ease of physical installation;
- provided ignition with electric spark (piloted ignition);
- sample mass loss measurement system.

Similar to the cone calorimeter, the mass loss calorimeter employs a conical electric heater to sustain a steady and uniform heat flux of up to 100 kW/m^2, enabling the replication of diverse fire conditions. Furthermore, the heat flux can be easily calibrated before each test.

The parameters measured with mass loss calorimeter are: heat release rate (HHR), time to ignition (tig), mass loss rate (MLR), Total Heat release (THR), and Effective Heat of Combustion (EHC) of materials.

- **Apparatus design**

The mass loss calorimeter instrument consists of the following assemblies:

1. Fire Model which consists of conical radiant heater, heater shutter assembly, spark igniter, 3 thermocouple sockets for cone heater control;
2. Control Unit;
3. Load Cell Assembly;
4. Chimney and Thermopile;
5. Calibration burner and flow meters;
6. Software interface and MLCCalc software.

Figure 2, extracted from the instruction manual for the mass loss calorimeter, illustrates the constituent elements of the device [47].

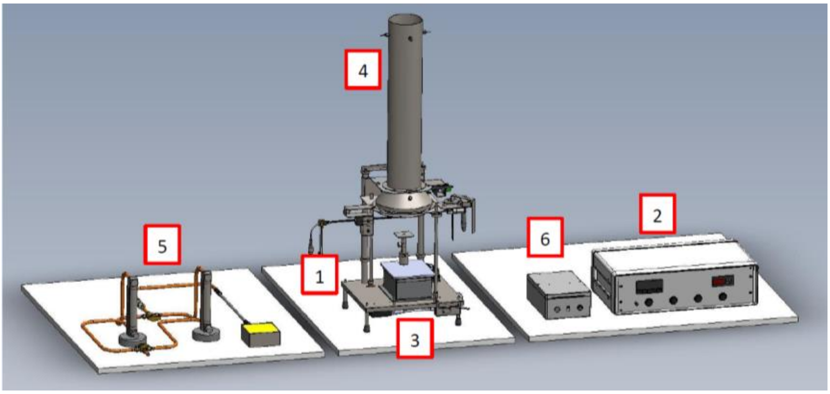

Fig. 2 Mass loss calorimeter components [47]

The basic mass loss calorimeter comprises solely a fire model and a load cell, intended for conducting mass loss and ignitability measurements primarily for screening purposes. However, the device discussed in this paper represents a modified version. To facilitate measurements of the heat release rate, an advanced calculation method was developed by the equipment producer. This method involves integrating an additional thermopile onto the fume stack, that allows for the digital deconvolution of the fume stack's thermal response into radiant and convective energy absorption components. Subsequently, the processed signal yields a composite value that exhibits a linear correlation with the measured HRR of reference materials [45].

- **Conical radiant heater**

The conical radiant heater can attain sufficiently high levels of irradiance, and maintain a uniformly distributed irradiance across the entire surface of the specimen. The room fire burning test reveals that maximum gas temperatures exceed 1000 °C, corresponding to irradiance levels reaching approximately 150 kW/m^2 on the walls and contents. In line with this, similar to the cone calorimeter, the conical heater within the mass loss calorimeter generates controlled heat fluxes ranging from 10 to 100 kW/m^2.

The design of the conical heater was borrowed from the ISO 5657 ignitability apparatus, specifically for its central hole feature [48]. This design effectively prevents the formation of a hot spot at the center of the sample and ensures that flames from the specimen do not splash onto the heater coil. The schematic view of the conical heater is shown in Figure 3.

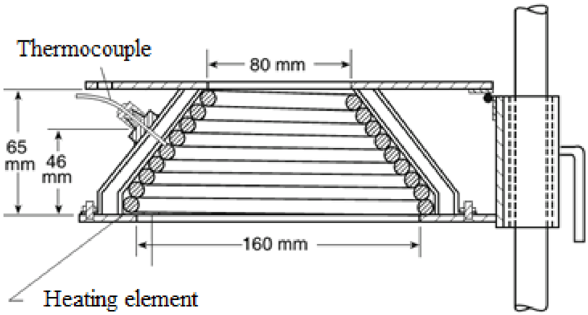

Fig. 3 Cross-section view through the heater [48]

Additionally, the conical heater is equipped with a removable radiation shield, which serves to protect the specimen from irradiance just before the commencement of the test.

- **Load cell**

A standard load cell has a maximum load capacity of 500 grams. The device has an accuracy of 0.1 g and a 90% response time of less than 3 seconds. The load cell measures the real-time change in mass loss of the specimen during the experiment. All data are recorded using the MLCCalc software, and the mass loss data changes are displayed on the control unit.

- **Specimen mounting**

Specimens are cut to 100 x 100 mm in size, and with thickness up to 50 mm. With the prepared size and shape, samples are inserted into the sample holder. The sample holder has the shape of a square pan with an opening of external dimensions measuring 106 by 106 mm at the top, and a depth of 25 mm. Equipped with a handle for easy insertion and removal, it also features a mechanism to ensure the central positioning of the specimen under the heater and proper alignment with the load cell. All test specimens must be tested with the retainer frame, which is part of the sample holder (see Fig. 4).

Adjustments for specimen thicknesses less than 50 mm can be made by adding extra refractory pad layers. A spacing of 25 mm needs to be set up between the bottom of the cone and the top of the specimen, to achieve uniform distribution of heat flux across the entire specimen surface. Before positioning the sample holder along with the sample, the sides of the testing specimen need to be protected with aluminum foil, ensuring a single piece fits the bottom and sides and is cut flush with the top.

The following procedure for specimen preparation is:

- Put the retainer frame on a flat surface facing downwards.
- Insert a foil-wrapped specimen into the retainer frame, with the exposed surface facing downwards.
- Put layers of ceramic fiber blanket on top of the sample, until 2 layers extend above the rim of the retainer frame.
- Fit the sample holder into the retainer frame.
- Position the sample holder atop the load cell, ensuring that the specimen holder is centered with respect to the cone heater.

Fig. 4 Sample holder with ceramic fiber insulating material and retainer frame

- **Spark ignitor**

The spark ignitor is placed where it is expected to reach the lower flammable limit as the specimen begins pyrolysis. However, it should not be positioned so close to the specimen surface that minor swelling of the specimen would disrupt the ignition process. In the mass loss calorimeter, the spark ignitors are ideally positioned 13 mm above the center of the specimen. Additionally, users have the option to choose between piloted ignition with a spark ignitor or simultaneous ignition without one.

- **Calibration**

The mass loss calorimeter utilizes three distinct calibrations.

First, calibration of the conical heater is necessary. This calibration aims to establish a correlation between the temperature of the heater and the heat flux it generates. It is conducted using a Schmidt-Boelter water-cooled fluxmeter, specifically calibrated for the heat flux intended for the test.

The temperatures of the conical heaters corresponding to the determined values of the heat flux on the mass loss calorimeter at the Faculty of Occupational Safety in Niš are presented in Table 1. Additionally, a comparative analysis of the temperatures specified in the [49] is provided. The measured temperature corresponding to the flow speed in the duct is 3.4 m/s, while below the cone heater, it is 0.1 ± 0.02 m/s.

Table 1 Heat flux from cone heater and temperature

Irradiance [kW/m^2]	Heater temperature at Faculty of Occupational Safety [°C]	Heater temperature in [49] [°C]
10	416	422
20	557	547
25	609	592
30	649	628
40	720	689
50	778	744
60	835	783
70	883	825

The second calibration is related to thermocouples, which are calibrated using a methane burner. This burner is designed to allow gas to flow out through the sand aggregate, ensuring an even distribution of the flame across the burner's entire surface. Initial calibration of the thermocouples is conducted for heat powers of 0.5 kW, 0.75 kW, 1 kW, 2 kW, 3 kW, 4 kW, and 5 kW. For each of these heat powers, the flow of methane with a purity of at least 99.5% is precisely regulated (refer to Table 2).

Table 2 The Flow of Methane Required for Thermocouple Calibration

Heat power [kW]	The flow of methane [l/min]
0.5	0.83
0.75	1.26
1	1.68
2	3.35
3	5.03
4	6.7
5	8.38

The objective of this calibration is to establish a correlation between the measured temperature on the thermocouples and the current heat output of the methane burner. In Figure 5, an example graph illustrating thermocouple calibration for a heat flux of 50 kW/m^2 can be observed.

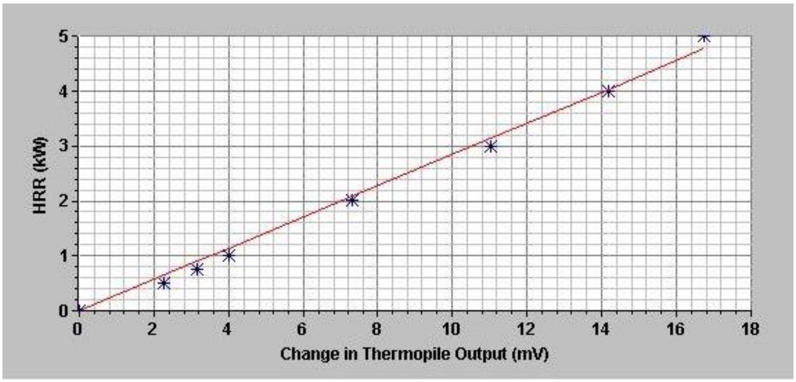

Fig. 5 Example of thermocouple calibration line for a heat flux of 50 kW/m^2

Additionally, alongside this calibration, it is essential to conduct a daily check of the heat release rate at 3 kW before commencing work with the device.

To measure the mass loss accurately, it is imperative to calibrate the scale before using the device. This calibration is conducted based on the expected mass of the sample, enhancing the precision of the measurement.

5.2. Sampling and measurement of fire effluents

A crucial aspect for evaluating the toxic hazard in fires involves understanding the variety, characteristics, and concentrations of toxic substances and smoke particles emitted in the fire effluent. Due to the frequently harsh conditions prevailing in fires, specialized methods for sampling and analysis are necessary to ensure meaningful results [50].

The GASMET DX-4000 is a gas analyzer specifically engineered for measuring the concentrations of different emission and immission gases. Its operational principle is rooted in utilizing Fourier transform infrared (FTIR) spectroscopy to determine gas concentrations. The DX-4000 analyzer is commonly employed in monitoring stack emissions, catalytic process control, and other scenarios requiring accurate monitoring of multiple gas compounds in hot and humid gases. The heating of the sampling cell ensures a condensation-free sampling process, even at high water vapor concentrations.

The GASMET DX-4000 gas analyzer includes the following components:

- GASMET DX-4000 gas analyzer;
- GASMET - Portable Sampling System;
- portable probe for gas sampling PSP4000-H;
- sampling line.

A sampling probe, designed in accordance with ISO/TS 21397, was used to sample effluents from the extraction system during the combustion process in the mass loss calorimeter [35].

The FTIR Gasmet DX4000 features a library of 16 gases that can be continuously measured: Water vapor (H_2O), Carbon dioxide (CO_2), Carbon monoxide (CO), Nitrous oxide (N_2O), Nitrogen monoxide (NO), Nitrogen dioxide (NO_2), Sulfur dioxide (SO_2), Ammonia (NH_3), Hydrogen chloride (HCl), Hydrogen fluoride (HF), Methane (CH_4), Ethane (C_2H_6), Ethylene (C_2H_4), Propane (C_3H_8), n-Hexane (C_6H_{14}) and Formaldehyde (CHOH).

According to information from the manufacturer, Gasmet's FTIR analyzers do not require any span or re-calibrations after the initial factory calibration. Performing a daily background spectrum measurement using zero gas, such as nitrogen (N_2), is sufficient to maintain measurement accuracy. The gas sampling interval can be configured with different time values, although 3 seconds is the theoretical minimum due to technical limitations of the instrument. Sampled gases were transported to an FTIR gas cell through a heated PTFE sampling line conditioned at 180 °C.

As the mass loss calorimeter and gas analyzer operate independently, it's essential to synchronize the time delay between these instruments. Suitable adjustments can be made before experiments, once all data are collected.

6. CONCLUSION

This study highlights the importance of rigorous fire testing for building materials to enhance safety and ensure compliance with local codes. By utilizing standardized methods and advanced equipment, reliable data on material flammability and fire effluent characteristics can be obtained.

Numerous studies in the literature focus on determining the flammability characteristics of materials with various structures and purposes using small bench-scale devices, such as Cone Calorimeters and Fire Propagation Apparatus. These instruments are considered state-of-the-art in fire engineering. However, as an alternative to these devices, the less expensive Mass Loss Calorimeter can be considered. This device employs the same fire model as the Cone Calorimeter but includes an additional stainless steel chimney equipped with a thermopile for measuring heat release rate. Hence, it represents a suitable alternative to the Cone Calorimeter for determining the flammability characteristics of materials.

In addition, this paper details a custom-made installation at the Fire Protection Laboratory of the Faculty of Occupational Safety, University of Niš, designed to assess the flammability parameters of various materials. This advanced setup, which includes a Mass Loss Calorimeter and an FTIR gas analyzer, enables thorough and simultaneous real-time measurement of flammability characteristics and fire effluent analysis.

Acknowledgement: *This research was sponsored by the NATO Science for Peace and Security Programme under grant SPS MYP G6006 "Acoustic Multi-Functional Composites for Environmental Risks and Health Hazards Reduction", ERASMUS+ Jean Monnet Module "Workplace and Process Safety in Next Generation Europe - Teaching for Learning" and by the Ministry of Science, Technological Development and Innovation of the Republic of Serbia under the contract no. 451-03-66/2024-03/200148.*

REFERENCES

1. Home - SFPE, https://www.sfpe.org/home
2. NFPA | The National Fire Protection Association, https://www.nfpa.org/en
3. ASTM International - Standards Worldwide, https://www.astm.org/
4. ISO - International Organization for Standardization, ISO https://www.iso.org/home.html
5. European Standards, CEN-CENELEC https://www.cencenelec.eu/european-standardization/european-standards/
6. UL Research Institutes | Discoveries in Safety, UL Research Institutes, https://ul.org/
7. ASTM E119-20, Standard Test Methods for Fire Tests of Building Construction and Materials
8. H. Stacy, D. Priest, Fire Resistance Testing of Fire Rated Gypsum Wallboard—The Last 20 Years, in: Centennial Symposium on Advances in Gypsum Technologies and Building Systems, ASTM International, 2015: pp. 1–9. https://asmedigitalcollection.asme.org/astm-ebooks/book/chapter-pdf/7215328/10_1520_stp158820150016.pdf
9. A. Ariyanayagam, M. Mahendran, Fire safety of buildings based on realistic fire time-temperature curves, in: Proceedings of the 19th International CIB World Building Congress, Brisbane 2013: Construction and Society, Queensland University of Technology, 2013: pp. 1–13. https://eprints.qut.edu.au/61929
10. M.J. Hurley, D. Gottuk, J.R. Hall, K. Harada, E. Kuligowski, M. Puchovsky, J. Torero, J.M. Watts, C. Wieczorek, eds., SFPE Handbook of Fire Protection Engineering, Springer New York, New York, NY, 2016. https://doi.org/10.1007/978-1-4939-2565-0.
11. V. Babrauskas, Ignition Handbook: Principles and Applications to Fire Safety Engineering, Fire Investigation, Risk Management and Forensic Science, Fire Science Pub, Issaquah, Wash, 2003.
12. ASTM D1929-20, Standard Test Method for Determining Ignition Temperature of Plastics.
13. ISO 871:2022, Plastics — Determination of ignition temperature using a hot-air furnace
14. M.M. Hirschler, Façade requirements in the 2021 edition of the US International Building Code, Fire and Materials 45 (2021) 586–597. https://doi.org/10.1002/fam.2803.
15. ISO 5660-1:2015, Reaction-to-fire tests — Heat release, smoke production and mass loss rate — Part 1: Heat release rate (cone calorimeter method) and smoke production rate (dynamic measurement)
16. ASTM E2058-19, Standard Test Methods for Measurement of Material Flammability Using a Fire Propagation Apparatus (FPA)
17. ASTM E1354-22b, Standard Test Method for Heat and Visible Smoke Release Rates for Materials and Products Using an Oxygen Consumption Calorimeter
18. ASTM E1321-18, Standard Test Method for Determining Material Ignition and Flame Spread Properties
19. ISO 5657:1997, Reaction to fire tests — Ignitability of building products using a radiant heat source
20. ASTM D2863-19, Standard Test Method for Measuring the Minimum Oxygen Concentration to Support Candle-Like Combustion of Plastics (Oxygen Index)
21. ISO 4589-2:2017, Plastics - Determination of burning behaviour by oxygen index — Part 2: Ambient-temperature test
22. C.F. Cullis, M.M. Hirschler, The combustion of organic polymers, (No Title) (1981). https://cir.nii.ac.jp/crid/1130000797750798976
23. J. G. Quintiere, The effects of angular orientation on flame spread over thin materials, Fire Safety Journal 36 (2001) 291–312. https://doi.org/10.1016/S0379-7112(00)00051-5
24. ASTM E84-23, Standard Test Method for Surface Burning Characteristics of Building Materials
25. NFPA 262, Standard Method of Test for Flame Travel and Smoke of Wires and Cables for Use in Air-Handling Spaces
26. ISO 5658-2:2006, Reaction to fire tests - Spread of flame - Part 2: Lateral spread on building and transport products in vertical configuration
27. ASTM E162-22, Standard Test Method for Surface Flammability of Materials Using a Radiant Heat Energy Source
28. J.G. Quintiere, M. Harkleroad, New concepts for measuring flame spread properties, Fire Safety Science and Engineering, ASTM STP 882 (1985) 239–267
29. ASTM E662-21ae1, Standard Test Method for Specific Optical Density of Smoke Generated by Solid Materials
30. ISO 5659-2:2017, Plastics - Smoke generation - Part 2: Determination of optical density by a single-chamber test
31. V. Babrauskas, R.H. Harris Jr, E. Braun, B.C. Levin, M. Paabo, R. Gann, Role of Bench-Scale Test Data in Assessing Real-Scale Fire Toxicity (NIST TN 1284), (1991). https://www.nist.gov/publications/role-bench-scale-test-data-assessing-real-scale-fire-toxicity-nist-tn-1284

32. V. Babrauskas, R.D. Peacock, Heat release rate: the single most important variable in fire hazard, Fire Safety Journal 18 (1992) 255–272
33. ISO/TC 92/SC 3 - Fire threat to people and environment
34. ISO 19702:2015, Guidance for sampling and analysis of toxic gases and vapours in fire effluents using Fourier Transform Infrared (FTIR) spectroscopy
35. ISO/TS 21397:2021, FTIR analysis of fire effluents in cone calorimeter tests
36. ISO 13344:2015, Estimation of the lethal toxic potency of fire effluents
37. ISO 19703:2018, Generation and analysis of toxic gases in fire - Calculation of species yields, equivalence ratios and combustion efficiency in experimental fires
38. V. Babrauskas, The Early History of the Cone Calorimeter, Fire Science and Technology 41 (2022) 21–31.
39. ASTM E906/E906M-17, Standard Test Method for Heat and Visible Smoke Release Rates for Materials and Products Using a Thermopile Method
40. C.P. Sarkos, R.G. Hill, R.M. Johnson, Implementation of heat release measurements as a regulatory requirement for commercial aircraft materials, Fire Calorimetry (1995) 173.
41. G.L. Nelson, ed., Fire and Polymers II: Materials and Tests for Hazard Prevention, American Chemical Society, Washington, DC, 1995. https://doi.org/10.1021/bk-1995-0599.
42. ASTM E1623-22, Standard Test Method for Determination of Fire and Thermal Parameters of Materials, Products, and Systems Using an Intermediate Scale Calorimeter (ICAL).
43. EN 13823:2020+A1:2022, Reaction to fire tests for building products - Building products excluding floorings exposed to the thermal attack by a single burning item
44. ASTM E2257-22, Standard Test Method for Room Fire Test of Wall and Ceiling Materials and Assemblies
45. M. Dietenberger, C. Boardman, HRR upgrade to Mass Loss Calorimeter and Modified Schlyter test for FR wood, in: Fire and Materials 2013, 13th International Conference and Exhibition, 2013: pp. 251–262.
46. M. Protić, N. Mišić, M. Raos, and L. Milošević, "Testing Fire Properties of Pmma in Mass Loss Calorimeter Coupled With Ftir Gas Analyzer," Facta Univ. Ser. Work. Living Environ. Prot., vol. 18, no. 3, pp. 177–186, 2021.
47. INSTRUCTION MANUAL MASS LOSS CALORIMETER, (2017).
48. V. Babrauskas, The Cone Calorimeter, in: SFPE Handbook of Fire Protection Engineering, pp. 952–980.
49. V. Babrauskas, Development of the Cone Calorimeter -- A Bench-Scale Heat Release Rate Apparatus Based on Oxygen Consumption, National Institute of Standards and Technology (NIST), 1982.
50. P. Fardell, E. Guillaume, Sampling and measurement of toxic fire effluent, in: Fire Toxicity, 2010: pp. 385–423. https://doi.org/10.1533/9781845698072.4.385.S. Fares et al., "Characterizing potential wildland fire fuel in live vegetation in the Mediterranean region," Ann. For. Sci., vol. 74, no. 1, 2017, doi: 10.1007/s13595-016-0599-5.

PREGLED UOBIČAJENIH METODA ZA ISPITIVANJE POŽARA

Ispitivanje materijala na dejstvo požara je ključno za procenu ponašanja građevinskih materijala u uslovima požara. Tokom ispitivanja dobija se neposredan uvid u važne promenljive poput zapaljivosti, brzine oslobađanja toplote i produkcije dima. Ovaj rad daje pregled uobičajenih metoda ispitivanja materijala na dejstvo požara, uključujući procedure za odabir testa, pripremu uzoraka, prikupljanje podataka i analizu. Metode ispitivanja definisane su u standardima koje izdaju globalno respektabilne institucije poput ISO, EN, ASTM i UL. Ovi standardi garantuju i obezbeđuju doslednost i pouzdanost propisanih metoda. Takođe, u ovom radu je dat detaljan opis instalacije u Laboratoriji za zaštitu od požara Fakulteta zaštite na radu Univerziteta u Nišu, koja se koristi za određivanje ključnih požarnih karakteristika za širok dijapazon materijala. Ova instalacija, koja se sastoji od kalorimetra za merenje toplotne snage i FTIR gasnog analizatora, može se koristiti za sveobuhvatno i istovremeno merenje parametara zapaljivosti u realnom vremenu i analizu efluenata požara.

Ključne reči: *ispitivanje požara, zapaljivost, efluenti požara, toplotna snaga, kalorimetar za merenje toplotne snage, gasni analizator.*

FACTA UNIVERSITATIS
Series: **Working and Living Environmental Protection** Vol. 21, Nº 1, 2024, pp. 37 - 48
https://doi.org/10.22190/FUWLEP240213003M

Review Paper

A LITERATURE REVIEW OF KEY FINDINGS IN FUNDAMENTAL FOREST FIRE RESEARCH

*UDC 630*43*

Nikola Mišić, Milan Protić, Miomir Raos, Ana Vukadinović

University of Niš, Faculty of Occupational Safety, Niš, Republic of Serbia

ORCID iDs:	Nikola Mišić	https://orcid.org/0000-0003-2314-4851
	Milan Protić	https://orcid.org/0000-0003-4957-7882
	Miomir Raos	https://orcid.org/0000-0001-5586-0276
	Ana Vukadinović	https://orcid.org/0000-0002-6228-1077

Abstract. *The purpose of this review is to examine key findings in the fundamental research of wildfire flammability characteristics. The review begins with a brief introduction, highlighting the growing need for more detailed research into the development of forest fires due to increasingly pronounced climate changes. This is followed by an overview of the application of devices operating on the principle of calorimetry, emphasizing additional possibilities for setting and adjusting these devices. Upon reviewing the literature, it becomes evident that the majority of research on the flammability of forest vegetation is primarily focused on the moisture content levels in fuels. For this reason, the third part of this paper is dedicated to exploring the influence of moisture content on the flammability of forest vegetation. Towards the end, an overview of the types and possibilities of igniting forest fuel is provided, with a particular emphasis on the creation of firebrands as a source of ignition for vegetative fuel.*

Key words: *forest fire, calorimetry, moisture content, ignition types.*

1. INTRODUCTION

With a warmer and drier climate projected for the future, the intensity and frequency of forest fires are expected to worsen. This escalation will pose an even greater threat to forestry, agriculture, and human well-being [1].

The term "wildfire behavior triangle" as found in the literature, explains that wildland fire behavior is influenced by three key factors: fuels, weather, and topography. Fuels can be categorized into two natural levels of organization: fuel particles and fuel beds. Fuel particles are associated with varying sizes, shapes, moisture content, and etc. While fuel beds are collections of fuel particles, and they are characterized by factors such as fuel quantity (loading), depth, compactness, and continuity. Additionally, vegetation attributes

Received February 13, 2024 / Accepted March 18, 2024
Corresponding author: Nikola Mišić
University of Niš, Faculty of Occupational Safety, Čarnojevića 10a, 18000 Niš, Serbia
E-mail: nikola.misic@znrfak.ni.ac.rs

such as fuel structure, spatial arrangement, moisture content, chemical composition, and the proportion of dead and live fuel varies during the year. Weather parameters, including precipitation, solar radiation, wind speed and direction, air temperature, and humidity, influence wildfire behavior. Topography directly influences fire behavior through slope steepness and indirectly through interactions with other environmental factors. [2].

Researchers investigating the flammability characteristics of forest vegetation have individually considered all previously mentioned factors, conducting numerous correlation analyses between flammability parameters and fuel traits to enhance understanding of the dynamics and spread of forest fires. To perform the aforementioned analyses, numerous devices were employed and developed. In [3], authors review 134 studies on tissue-level flammability, emphasizing the methods employed. The most common methods identified include the epiradiator chamber, muffle furnaces, wind tunnels, and direct flame approaches.

In [4], the authors underscore the significance of comprehending litter flammability in predicting fire behavior and understanding ecological impacts in fire-prone ecosystems. Additionally, they evaluate the needs and challenges of scaling up laboratory findings to field observations of fire behavior.

The purpose of this work is to review key findings from scientific literature, emphasizing properties most frequently associated with exploring the flammability of forest vegetation.

2. Characterizing Forest Fuel Flammability through Calorimetric Analysis

The heat of combustion represents the energy released during the complete combustion of a unit mass of fuel in a pure oxygen atmosphere. In theory, the heat of combustion can be calculated by understanding the energies of reactants and products, as derived from the chemical reaction. However, due to the imperfect stoichiometric conditions during combustion in wildland fires, predicting the exact formation of combustion products becomes challenging. Therefore, a more precise and reliable approach is to measure the heat of combustion, rather than relying solely on theoretical calculations [2]. The standardized method for measuring the heat of combustion is defined by ASTM D 5865 (Test method for gross calorific value of coal and coke), which employs the oxygen bomb calorimeter.

In [5], the authors explore the relationship between flammability characteristics and species within the same genus. The researchers utilized an oxygen calorimeter to determine the energy content of plant samples based on their dry weight. This instrument measures the combustible quantity of the sample and calculates the energy released during combustion. In [6], the authors suggest that assessing flammability in an oxygen bomb calorimeter may have limitations in capturing certain aspects, especially those associated with physical processes and physiological changes in plant parts. Results obtained from an oxygen bomb calorimeter might not fully capture the significance of gas diffusion through the fuel during a rapid flaming phase, a critical factor in determining flammability.

Unlike oxygen bomb calorimeter tests where fuels are fully consumed, wildland fuels are never completely burned in fires. This discrepancy can lead to measurements indicating higher heat of combustion than what occurs in reality during wildland fires [7]. In their study, Della Rocca et al. (2015) employed various devices for a comprehensive characterization of flammability, considering different aspects such as ignitability, sustainability, combustibility, and heat release rate. The oxygen bomb calorimeter was utilized to measure the gross heat of combustion, offering additional insights into the flammability of the samples. The heat content of the analyzed samples was consistently higher in the oxygen bomb tests compared to the mass loss calorimeter tests [8], aligning with the statements in [7]. Additionally, the results in [9] show that the effective heat of combustion is between 18% and 44% lower than the gross heat of combustion.

Unlike results obtained from a bomb calorimeter, more realistic values can be derived from various standardized testing techniques, particularly those based on the principles of calorimetry [10]. Devices like the cone calorimeter (CC), fire propagation apparatus (FPA), and mass loss calorimeter (MLC) enable the measurement of heat of combustion for incomplete combustion, considering char formation.

In addition to measuring the temperature and geometry of flames, a common goal in fire science is to quantify the size of a fire by assessing the heat release rate (HRR) [11]. The calculation of HRR during combustion depends on the employed devices. It can be determined by measuring combustion products such as CO and CO2 in an exhaust duct, a method related to the FPA. Alternatively, oxygen sensors can be used to measure the amount of oxygen consumed during combustion to determine the HRR, as is the case with the CC. Regarding the MLC, the HRR value can be determined by measuring the temperature of the products formed during combustion.

The results obtained from these devices can be utilized to describe the components of the flammability of forest vegetation, as stated in [12], [13]:

- Ignitability - the ignitability of the sample is determined by recording the time for sustained ignition;
- Sustainability - the sustainability of a fire depends on the ignition characteristics of the fuel and the total heat released during the combustion of the fuel;
- Combustibility – the combustibility reflects the speed at which a fire burns and can be expressed through the heat release rate;
- Consumability – the consumability provides information on the extent to which the fuel is consumed, measured through the residual mass fraction.

For small bench-scale devices based on the calorimetry principle, the recommended sample size is 10 x 10 cm to ensure uniform incident radiant heat flux onto the specimen surface [14]. These devices are equipped with load cells that can be used to measure the mass loss rate while the samples are burning. Moreover, the FPA possesses the capability to control the airflow through the sample. Depending on the volume of the sample holder, the fuel mass may vary. Consequently, different bulk densities can be produced, influencing the burning behavior. In study [15], the FPA was used to examine the effects of transport in the fuel beds by controlling the airflow, and analyze variables such as time to ignition, duration of flaming combustion, and peak heat release rate for two species of pine needles. For the first time in calorimetric studies, the authors introduce a custom-made sample holder. These holders are employed to systematically study the porous properties of fuel beds, enhancing understanding of the effects of airflow transport within the fuel beds, and assessing the flammability characteristics of forest fuels [15]. These approaches represent new trends in investigating the flammability characteristics of forest vegetation using calorimetric devices.

In their study, Bartoli et al. (2011) explore the role of surface-to-volume ratio, fuel packing ratios, and chemical properties in the burning dynamics of pine needles using the FPA. They observe that increasing the flow magnitude can result in a delay in burning and induce a cooling effect on combustion. [16]. Besides surface-to-volume ratio, factors such as fuel packing ratios, chemical properties, flow conditions, fuel species particularities, and their interactions contribute to the governing of burning dynamics. The sample holder design allowed for the examination of internal porous fuel bed characteristics and their interaction with flow conditions and fuel species properties, contributing to a better understanding of the factors governing burning dynamics.

Santoni et al. (2015) conducted a study on the scale effects and experimental setups concerning heat release rate, smoke production rate, and species yields during the burning of a vegetation bed. They investigated the burning of a vegetation bed using both the cone calorimeter and the furniture calorimeter on small and large scales. This work represents an initial effort to highlight the scale effect and the influence of combustion setups on flammability parameters. The study concludes that results obtained at the bench scale cannot be directly extrapolated to the full scale, even for litter with a high packing ratio [17].

Unlike CC and FPA devices, the mass loss calorimeter (MLC) device offers an alternative approach to measuring heat release. From the obtained results in [18], the authors demonstrated that the MLC device exhibits good repeatability and provides a reasonable approximation to the heat release rate (HRR) values obtained with a cone calorimeter. The MLC device allows for the evaluation of forest fuel flammability and combustion properties.

The study in [6] focuses on evaluating the flammability of gorse (*Ulex europaeus L.*) plant parts and whole plants after prescribed burning. The aim is to understand the changes in flammability over time, utilizing both full-scale methods such as an outdoor wind tunnel and epiradiator with a flaming firebrand as the point ignition source, and bench-scale devices like a mass loss calorimeter with a porous holder. The results indicate that ignitability is highly dependent on the type of ignition source, while combustibility is more influenced by the dead fraction of the plant.

Melnik et al. (2022) introduced a novel method that assesses flammability by quantifying the fuel's net contribution to the energy release of the incoming flame, employing in-flame flammability testing. This method utilizes oxygen consumption calorimetry to gauge the energy release contribution of live fuel to the methane flame in comparison to the methane flame alone. The energy release contribution of live fuel is determined as the difference in energy release between the methane flame interacting with live fuel and the methane flame in isolation. In-flame testing results in fuel ignition and consumption similar to those observed in wildfires, rendering it a realistic approach for measuring flammability [19].

To determine the flaming ignition time of samples, one criterion is the ignition temperature. However, the ignition temperature can vary due to conditions and testing methods applied. For instance, the ignition temperature for wood can range between 296 and 497 °C [20]. In this context, it is more practical to conduct flammability tests with fixed parameters, such as heat flux.

An important feature of devices based on the calorimetry principle is their ability to establish burning conditions with a fixed heat flux value. Heat flux is defined as the amount of energy transferred to a sample per unit area and typically has units of kW/m^2 in fire applications. The heat flux from the fire to the surface includes contributions from both radiation and convection [21]. In calorimetry principle devices, heat flux is measured by water-cooled gauges, commonly including Schmidt-Boelter type. The Schmidt-Boelter gauge, utilizing a thermopile-style design, measures temperature at various locations across a substrate. Due to its ability to measure heat flux accurately in environments with both radiation and convection, it is considered more accurate device for assessing heat transfer in fire environments [21].

Table 1 summarizes the most cited authors whose experiments involve the application of bench-scale devices for analyzing the flammability of forest vegetation. The table is formed based on the following criteria: apparatus used, applied heat flux, analyzed samples, and type of sample holder.

Table 1 A review of research on the flammability characteristics of forest vegetation using bench-scale devices based on the calorimetry principle

Authors	Apparatus	Heat flux [kw/m^2]	Samples	Sample holder type
Schemel et al. (2008) [15]	Fire propagation apparatus	-	Pine needles	Circular porous (0%, 26% and 63% opening)
Bartoli et al. (2011) [16]	Fire propagation apparatus	25	Pine needles	Circular porous (0%, 26% and 63% opening)
Simeoni et al. (2012) [22]	Fire propagation apparatus	8.5 - 60	Pine needles	Circular porous (26% and 63% opening)
Lamorlette et al. (2015) [23]	Fire propagation apparatus	8 - 55	Pine needles	Basket (0% opening)
Jervis et al. (2016) [24]	Fire propagation apparatus	50	Pine needles	Circular porous (63% opening)
Weise et al. (2005) [25]	Cone calorimeter Intermediate-scale calorimeter	25 -	Ornamental vegetation (foliage and branches)	Square 100x100 mm -
Blank et al. (2006) [26]	Cone calorimeter	30	Grass - cheatgrass	Square 100x100 mm
Dibble et al. (2007) [27]	Cone calorimeter	25	Invasive and non-invasive species (different growth forms)	Square 100x100 mm
Santoni et al. (2015) [17]	Cone calorimeter Furniture calorimeter	-	Pine needles	Circular porous (99% opening)
Fateh et al. (2016) [28]	Cone calorimeter	10 - 50	Pine needles	Basket (0% opening)
Madrigal et al. (2009) [18]	Mass loss calorimeter	50	Pine needles Twigs and leaves Moss	Square porous (63% opening)
Madrigal et al. (2011) [9]	Mass loss calorimeter	50	26 forest fuels (stalks, leaves, twigs, needles)	Square porous (63% opening)
Fernandez-Gomez et al. (2011) [29]	Mass loss calorimeter	50	Pine needles Twigs with leaves of *Cistus laurifolius L.*	Square porous (63% opening)
Madrigal et al. (2012) [6]	Mass loss calorimeter Oxygen bomb calorimeter Full scale (outdoor wind tunnel)	50 - -	Shrubs	Square porous (63% opening) - -
Madrigal et al. (2012) [30]	Mass loss calorimeter	25 and 50 50	Pine needles Leaves and twigs of shrub species	Square porous (63% opening)
Possell et al. (2012) [31]	Mass loss calorimeter	25	Eucalyptus foliage	Square porous (27% opening)

During wildland fires, radiant heat fluxes typically range from 50 to 250 kW/m^2 [32]. Based on literature review presented in Table 1, most research are conducted for heat flux up to 50 kW/m^2.

The critical heat flux necessary for ignition is the heating rate that balances the cooling rate and consequently raises the temperature precisely to the moment at which ignition will occur. This value depends on heat transfer, weather conditions, and fuel properties, including its ignition temperature, porosity, compactness, and moisture content. Sabi et al. (2021) propose a new method for estimating the critical heat flux for the ignition of porous fuels. They compare the experimental data obtained from the cone calorimeter with analytical and numerical results from a model that incorporates energy and temperature ignition criteria. The experimental setup aimed to investigate the probabilistic ignition behavior observed in the critical region, which is ignored by deterministic methods used in literature for estimating the critical heat flux for ignition [33].

3. Fuel Moisture as Main Driver of Forest Flammability

The moisture content (MC) stands out as the crucial fuel factor influencing the behavior of wildfires. Moisture content is traditionally reported in the literature on a dry weight basis, expressed as a percentage of oven-dry weight. This can be calculated using the following equation:

$$MC\% = \frac{\text{fresh weight - dry weight}}{\text{dry weight}} \times 100\% \quad (1)$$

Moisture content influences nearly all fire processes, like ignition, combustion, and smoldering. High level of moisture content can slow the rate of burning and fuel consumption. Upon exposure to heat, the water is the first to evaporate, slowing down the ignition and combustion process. If the ignition occurs, with a higher level of moisture content, it can result in less flaming combustion but increased smoldering, and decreased fuel consumption [34].

The classical combustion model assumes that all moisture will initially evaporate from the sample at a temperature near the boiling point of water. However, Picket et al. (2010) revealed that substantial amounts of moisture persisted in the individual samples even after ignition [35].

Most flammability experiments on forest vegetation involve dead ground fuels with very low moisture content. The primary hypothesis in this line of research is that wildfires in many ecosystems are dominated by ground fuels with moisture contents less than 5% on an oven-dry weight basis.

The oscillation of moisture content in dead fuels can be best understood by considering the concept of equilibrium moisture content. Equilibrium moisture content refers to the period when fuel particles neither gain moisture from the air and environment nor lose moisture. Fuel particles reach equilibrium moisture content when the water vapor pressure within the particle matches the vapor pressure of the air in contact with its surface, preventing any moisture exchange between the air and the wood fuel. However, this equilibrium state is rarely achieved in nature because air temperature, humidity, and solar radiation continually fluctuate throughout the day and night [2].

Research on the combustion characteristics of live fuels is limited, due to the assumption that live fuels behave like wet dead fuels. Jervis and Rein (2016) discovered that live *Pinus halepensis* needles ignite approximately four times slower and burn with lower power and heat of combustion compared to dead needles. Oven drying of live samples results in significant variations in fire behavior, indicating that drying conditions and changes in plant chemistry are crucial factors [24].

On the other hand, some researchers focus on the differences in the burning behavior of live and dead leaves. In the article [36], the authors conducted measurements to analyze flame patterns and retained moisture in live and dead leaves. The live groups had approximately 34% and 63% moisture content, while the dead groups were dried to about 4% moisture content, with one group rehydrated back up to 26% moisture content. The results indicate that the temperatures, slopes, and durations of rehydrated and dehydrated leaves differed. This suggests that moisture held in live leaves has a stronger effect on leaf temperature than moisture held in dead leaves.

McAllister et al. (2012) investigated the thermal behavior of both live and dry needles, collecting samples throughout the growing season to analyze variations in moisture content and chemical composition. The study compares the ignition behavior of live fuels, specifically lodgepole pine and Douglas-fir, through piloted ignition experiments. It evaluates various correlations from the literature for ignition time concerning moisture content and finds that these correlations do not accurately capture the trends with live fuels [32].

Jolly et al. (2012) explore the fuel characteristics and ignition potential of *Pinus contorta* (lodgepole pine) foliage in the initial phases of a mountain pine beetle attack. The study measures the fuel moisture content, chemical composition, and time to ignition of needles across various attack categories. Understanding the time to ignition of needles assists in determining the minimum surface fire intensity needed for a fire to escalate into the crowns of trees. Reduced moisture content and alterations in foliar chemistry amplify the flammability of mountain pine beetle-attacked trees, indicating an increased likelihood of crown fires in affected stands as long as foliage is retained on the trees [37].

The study in [38] explores the influence of moisture on the combustion of pyrolysis gases in wildland fires. The moisture released from vegetation during pyrolysis impacts the characteristics of the gaseous flame and the temperature distribution within both opposed diffusion and premixed laminar flames. The findings indicate that the presence of water vapor derived from vegetation moisture influences the distribution of key gas components, including O_2 and H, in both non-premixed and premixed flames.

Pinto et al. (2020) present a novel approach to influence the moisture content on the radiant heat flux emitted by a laminar non-premixed flame. With increasing moisture content, both flame height and mass loss evolution decrease, resulting in a decrease in the radiant fraction emitted. Interestingly, the research indicated that the fuel moisture content does not alter the shape of the flame, which is modeled as a cone. Both flame height and radius diminish as fuel moisture content increases. Notably, the variable with the most significant impact on the flame's radiative behavior over time is the mass loss rate [39].

Some authors have played a key role in driving the ongoing development of new approaches to determine the flammability parameters of wildland fuels, particularly those related to moisture content. The study in [30] introduces a novel bench-scale methodology that integrates the use of a mass loss calorimeter and a moisture analyzer to estimate flammability parameters and assess fuel moisture content. This approach ensures fixed conditions for laboratory tests. The proposed method is directly applicable to forest fuels in devices with the same configuration, such as the cone calorimeter and the fire propagation apparatus.

Precise assessment of flammability is essential to enhance understanding of the risk of vegetation fires. Research in [40] offers insights into the flammability characteristics of tree species, helping to identify suitable species for fuel brakes in forest fire prevention based on varying moisture content.

In addition to moisture content, the authors in [41] underscore the importance of employing appropriate testing methods, sample preparation, and considering factors such as sample size and moisture content when investigating the flammability of wildland fuels using bench-scale devices. Their study reveals significant influences of fuel bed diameter and moisture content on the ignition and burning behavior of Eucalyptus leaves. Additionally, the increase in emission factors for volatile organic compounds (VOCs) with higher fuel moisture content underscores the importance of considering moisture levels when assessing the impact of fire on air quality [31].

Regarding the flammability of live forest fuels, the study [32] suggests that moisture content alone is not sufficient to predict the ignition time of live fuels, as there is another mechanism controlling ignition time. The thermal properties of live foliage, such as density, thermal conductivity, and specific heat, are largely unknown and may influence the ignition time of live fuels. Similarly, the results of the study in [24], show that there are fundamental differences in the physics and chemistry of the flames of live, aged, and dead needles, and that moisture content alone cannot account for the variations in burning behavior.

4. Influence of Ignition Types on Burning of Forest Fuels

Combustion is a chemical reaction involving fuel and oxidizer, leading to the rapid release of energy in the form of heat and light [42]. This process subsequently results in the production of various chemical products. Upon exposure to thermal radiation, the surface temperature of the samples increases, leading to the production of pyrolysis gases. As the pyrolysis temperature is reached and continues to rise, fuel gases may become visible, transforming into more reactive gases in larger quantities. At this stage, pyrolysis gases begin to mix with the surrounding air, and as the temperature rises further, the lower flammability limit is reached. At this point, any external spark can ignite the formed gaseous mixture [2]. An important feature of calorimetric devices is the capability to use piloted ignition, such as an electric spark. This ignition method accelerates the local reaction and heat release rate, which then continues as self-sustaining combustion of the sample. In the references listed in Table 1, primarily involving calorimetric devices, piloted ignition in the form of an electric spark was employed.

McAllister et al. (2012) investigated the piloted ignition behavior of live fuels, considering their moisture content and chemical composition throughout the growing season. The study aimed to test the applicability of existing correlations for predicting live fuel ignition based on moisture content alone [32]. Mindykowski et al. (2011) determined the critical (minimum) heat flux for the piloted ignition of wildland fuel litters (needles and leaves) by employing the Fire Propagation Apparatus (FPA). The assumption is made that ignition occurs precisely when the average temperature within the penetration depth of radiation attains a critical value [43].

Another type of ignition is self (auto)-ignition, also known as spontaneous ignition, which depends on the balance between the heat produced and the heat given to the environment. Spontaneous ignition requires a higher gas phase ignition temperature than that required for piloted ignition [2]. Tihay-Felicelli et al. (2016) performed autoignition experiments in a cone calorimeter to investigate the effect of the diameter of dead twigs on flammability parameters such as time to ignition, surface temperature and mass loss [44].

One characteristic of the spread of forest fires in urban environments is the generation of combustible fragments from burned forest biomass, that once lofted, become firebrands. Upon depositing on vegetative fuels, firebrands with sufficient energy initiate the ignition processes. They can initiate either a smoldering combustion reaction or a flaming combustion reaction. Understanding the transport and ignition of firebrands presents a significant challenge, particularly in dealing with the actual showers of firebrands generated in wildland and Wildland-Urban Interface (WUI) fires [45].

To investigate structural vulnerabilities resulting from firebrand showers, Manzello et al. (2011) conducted a series of full-scale tests to quantify firebrand penetration through building vents. The aim was to determine whether firebrands have the potential to accumulate in front of structures and ignite materials placed nearby [46]. The research presented in the [47] examines the spontaneous ignition time of idealized firebrands under controlled radiative heat flux, including variations in the physical characteristics of the fuel litter.

Reszka et al. (2020) presented additional research exploring the types of ignition. The authors analyze continuous and discontinuous types of ignition. Continuous ignition is characterized by a heat flux from a radiative and/or convective source, while discontinuous ignition involves the transfer of mass and energy due to the transport and landing of hot particles, such as embers or firebrands. This paper addresses the need to experimentally and theoretically determine whether firebrands are capable of igniting live vegetation. This underscores the importance of understanding the role of firebrands in fire propagation and the ignition of live vegetation [48].

5. Conclusion

Based on the literature search discussed in this paper, the overarching conclusion is that the scientific community has not established a standard methodology for determining the flammability characteristics of forest vegetation. Among the devices whose working principles are determined by international standard organizations, those operating on the principles of calorimetry (fire propagation apparatus, cone calorimeter, mass loss calorimeter) stand out. Among researchers worldwide addressing this issue, the literature reveals numerous commercial devices for determining the flammability characteristics of forest vegetation, as well as devices created as personal innovations by researchers. Additionally, the data obtained from these devices can serve as input information in various systems, providing decision support for managing forest fires.

A limiting factor in comprehending the spread and development of wildfires, attributed to high expenses, is the implementation of large-scale experiments. To overcome this limitation, various numerical models based on the principles of numerical fluid dynamics have been developed to attain the desired results. Extensive statistical analyses were employed to process the data and draw general conclusions about the dynamics of forest fire development.

The references analyzed in this literature review reveal that research on the flammability of forest vegetation predominantly concentrates on surface dead fuels, with limited attention given to canopy fuels. In particular, the lack of canopy fuel analysis on devices that work on the principle of calorimetry was noticed. In the application of these devices, a widely accepted approach involves preparing samples on custom-made sample holders, intending to analyze their position to correspond with the field position. Given the existence of various sample holder configurations, future research should focus on determining reliability coefficients for the application of different sample holders.

Predicting the ignition time of a forest fuel based solely on moisture content is not sufficient, as numerous mechanisms control the ignition time of a fuel. Characterizing the flammability of forest fuel solely based on flammability parameters (such as heat released, flame geometry, temperature, etc.) obtained by numerous experimental methods is not possible without considering the physical and chemical characteristics of the fuel.

Acknowledgement: *This work was financially supported by the Ministry of Education, Science and Technological Development of the Republic of Serbia, Grant No. 451-03-66/2024-03/ 200148.*

REFERENCES

1. S. Fares et al., “Characterizing potential wildland fire fuel in live vegetation in the Mediterranean region,” Ann. For. Sci., vol. 74, no. 1, 2017, doi: 10.1007/s13595-016-0599-5.
2. M. Finney, S. McAllister, T. Grumstrup, and J. Forthofer, Wildland Fire Behaviour:Dynamics, Principles and Processes. 2021.
3. J. V. Celebrezze, I. Boving, and M. A. Moritz, “Tissue-Level Flammability Testing: A Review of Existing Methods and a Comparison of a Novel Hot Plate Design to an Epiradiator Design,” Fire, vol. 6, no. 4, 2023, doi: 10.3390/fire6040149.
4. J. Morgan Varner, J. M. Kane, J. K. Kreye, and E. Engber, “The flammability of forest and woodland litter: A synthesis,” Curr. For. Reports, vol. 1, no. 2, pp. 91–99, 2015, doi: 10.1007/s40725-015-0012-x.
5. A. L. Behm, M. L. Duryea, A. J. Long, and W. C. Zipperer, “Flammability of native understory species in pine flatwood and hardwood hammock ecosystems and implications for the wildland-urban interface,” Int. J. Wildl. Fire, vol. 13, no. 3, pp. 355–365, 2004, doi: 10.1071/WF03075.
6. J. Madrigal, E. Marino, M. Guijarro, C. Hernando, and C. Díez, “Evaluation of the flammability of gorse (Ulex europaeus L.) managed by prescribed burning,” Ann. For. Sci., vol. 69, no. 3, pp. 387–397, 2012, doi: 10.1007/s13595-011-0165-0.
7. M. A. Finney, S. S. Mcallister, T. Grumstrup, and J. M. Forthofer, “Combustion,” in Wildland Fire Behaviour: Dynamics, Principles and Processes, 2021, pp. 82–113.
8. G. Della Rocca et al., “Possible land management uses of common cypress to reduce wildfire initiation risk: A laboratory study,” J. Environ. Manage., vol. 159, pp. 68–77, 2015, doi: 10.1016/j.jenvman.2015.05.020.
9. J. Madrigal, M. Guijarro, C. Hernando, C. Díez, and E. Marino, “Effective Heat of Combustion for Flaming Combustion of Mediterranean Forest Fuels,” Fire Technol., vol. 47, no. 2, pp. 461–474, 2011, doi: 10.1007/s10694-010-0165-x.
10. R. H. White and W. C. Zipperer, “Testing and classification of individual plants for fire behaviour: Plant selection for the wildlandurban interface,” Int. J. Wildl. Fire, vol. 19, no. 2, pp. 213–227, 2010, doi: 10.1071/WF07128.
11. R. M. Hadden, “Heat Release Rate BT - Encyclopedia of Wildfires and Wildland-Urban Interface (WUI) Fires,” S. L. Manzello, Ed. Cham: Springer International Publishing, 2020, pp. 603–610.
12. H. E. Anderson, “Forest fuel ignitibility,” Fire Technol., vol. 6, no. 4, pp. 312–319, 1970, doi: 10.1007/BF02588932.
13. R. Martin, “Assessing the flammability of domestic and wildland vegetation,” 12th Conf. Fire For. Meteorol. Jekyll Island, GA, USA, Vol. pages 26-28, no. November, pp. 26–28, 1994, doi: 10.13140/RG.2.1.3999.3680.
14. M. Janssens, “Calorimetry BT - SFPE Handbook of Fire Protection Engineering,” in SFPE Handbook of Fire Protection Engineering, M. J. Hurley, D. Gottuk, J. R. Hall, K. Harada, E. Kuligowski, M. Puchovsky, J. Torero, J. M. Watts, and C. Wieczorek, Eds. New York, NY: Springer New York, 2016, pp. 905–951.
15. C. F. Schemel, A. Simeoni, H. Biteau, J. D. Rivera, and J. L. Torero, “A calorimetric study of wildland fuels,” Exp. Therm. Fluid Sci., vol. 32, no. 7, pp. 1381–1389, 2008, doi: 10.1016/j.expthermflusci.2007.11.011.
16. P. Bartoli, A. Simeoni, H. Biteau, J. L. Torero, and P. A. Santoni, “Determination of the main parameters influencing forest fuel combustion dynamics,” Fire Saf. J., vol. 46, no. 1–2, pp. 27–33, 2011, doi: 10.1016/j.firesaf.2010.05.002.

17. P. A. Santoni, E. Romagnoli, N. Chiaramonti, and T. Barboni, “Scale effects on the heat release rate, smoke production rate, and species yields for a vegetation bed,” J. Fire Sci., vol. 33, no. 4, pp. 290–319, 2015, doi: 10.1177/0734904115591176.
18. J. Madrigal, C. Hernando, M. Guijarro, C. DÃez, E. Marino, and A. J. De Castro, “Evaluation of forest fuel flammability and combustion properties with an adapted mass loss calorimeter device,” J. Fire Sci., vol. 27, no. 4, pp. 323–342, 2009, doi: 10.1177/0734904109102030.
19. O. M. Melnik et al., “New in-flame flammability testing method applied to monitor seasonal changes in live fuel,” Fire, vol. 5, no. 1, pp. 1–29, 2022, doi: 10.3390/fire5010001.
20. V. Babrauskas, “Ignition of Wood: A Review of the State of the Art,” J. Fire Prot. Eng., vol. 12, no. 3, pp. 163–189, 2002, doi: 10.1177/10423910260620482.
21. B. Y. Lattimer, “Heat Transfer from Fires,” in Encyclopedia of Wildfires and Wildland-Urban Interface (WUI) Fires, S. L. Manzello, Ed. Cham: Springer International Publishing, 2018, pp. 1–10.
22. A. Simeoni et al., “Flammability studies for wildland and wildland-urban interface fires applied to pine needles and solid polymers,” Fire Saf. J., vol. 54, pp. 203–217, 2012, doi: 10.1016/j.firesaf.2012.08.005.
23. A. Lamorlette, M. El Houssami, J. C. Thomas, A. Simeoni, and D. Morvan, “A dimensional analysis of forest fuel layer ignition model: Application to the ignition of pine needle litters,” J. Fire Sci., vol. 33, no. 4, pp. 320–335, Jul. 2015, doi: 10.1177/0734904115591177.
24. F. X. Jervis and G. Rein, “Experimental study on the burning behaviour of Pinus halepensis needles using small-scale fire calorimetry of live, aged and dead samples,” Fire and Materials, vol. 40, no. 3. pp. 385–395, 2016, doi: 10.1002/fam.2293.
25. D. R. Weise, R. H. White, F. C. Beall, and M. Etlinger, “Use of the cone calorimeter to detect seasonal differences in selected combustion characteristics of ornamental vegetation,” Int. J. Wildl. Fire, vol. 14, no. 3, pp. 321–338, 2005, doi: 10.1071/WF04035.
26. R. R. Blank, R. H. White, and L. H. Ziska, “Combustion properties of Bromus tectorum L.: Influence of ecotype and growth under four CO2 concentrations,” Int. J. Wildl. Fire, vol. 15, no. 2, pp. 227–236, 2006, doi: 10.1071/WF05055.
27. A. C. Dibble, R. H. White, and P. K. Lebow, “Combustion characteristics of north-eastern USA vegetation tested in the cone calorimeter: Invasive versus non-invasive plants,” Int. J. Wildl. Fire, vol. 16, no. 4, pp. 426–443, 2007, doi: 10.1071/WF05103.
28. T. Fateh, F. Richard, B. Batiot, T. Rogaume, J. Luche, and J. Zaida, “Characterization of the burning behavior and gaseous emissions of pine needles in a cone calorimeter - FTIR apparatus,” Fire Saf. J., vol. 82, pp. 91–100, 2016, doi: 10.1016/j.firesaf.2016.03.008.
29. I. Fernández-Gómez et al., “Characterization of forest fuels in a Mass Loss Calorimeter by short open-path FTIR spectroscopy,” J. Quant. Spectrosc. Radiat. Transf., vol. 112, no. 3, pp. 519–530, 2011, doi: 10.1016/j.jqsrt.2010.10.004.
30. J. Madrigal, C. Hernando, and M. Guijarro, “A new bench-scale methodology for evaluating the flammability of live forest fuels,” J. Fire Sci., vol. 31, no. 2, pp. 131–142, 2013, doi: 10.1177/0734904112458244.
31. M. Possell and T. L. Bell, “The influence of fuel moisture content on the combustion of Eucalyptus foliage,” Int. J. Wildl. Fire, vol. 22, no. 3, pp. 343–352, 2013, doi: 10.1071/WF12077.
32. S. McAllister, I. Grenfell, A. Hadlow, W. M. Jolly, M. Finney, and J. Cohen, “Piloted ignition of live forest fuels,” Fire Saf. J., vol. 51, pp. 133–142, 2012, doi: 10.1016/j.firesaf.2012.04.001.
33. F. Z. Sabi et al., “Ignition/non-ignition phase transition: A new critical heat flux estimation method,” Fire Saf. J., vol. 119, no. April 2020, p. 103257, 2021, doi: 10.1016/j.firesaf.2020.103257.
34. Robert E. Keane, Wildland Fuel Fundamentals and Applications. Springer, 2015.
35. B. M. Pickett, C. Isackson, R. Wunder, T. H. Fletcher, B. W. Butler, and D. R. Weise, “Experimental measurements during combustion of moist individual foliage samples,” Int. J. Wildl. Fire, vol. 19, no. 2, pp. 153–162, 2010, [Online]. Available: https://doi.org/10.1071/WF07121.
36. D. R. Prince and T. H. Fletcher, “Differences in burning behavior of live and dead leaves, Part 1: Measurements,” Combust. Sci. Technol., vol. 186, no. 12, pp. 1844–1857, 2014, doi: 10.1080/00102202.2014.923412.
37. W. M. Jolly et al., “Relationships between moisture, chemistry, and ignition of Pinus contorta needles during the early stages of mountain pine beetle attack,” For. Ecol. Manage., vol. 269, pp. 52–59, Apr. 2012, doi: 10.1016/j.foreco.2011.12.022.
38. S. C. Ferguson, A. Dahale, B. Shotorban, S. Mahalingam, and D. R. Weise, “The role of moisture on combustion of pyrolysis gases in wildland fires,” Combust. Sci. Technol., vol. 185, no. 3, pp. 435–453, 2013, doi: 10.1080/00102202.2012.726666.
39. P. Pinto et al., “Effects of wildland fuel moisture content on radiant heat flux emitted by a laminar non-premixed flame,” Appl. Therm. Eng., vol. 181, no. September, p. 115968, 2020, doi: 10.1016/j.applthermaleng.2020.115968.

40. G. Zhou, Y. Zhou, S. Yu, S. Bai, and F. Lu, “Schima superba as a fuelbreak: Litter combustibility of three tree species with five water content levels using a cone calorimeter,” Front. For. China, vol. 4, no. 2, pp. 178–184, 2009, doi: 10.1007/s11461-009-0022-6.
41. M. L. Ramadhan, S. Zarate, J. Carrascal, A. F. Osorio, and J. P. Hidalgo, “Effect of fuel bed size and moisture on the flammability of Eucalyptus saligna leaves in cone calorimeter testing,” Fire Saf. J., vol. 120, no. January, p. 103016, 2021, doi: 10.1016/j.firesaf.2020.103016.
42. N. May and M. J. Gollner, “Fire Emissions,” in Encyclopedia of Wildfires and Wildland-Urban Interface (WUI) Fires, Tokyo: Springer, 2020, p. 1210.
43. P. Mindykowski, A. Fuentes, J. L. Consalvi, and B. Porterie, “Piloted ignition of wildland fuels,” Fire Saf. J., vol. 46, no. 1–2, pp. 34–40, 2011, doi: 10.1016/j.firesaf.2010.09.003.
44. V. Tihay-Felicelli, P. A. Santoni, T. Barboni, and L. Leonelli, “Autoignition of Dead Shrub Twigs: Influence of Diameter on Ignition,” Fire Technol., vol. 52, no. 3, pp. 897–929, 2016, doi: 10.1007/s10694-015-0514-x.
45. S. L. Manzello, “Firebrand Processes in Wildland Fires and Wildland-Urban Interface (WUI) Fires BT - Encyclopedia of Wildfires and Wildland-Urban Interface (WUI) Fires,” S. L. Manzello, Ed. Cham: Springer International Publishing, 2019, pp. 1–6.
46. S. L. Manzello, S. H. Park, S. Suzuki, J. R. Shields, and Y. Hayashi, “Experimental investigation of structure vulnerabilities to firebrand showers,” Fire Saf. J., vol. 46, no. 8, pp. 568–578, 2011, doi: 10.1016/j.firesaf.2011.09.003.
47. N. Hernández, A. Fuentes, J. L. Consalvi, and J. C. Elicer-Cortés, “Spontaneous ignition of wildland fuel by idealized firebrands,” Exp. Therm. Fluid Sci., vol. 95, no. January, pp. 88–95, 2018, doi: 10.1016/ j.expthermflusci.2018.01.037.
48. P. Reszka et al., “Ignition delay times of live and dead pinus radiata needles,” Fire Saf. J., vol. 112, no. September 2019, 2020, doi: 10.1016/j.firesaf.2020.102948.
49. F. R. Scarff, B. F. Gray, and M. Westoby, “Exploring phosphate effects on leaf flammability using a physical chemistry model,” Int. J. Wildl. Fire, vol. 21, no. 8, pp. 1042–1051, 2012, doi: 10.1071/WF09065.
50. H. Fazeli, W. M. Jolly, and D. L. Blunck, “Stages and time-scales of ignition and burning of live fuels for different convective heat fluxes,” Fuel, vol. 324, no. PA, p. 124490, 2022, doi: 10.1016/j.fuel.2022.124490.
51. G. Rein, “Smouldering Combustion Phenomena in Science and Technology,” Int. Rev. Chem. Eng., vol. 1, pp. 3–18, 2009, [Online]. Available: http://www.era.lib.ed.ac.uk/handle/1842/1152.

PREGLED LITERATURE KLJUČNIH NALAZA U FUNDAMENTALNIM ISTRAŽIVANJIMA ŠUMSKIH POŽARA

Svrha ovog pregleda je da izvrši ispitivanje ključnih nalaza u fundamentalnim istraživanjima karakteristika upaljivosti šumskih požara. Pregled počinje kratkim uvodom, naglašavajući rastuću potrebu za detaljnijim istraživanjem razvoja šumskih požara usled sve izraženijih klimatskih promena. Zatim sledi pregled primene uređaja koji rade na principu kalorimetrije, sa akcentom na dodatne mogućnosti podešavanja i prilagođavanja tih uređaja. Pregledom literature postaje evidentno da je većina istraživanja o zapaljivosti šumske vegetacije prvenstveno usmerena na nivoe vlage u gorivima. Iz tog razloga, treći deo ovog rada posvećen je uticaju sadržaja vlage na upaljivost šumske vegetacije. Na kraju je dat pregled vrsta i mogućnosti paljenja šumskog goriva, sa posebnim naglaskom na stvaranje tinjajućeg žara kao izvora paljenja vegetativnog goriva.

Ključne reči: *šumski požari, kalorimetrija, sadržaj vlage, tipovi paljenja*.

FACTA UNIVERSITATIS
Series: **Working and Living Environmental Protection** Vol. 21, Nº 1, 2024, pp. 49 - 57
https://doi.org/10.22190/FUWLEP231201004C

Review Paper

NO-CONTACT DIAGNOSTICS IN THE FUNCTION OF RISK-BASED MAINTENANCE ON A WIND GENERATOR MODEL

UDC 621.311.245:620.92

Miljan D. Cvetković, Ivan M. Mijailović

University of Niš, Faculty of Occupational Safety, Niš, Serbia

ORCID iDs: Miljan D. Cvetković https://orcid.org/0000-0001-5763-7617
Ivan M. Mijailović https://orcid.org/0000-0002-4782-9591

Abstract. *When it comes to risk-based maintenance of technical systems, selecting a diagnostic procedure is the weakest link in the chain of steps that guarantee the system's availability, sustainability, and safe operation while utilizing its working characteristics.*
The model of a wind generator, which by virtue of its technological structure represents an increasingly widespread system in the geographical and topographical sense, was used to examine diagnostics based on non-contact, remote collection of pertinent information, which is essential for assessing the state of the technical system. In addition, the fact that the system is not physically accessible to the maintenance teams emphasizes the necessity of taking prompt action to rectify work in order to preserve production capacity and the security of the exploitation process.
When applied to the wind generator model, proactive maintenance based on risk allows for enhanced interconnected machine efficiency, optimal maintenance process planning, and real-time production process control. These factors contribute to the advancement and refinement of the contemporary 4K industry philosophy.
The concept of remote diagnostics in complex technological structures is of interest to the authors. The goal is to process information about the condition through the lens of risk, paying particular attention to the diagnostic method's reliability and improving prediction accuracy in the maintenance of industrial plant machinery.

Key words: *wind generator, diagnostics, maintenance.*

1. INTRODUCTION

Because wind energy is dependable, sustainable, and efficient, it is the renewable energy source with the fastest rate of growth in the world. In order to turn wind energy into electricity, both onshore and offshore wind generators are frequently utilized. Not only is wind energy a renewable energy source, but it also emits no CO_2 or SO_2 into the atmosphere.

Received December 1, 2023 / Accepted April 24, 2024
Corresponding author: Miljan Cvetković
University of Niš, Faculty of Occupational Safety, Čarnojevića 10a, 18000 Niš, Serbia
E-mail: miljan.cvetkovic@znrfak.ni.ac.rs

Fossil fuel prices have always had an impact on interest in wind energy. Fuel became less expensive after World War II. Interest in wind energy starts to wane at that point. The Organization of the Petroleum Exporting Countries imposed an embargo and fuel costs increased in the 1970s, which piqued interest. The need to increase wind generator productivity and optimize wind farm ROI grew along with this expansion.

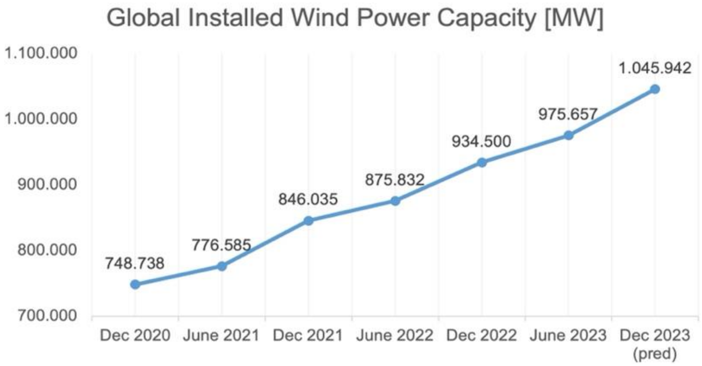

Fig. 1 Global installed capacities of wind generators [1]

Since "the net income from a wind farm is the income generated from the sale of electricity less operation and maintenance [2]," appropriate (technically feasible and economically profitable) maintenance strategies will be needed for successful future development.

According to data from the World Wind Energy Association, 1.045.942 MW of electricity could be produced using wind power by the end of 2023. In 2020, an additional 93 GW of energy was added. The generation of wind power has increased by 58% during the past five years. [1]

Wind generators require frequent monitoring and maintenance because they typically operate in harsh environments, but accessing them can be challenging due to their remote locations. Thus, one of the primary obstacles impeding the growth of wind energy is the expense of maintenance.

2. Wind Generator Components

The tower, rotor, and casing are the three main components of a wind generator. The housing that holds the brake, control device, generator, and transmission system is attached to the rotor.

The case's function is to safeguard the internal components as well. The generator and transmission system are the two main components of the wind generator.

Hub, main shaft (relatively), bearings, couplings, and gear transmission make up the transmission system Fig 2 [3]. Gray cast iron is used to make the head because of its unique shape. Forging steel is the most common method of creating the main shaft. The main shaft rotates at 40–60 revolutions per minute. Typically, bearings are made of spherical rollers. In order to minimize wear and tear and the ingress of water and dirt into the bearing, the sealing is labyrinthine. The torque is transmitted from the main shaft to the gear transmission through a friction coupling.

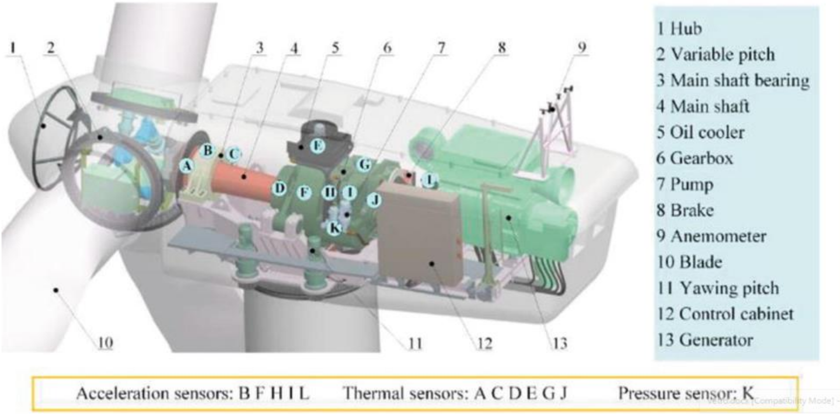

Fig. 2 The main components of wind generators [4]

Large, heavy gears are needed for the gear transmission's function of raising the main shaft's rotational speed from 40–60 rpm to 1500–1800 rpm. Transmission can be two-stage (150 MW), three-stage (300 MW), or planetary (above 450 MW) depending on the output power. A rigid coupling connects the transmission's output shaft to the generator.

3. Reliability and Maintenance of the System

The use of contemporary maintenance techniques is necessary to meet the system's current needs for high dependability in wind generators. Larger, heavier constructions are the tendency in modern wind generator development, which raises the failure rate. In actuality, offshore and onshore wind turbine systems of the same type have very different failure rates. The failure rates of wind generating systems and parts are depicted in the Fig 3 [5].

Damage to the wind generator, or to a structural component, is what we mean when we say that the production situation is unacceptable. Put differently, damage denotes a notable departure from the initial functioning state and, as such, is unacceptable to the owner. Two categories of harm stand out in this regard:

1. Functional damage to the wind generator is defined as its inability to meet all of the performance requirements listed in the relevant technical file. As such, it is typically detected by the machine operator, who is the process owner.
2. The physical state of the equipment suggests that functional damage is highly likely to occur, which presents potential damage to the wind generator. The maintenance department is usually the one to identify this problem.

Because they carry extremely high loads during the exploitation process, the bearings in wind generator subassemblies are the most vulnerable parts of the assembly. The bearings may have to support big loads at low speeds or modest loads at high speeds, depending on the subassembly's location and the operating load. Low wind speeds can result in high stresses at low speeds, which can rupture the oil film and reduce the bearing's lifespan. Typically, an automatic lubrication system is used to grease the bearings in the gear transmission. High oil purity is guaranteed by the oil filter, which is independent of the oil cooling system.

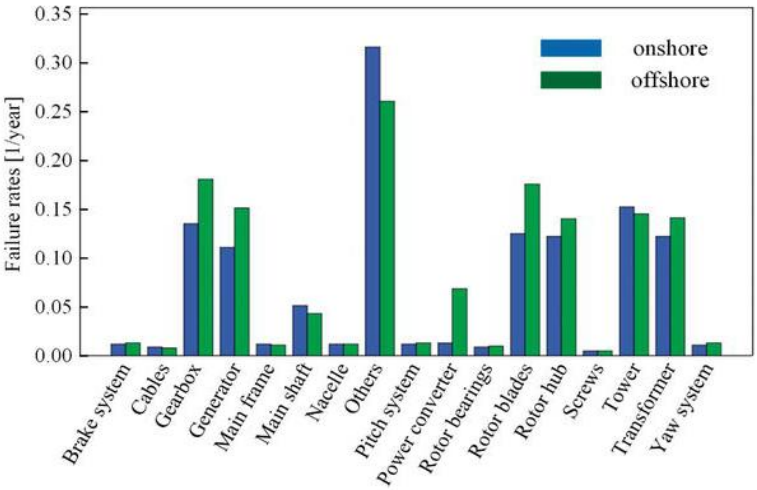

Fig. 3 Failure rates for onshore and offshore wind turbine subassemblies [5]

This is a critical solution for arid climates, where airborne dust particles can abrasively wear down toothed gears. Salt and moisture are constant risk considerations for wind turbines situated on offshore platforms. The toothed transmission can become contaminated during installation, through wear and tear, leaks through vents and seals, and negligent maintenance diagnosis. For these reasons, it's crucial to ensure that the oil is clean.

Assembling under unsuitable settings results in the introduction of contaminants during installation. These contaminants are the most hazardous to start since the oil filter cannot get rid of them right away. The main sources of impurities that develop inside the transmission are bearings, gears, and other component wear. Wear can show up as fretting, adhesion, abrasion, micro pitting, and macro pitting. Seals and vents allow dirt to enter the transmission. It is important to do maintenance, such as relubrication, to stop contaminants from penetrating. Preventive maintenance, which involves monitoring for water presence, viscosity, acidity, and oil pollution, can help lower the frequency of failures.

The rotor blades are the second most susceptible structural component of the wind generator to damage. Wind energy powers the rotor blades of wind turbines, converting it into mechanical energy. Blades have high failure rates due to their frequent alternating stress; fatigue, fracture, cracking, wear, inadequate resistance to low temperatures, and sensor failure are the main causes of failure. The rotor blades' location within the structure makes maintenance and repair challenging, and any malfunction raises the cost of extraction. Therefore, in order to create highly reliable blades, it is crucial to thoroughly and meaningfully investigate the elements that contribute to damage.

4. Maintenance Strategies

A contractual guarantee of two to five years is typically included with wind turbines, and it covers both preventive and corrective (time-based) maintenance methods. These tactics are typically used for the wind generator's ongoing maintenance after the contract time expires [6, 7]. Operating the wind turbine or any of its components until they break is known as fault-based maintenance. This tactic is typically used in situations where failing won't have an adverse effect on customer happiness, revenue, or health and safety. Critical component failures in wind turbines, however, can have detrimental effects on operations as well as public health, safety, and the environment.

The maintenance plan for wind generators is often implemented following the predetermined warranty period [7, 8], giving the owner the opportunity to make an informed decision and put their faith in the most dependable idea.

4.1. Maintenance concepts

Vibrations develop under operating conditions as a result of inertial disturbance forces produced by the machine system's complicated structure and the dynamic activity of its unbalanced elements during technological engagement. It has been demonstrated by contemporary practice that undesired vibrations can be an effective diagnostic tool for preventive engineering and machine system maintenance. All actions taken by the process owner to plan and carry out work aimed at keeping the machine in operable condition are collectively referred to as maintenance. Four well-known models serve as the foundation for the idea of guaranteeing production conditions and operational circumstances from the perspective of machine maintenance:

1. Corrective maintenance is maintenance performed after a failure;
2. Preventive or scheduled maintenance is maintenance carried out on schedule;
3. Preventive maintenance based on equipment condition monitoring is maintenance carried out on schedule;
4. Proactive maintenance.

The pros and cons of each of the aforementioned principles are considered while selecting the best model for sustaining the current equipment.

Operating the wind turbine or any of its parts until failure occurs is known as failure-based maintenance. This tactic is typically used in situations where failing won't have an adverse effect on customer happiness, revenue, or health and safety. Critical component failures in wind turbines, however, have the potential to be disastrous and have negative effects on operations, safety, and the environment.

Planned maintenance, or scheduled maintenance, is carrying out maintenance duties on a prearranged, regular basis. When the failure pattern is well-known, this tactic is frequently used to install original components without nullifying the manufacturer's warranty. The challenge lies in selecting the appropriate period because an interval that is too frequent raises operating expenses, wastes production time, and necessitates the replacement of components that are still in good condition, while unexpected failures frequently happen in the intervals that are too long [9]. As a result, money and resources are typically allocated to maintenance without much awareness of the equipment's actual condition.

The other two models, numbered 3 and 4, illustrate a contemporary idea of equipment maintenance. Preventive maintenance, also known as maintenance according to condition, suggests that machines be stopped for overhauls based on the values of characteristic parameters, or indicators (temperature, pressure, voltage state, vibrations), whose changes are regularly (sometimes) observed off lines or continuously (on line).

It is possible to identify and comprehend the underlying causes of typical machine failure modes through proactive maintenance. Preventive maintenance and root cause analysis, or RCFA, or root cause failure analysis, are combined in proactive maintenance. This makes preventative maintenance different from traditional preventive maintenance, which typically identifies the problem's effect rather than its cause, which is then further eradicated. In order to eliminate issues that have arisen in the past, a proactive strategy frequently calls for fundamental changes to the machine.

The risk-based maintenance paradigm of RBI, or Risk-Based Inspection, and proactive maintenance are extremely similar. The primary objective of the maintenance management process is to prioritize maintaining the necessary availability and dependability, or the proper probability of failure, before addressing the unfavorable effects of these occurrences. In actuality, it is far more convenient to keep an eye on both of these variables at the same time-that is, the likelihood that undesirable occurrences will occur and their effects. Combining these two elements will enable more logical and sensible judgments to be made, as risk is defined as the product of the likelihood of an undesirable event and its effects.

The requirement to evaluate the risks resulting from the Machinery Safety Directive and its associated standards just serves to validate the notion that a machine's operational life officially commences with commissioning following installation in a production facility. Products that are put on the market must adhere to the fundamental standards for health and safety protection in order to be allowed to remain in the single market (Europe). The life cycle of the machine is depicted in Fig 04 in stages. The manufacturing of components and the assembling of assemblies come first, followed by testing to ensure that labeling and the new, worldwide approach are followed. The machine is assembled upon delivery, and following functional testing, it is turned on. From that point on, the machine is the focus of the maintenance service's process owner. All phases of the life-work cycle involve interaction with the machine in the maintenance role.

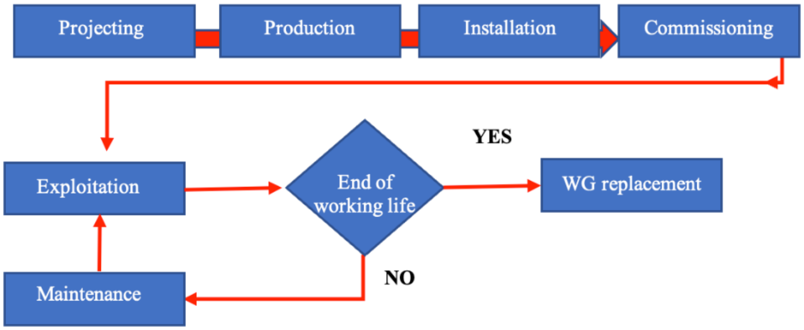

Fig. 4. Stages of the life-work cycle of a working machine-wind-generator

A machine's availability will be decreased by a failure at any point during its life cycle. All machine damage is related to commonplace, basic physical processes such as wear and tear, friction, erosion, corrosion, and shock loads. The way the operator or members of the maintenance department interact with the machine largely determines whether and how much these causal factors manifest on the machine.

It has been determined that condition-based maintenance, which comes from a proactive manner, is the most economical for maintaining important equipment [10-11]. When equipment or component performance declines as indicated by the condition monitoring process, a condition-based maintenance plan is implemented to fulfill the needs of the maintenance process [12]. Condition-based maintenance is a huge field of study that also includes wind turbines and related power facilities, but it has received little attention. While thermal imaging and acoustic emission are used to monitor the structural integrity of turbine blades [13–14], performance monitoring [15], temperature monitoring systems, and online analysis [16–17] are also used.

Table 1 Condition monitoring techniques in WT,

	Blades	Rotor	Gearbox	Generator	Bearing	Tower
Vibration	a, f	a,c	a, b, c, d, e, f, bef, eb, fg		a, c, d, f, g	d
Acoustic emission	a, f,	f	a, f,		a, b, de	
Ultrasonic techniques	a, f,					
Oil analysis			b		a	
Strain	a, c					
Shock Pulse methods					de, a, f	
Performance monitoring	a		c	a, b,	cd	

a: Statistical methods; b: Time domain analysis; c: Cepstrum analysis; d: Fast Fourier transformation (FFT); e: Amplitude demodulation; f: Wavelet transformation; g: Hidden Markov models; h: Novel techniques. [18]

One of the sophisticated diagnostic techniques that aligns with the idea of proactive maintenance of technological systems is contactless signal transmission Table 1, which provides information on physical phenomena that represent the condition of equipment in permanent exploitation mode. With good data acquisition and appropriate signal processing, faults can thus be detected while components are operational and appropriate actions can be planned in time to prevent damage or failure of components. FALCON's module for automatic non-contact diagnostics was mandated in order to put the concept of proactive maintenance for wind generators into practice. This module offers pertinent and trustworthy data on the value of diagnostic parameters required to describe the functional state of particular wind generator elements under operating conditions.

A wide range of flaws, including unbalance, misalignment, inappropriate assembly, friction, structural resonance, lubrication defects, bearing defects, gear defects, pump cavitation, and more, are identified by the module as prevalent in the industry. There is a high degree of dependability and confidence in the identification of errors, which are expressed precisely and clearly.

The synchronous acquisition shortens the time needed for data collection and equipment condition decision-making, and the outstanding measuring capabilities of the three-axis wireless sensor FALCON significantly boost production. The wireless sensors are swiftly mounted, and then automated sensor positioning is used to make measurements remotely. The reproducibility of the data is guaranteed by the monitoring of the controlled parameters, and errors resulting from the wiring and measurement point placement are totally eliminated. The module is the quickest gadget in the technical diagnostics industry since it allows real-time signal processing. By doing this, it is possible to arrange maintenance procedures and identify flaws in rotating machinery several months ahead of time, preventing unscheduled shutdowns and lost output.

5. CONCLUSION

Costs or lost benefits from production loss, component failure-related damage escalation, and repaired damaged components are incurred for corrective maintenance. Proactive maintenance in accordance with the risk-based condition will incur more costs for the process owner, but it will also lessen missed production and progressive damage.

In the context of the wind generator model, proactive maintenance based on risk refers to maximizing the productivity of networked and self-governing machinery as well as optimally scheduling maintenance procedures and controlling production in real-time, all of which facilitate the adoption of the 4K industry philosophy.

Non-contact diagnostics, or remote equipment condition monitoring, has an advantage over all other diagnostic techniques because it provides access to information about the state of a complex technical-technological system under actual operating conditions. This is made possible by advancements in sensor technology. The idea of technical advancement enables process automation, which gives the process owner remote control over all connected devices and visibility into the process, ultimately leading to a higher level of process management.

Acknowledgement: *This work was supported by the University of Niš, Faculty of Occupational Safety, Project number NIR_EK_2023*

REFERENCES

1. https://wwindea.org/wwea-half-year-report-2023-additional-momentum-for-windpower-in-2023/ [13.12.2023]
2. Learney, V. C., Sharpe, D. J. and Infield, D., Condition monitoring technique for optimization of wind farm performance, International Journal of COMADEM,1999, 2(1), 5–13.
3. Wilkinson, M. R. and Tavner, P. J. Extracting condition monitoring information from a wind turbine drive train, Proceedings of the 39th International Universities Power Engineering Conference, IEEE Cat. No. 04EX858, 2004, 1(1), 591–595
4. Caselitz, P., Giebhardt, J. and Mevenkamp., Application of condition monitoring system in wind energy converters, Proceedings of European Wind Energy Council, Dublin, 1997, 579–582
5. D. Barr, Modern Wind Turbines: A Lubrication Challenge, Machinery Lubrication, SeptemberOctober 2002, 36-45
6. Rademakers, L. W. and Verbruggen, T., Maintenance manager to control operation and maintenance of offshore wind farms, International Journal of Environment and sustainable Development, 2002, 1(4), 370–378.
7. Conover, K., Vanden Bosche, J., Rhoads, H. and Smith, B., Review of operation and maintenance experience in the DOE-EPRI wind turbine verification program, Proceedings of American Wind Energy Association's Wind Power 2000, NREL/CP-500-28620.
8. Verbruggen, T. Wind turbine operation and maintenance based on condition monitoring WT & OMEGA; final report, Technical Report, ECN-C–03-047, 2003, Energy Centre Netherlands.
9. Thorpe, C., Condition-Based Maintenance for CVN-21and DD, Empfasis, 2005, URL: http://www.empf.org/empfasis/july05/cbm705.htm [August 2022].
10. Arthur, N. and Dunn, M., Effective Condition Based Maintenance of reciprocating compressors on an offshore oil and gas installation, IMechE International Conference on Compressor and their system, 2001.
11. Saranga, H. and Knezevic, J., Reliability prediction for Condition-Based maintained systems, Reliability Engineering and System Safety, 2001, 71, 219–224.
12. Moubray, J., Reliability-Centred Maintenance II, Butter-Heinemann, 1991
13. Clayton, B. R., Dutton, A. G., Aftab, N., Bond, L., Lipman, N. H. and Irving, A. D., Development of structural condition monitoring techniques for composite wind turbine blades, Proceedings of European Community Wind Energy Conference, 1990, 10–14.
14. Philippidis, T. P. and Vassilopoulos, A. P., Life prediction methodology for GFRP laminates under spectrum loading, Renewable Energy, 2004, 35, 657–666.

15. Learney, V. C., Sharpe, D. J. and Infield, D., Condition monitoring technique for optimisation of wind farm performance, International Journal of COMADEM,1999, 2(1), 5–13
16. H. Stiesdal, The Wind Turbine Components and Operation, Bonus Energy A/S newsletter, 1999, Web site: www.bonus.dk
17. Dinmohammadi F, Shafiee M. A fuzzy-FMEA risk assessment approach for offshore wind turbines. IJPHM Special Issue on Wind Turbine PHM (Color); 2013:59
18. F. P. G. Márquez, A. M. Tobias, J. M. Pinar Pérez, M. Papaelias; Condition monitoring of wind turbines: Techniques and methods. Renewable Energy 46 (2012) 169-178
19. R. Errichello, J. Muller, Oil Cleanliness in WindTurbine Gearboxes, Machinery Lubrication, July-August 2002
20. Wouter, E.; Obdam, T.; Savenije, F. Current Developments in Wind—2009; Technical Report for Energy Research Centre of The Netherlands: Petten, The Netherlands, 2009.
21. Chou, J.-S.; Tu, W-T. Failure analysis and risk management of a collapsed large wind turbine tower. Eng. Fail. Anal. 2011, 18, 295–313.

BEZKONTAKTNA DIJAGNOSTIKA U FUNKCIJI ODRŽAVANJA ZASNOVANOG NA RIZIKU NA MODELU VETROGENERATORA

Izbor dijagnostičke procedure u funkciji održavanja tehničkih sistema zasnovanog na riziku, predstavlja najslabiju kariku u lancu procedura koje obezbeđuju bezbednu funkcionalnost, raspoloživost i održivost sistema u eksploataciji raspoloživih radnih karakteristika.

Dijagnostika zasnovana na bezkontaktnom, daljinskom prikupljanju relevantnih informacija, bitnih za ocenu stanja tehničkog sistema, razmatrana je na modelu vetro-generatora, koji po svojoj tehnološkoj strukturi predstavlja sve rasprostranjeniji sistem u geografskom i topografskom smislu. Istovremeno se radi o sistemu koji nije fizički dostupan timovima za održavanje, što dodatno ističe potrebu za blagovremeno preduzimanje mera korekcije rada u cilju održavanja proizvodnih kapaciteta i bezbednosti procesa eksploatacije.

Proaktivno održavanje zasnovano na riziku, aplicirano na modelu vetro-generatora, omogućuje povećanje efikasnosti međusobno povezanih mašina i optimalno planiranje procesa održavanja i kontrolu procesa proizvodnje u realnom vremenu, što omogućuje razvoj i unapređenje savremene filozofije industrije 4K.

Interesovanje autora je razvoj koncepta dijagnostike na distanci u složenim tehnološkim strukturama, sa ciljem da se informacije o stanju procesuiraju kroz aspekt rizika posebnim osvrtom na pouzdanost dijagnostičke metode i povećanja tačnosti predikcije u funkciji održavanja mašina industrijskih pogona.

Ključne reči: *vetrogeneratori, dijagnostika, održavanje*.

FACTA UNIVERSITATIS
Series: **Working and Living Environmental Protection** Vol. 21, Nº 1, 2024, pp. 59 - 70
https://doi.org/10.22190/FUWLEP240410005V

Original Scientific Paper

PREDICTION OF RUNOFF FROM ROOFS IN THE CENTRAL PART OF THE CITY OF NIŠ BASED ON L-MOMENT AND GIS APPROACH

UDC 628.2:[007:528.9(497.11Niš)

Petar Vranić, Lazar Z. Velimirović, Ivana Petkovski

Mathematical Institute of the Serbian Academy of Sciences and Arts, Belgrade, Serbia

ORCID iDs:	Petar Vranić	https://orcid.org/0000-0002-9671-992X
	Lazar Z. Velimirović	https://orcid.org/0000-0001-8737-1928
	Ivana Petkovski	https://orcid.org/0000-0001-7692-8436

Abstract. *Serbia, like many other countries, works to manage and protect water resources, promote sustainable practices, and improve infrastructure. However, there is no systematic advocacy for the implementation of sustainable stormwater management practices (SWM) in urban areas in Serbia. As highlighted by the Development Plan of the City of Niš For the Period 2021-2027, in the last decade the number of flash floods has increased, causing infrastructure and property damages. As a result, reducing the risk of flooding by external and internal waters is prioritized under the territorial development and environmental protection axis. As a contribution to the development of SWM practice, in this research, the prediction of the potential of runoff from roofs in the city of Niš, was performed using L-Moment and GIS. The research included 262 buildings in the city center and results indicate an increasing trend in average runoff from roofs across all sectors.*

Key words: *L-Moment, GIS, Decision Support, sustainable stormwater management practices.*

1. INTRODUCTION

Rapid urbanization and increased flash floods can be recognized as one of the main challenges urban areas are facing today [1-6]. High levels of urbanization are confronting varying hydrological phenomena [1]. Extreme weather conditions that are a consequence of long-term climate change and increased rainfalls that cause problems in managing water resources [6] are becoming more frequent and severe due to inadequate drainage systems and increased impermeable surfaces in urban areas. As cities expand, the increase in impermeable surfaces like roads, rooftops, and pavements leads to higher volumes of runoff during rainfall events. They can cause extensive infrastructure damage and significant

Received April 10, 2024 / Accepted June 20, 2024
Corresponding author: Petar Vranić
Mathematical Institute of the Serbian Academy of Sciences and Arts, Kneza Mihaila 36, 11001 Belgrade, Serbia
E-mail: petarvvv@gmail.com

economic losses, and they can also disrupt transportation networks, and carry pollutants, debris and sewage into natural water bodies, resulting in water contamination that affects the overall functioning of the city. On the other extreme, along with population growth, economic development and industrial progression, rapid urbanization is one of the main contributors to the global water scarcity problem [7,8]. Some estimations are that every fifth person globally is facing water scarcity [8]. Considering that two-thirds of the population will live in the cities by 2050 [3], water scarcity will become dominantly an urban issue.

Urgency in solving the mentioned challenges led to a number of scientific discoveries that suggest various solutions under the wider umbrella of sustainable stormwater management (SuDS, WSUD, LID, BMPs, etc.) and ecologically based urban planning approaches NbS, EbA, UGI, BGI, etc.) [9-21]. In a broader sense, urban stormwater management (SWM) involves the collection, control, and treatment of rainwater runoff in urban areas to prevent flooding, reduce water pollution, and manage water resources sustainably. In urban planning and design, stormwater management is integrated into the overall strategy for creating sustainable, resilient cities involving but not limited to: 1) infrastructure development - incorporating green infrastructure, such as green roofs, permeable pavements, rain gardens, and bioswales, helps absorb and filter runoff, reducing the load on conventional drainage systems; 2) water quality improvement - treating runoff to remove pollutants before it reaches natural water bodies, using constructed wetlands or retention ponds; and 3) flood prevention: designing urban landscapes to manage large volumes of water, minimizing the risk of floods through proper grading, stormwater basins, and overflow routes [9-21]

Almost 40 to 50% of the unused impermeable space for collecting atmospheric precipitation is discovered in roofs, making them a significant agent in SWM [22]. In addition, fast urbanization in the future will lead to growth in the number of buildings due to intensified migration to cities leaving the possibility to increase total roof surface [23]. Other than ground-surface stormwater collection, harvested rainwater is naturally the cleanest source of water that is at the same time sustainable because the rainfalls are captured before they touch the surface [24]. Latest discoveries showed that more than 70% of non-drinking water demand in non-residential buildings such as industry, retail, offices and recreational space could be replaced by the use of rainwater [25]. However, such collected atmospheric water cannot be used as freshwater drinkable water unless it is treated well [9]. Except for being useful for water scarcity problems, management of runoff from the roofs mitigates failure of the urban drainage system and minimizes flood hazard events [36]. It brings flexibility to existing conventional water supply systems and allows for secure water supply in times of climate change [24,26].

The need for sustainable water management is evident in Serbia. Consequences of climate change are recognized as well, however, there is no information on advocacy and effort for the systemic implementation of a sustainable SWM system in urban areas in Serbia. As highlighted by the Development Plan of the City of Niš For The Period 2021-2027[1], in the last decade the number of flash floods has increased, causing infrastructure and property damages, and reducing the risk of flooding by external and internal waters are recognized as a priority under the territorial development and environmental protection axis: Improving territorial development while preserving the environment. In line with above mentioned, the objective of this study is to contribute to SWM by analyzing one of its aspects, runoff from the roofs, by predicting potential runoff in the exemplary city area

[1] https://www.eupropisi.com/dokumenti/NI_036_2021_003.pdf

in the city of Niš, to inform the development of SWM strategies and urban planning and design practice. The rest of the paper is organized as follows: Section 2 describes the research methods. Section 3 presents the results. Section 4 discusses the results and provides suggestions for future research.

2. MATERIALS AND METHODS

The runoff from the roofs (in L/year) may be computed using catchment area (A, in m2), runoff coefficient (RC, non-dimensional), and local precipitation (P, in mm/year). These variables and the methods used for their estimation are explained below.

2.1. The case study

The study area of 0.2 km2 is located within a mixed-use neighbourhood of the central zone of the City of Niš. The selected area has similar spatial morphological characteristics as the wider city central zone that includes: a high level of impermeable surface area, small parcels, functional diversity, and a low percentage of green spaces. Thus, it is representative of the large part of the city and similar dense urban areas. The city of Niš is a regional hub, an administrative and socio-economic centre of the Region of South and East Serbia [27]. With a population of 249.816 inhabitants, Niš is the third-largest Serbian city [28]. According to the reports of the Republic Hydrometeorological Institute of Serbia a mean maximum temperature of 19.9^{o}C and the annual mean rainfall of 534.9 mm. The temperature of this area is +10·75 °C, varying from −1.9 to +24.6 °C from winter to summer. The coldest and hottest months are February and August, respectively. Climate change scenarios for Serbia indicate a prominent increase in temperature towards the end of the century for the whole territory. Thus, it is reasonable to expect increased pressure on water resources. Current urban planning and construction practice do not recognize the systemic application of SWM.

2.2. Data

For the purpose of this study, a spatial database is created in widely available, free and open access, and open source Geographic Information System software QGIS3.4.

2.2.1. Roof catchment area (RCA)

The catchment area contains 262 buildings in the city center zone (Figure 1). The footprint shapefile of the objects is generated from the Open Street Maps (OSM) using the QuickOSM plug-in.

Since the total roof surface covers approximately half of the surface of the study area (0.09 km2) they significantly contribute to the total urban storm-water runoff flow. Roof type and material for each roof are analyzed firstly through the desktop analysis using Google Earth Pro while afterwards they are confirmed by on-sight observation. Identified roof covers include clay tiles, metal, bitumen and gravel. The majority of roofs fall in the category of pitch roofs covered by clay tiles. The clay tiles for the local climate require a slope between 25 and 35 degrees. Therefore, for the calculation of RCA an average slope of 30 degrees is applied.

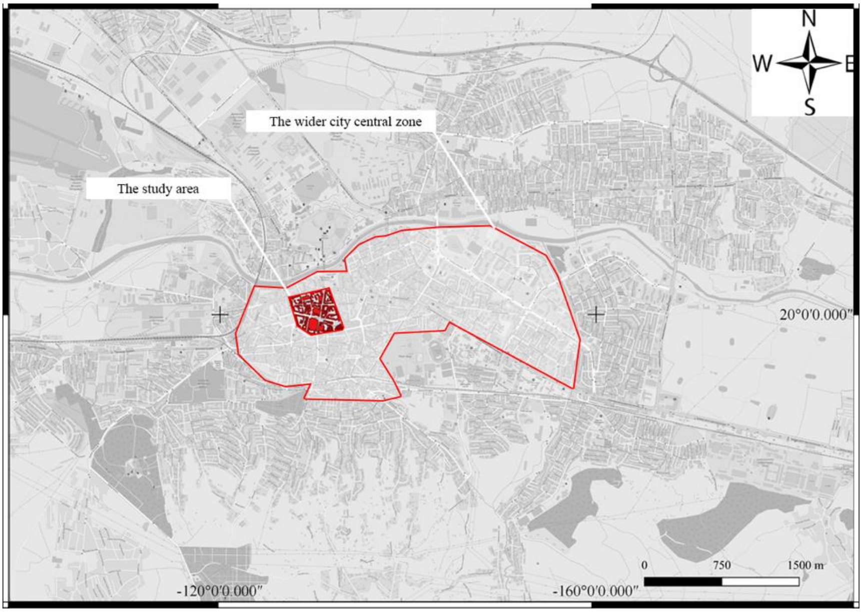

Fig. 1 Study area.

2.2.2. RC coefficient and RCA

The collection of rainwater is usually represented by a runoff coefficient (RC). The RC is a dimensionless value that estimates the portion of rainfall that becomes runoff, taking into account losses due to spillage, leakage, catchment surface wetting and evaporation. For instance, an RC of 0.75 means that 75% of the rainfall will be accumulated. So, the higher the runoff coefficient, the more rain that will be collected. Thus, the RC is useful for predicting the potential water running off a surface, which can be conveyed to a rainwater storage system. The roof RC varies significantly on the basis of the characteristics of the recipient surface of the rainfall (slope, impermeability, etc.). In this context, in the assessment of the quantitative potential of runoff from roofs in the study area, several types of roofs are identified and relevant RCs are assigned (Table 1). We used the average value of RC suggested by the literature.

Table 1 Runoff coefficients for traditional roofing materials.

Roof type	Runoff Coefficient (RC)	Source
Pitched roofs		
Concrete/asphalt	0.9	[29]
Metal	0.9	[29,30,31]
Bituminous tiles	0.8	[32]
Clay tiles	0.84	[31]
Flat roofs		
Gravel	0.83	[29,31]
Bitumen	0.7	[33]
Flat cement roofs	0.65	[34]

2.2.3. Local precipitation

The amount and frequency of precipitation in a city are key factors in determining its water-collecting potential. Cities with consistent and relatively high rainfall are more likely to have a substantial amount of water that can be collected. For the calculation of local precipitation the L – moment methodology is applied [35,36]. Time series of meteorological data used for the prediction of local participation covers the period 1946-2019 (Table 2).

Table 2 Parameters of the annual precipitation of the City of Nis for the period 1946-2019

Station name	Longitude (E)	Latitude (N)	Elevation (m a.s.l.)	Mean precipitation (mm)	Standard deviation (mm)
Nis	21°54'	43°20'	204	587.0	116.2

For this purpose, three distributions were fitted to the annual precipitation data collected from meteorological stations in Nis for the period 1946–2019 using the method of L-moment: generalized extreme value (GEV), generalized Pareto (GPD), and generalized logistic (GLO) [3]. The goodness-of-fit for the selected three distributions was confirmed using the L-diagram and three measures namely relative root mean squared error (RRMSE), relative mean absolute error (RMAE), and probability plot correlation coefficient (PPCC). From the results of this analysis, the GLO distribution was selected as the best-fitting distribution of the annual precipitation data for the City of Nis:

$$f(x)=\begin{cases}\dfrac{\left(1+\kappa\dfrac{x-\xi}{\alpha}\right)^{-1-\frac{1}{\kappa}}}{\alpha\left(1+\left(1+\kappa\dfrac{x-\xi}{\alpha}\right)^{-\frac{1}{\kappa}}\right)^{2}}, \kappa\neq 0\\[2ex] \dfrac{e^{-\frac{x-\xi}{\alpha}}}{\alpha\left(1+e^{-\frac{x-\xi}{\alpha}}\right)^{2}}, \kappa=0\end{cases} \tag{1}$$

where:

$$\kappa=-\tau_3$$
$$\alpha=\frac{\lambda_2}{\Gamma(1+\kappa)\Gamma(1-\kappa)} \tag{2}$$
$$\xi=\lambda_1+\frac{\lambda_2-\alpha}{\kappa}$$

(ξ ,α, κ are location, scale and shape parameters of distributions; Γ is the symbol of gamma function).

Best fitting distribution based on L-diagram and determined based on the combined RRMSE, RMAE, and PPCC goodness-of-fit measures for stations of the City of Niš is generalized logistic (GLO). In our case, estimates of the parameters for GLO distribution for the City of Nis using *L*-moments are:

$$\xi = 589.2500, \alpha = 63.0145, \kappa = -0.0153$$

In accordance with that, the GLO distribution was used to determine precipitation estimates for different return periods from 2 to 1000 years for the City of Niš stations. The T-year return level namely x_T is the level exceeded on average only once every T years. By the inverting $F(x_T) = 1 - 1/T$ in GLO:

$$x_T = \xi + \frac{\alpha}{\kappa}\left(1 - \left(\frac{1}{T-1}\right)^{\kappa}\right), \kappa \neq 0 \quad (3)$$

The estimated precipitation in the City of Nis for different return periods from 2 to 1000 years is presented in Table 3.

Table 3 The City of Nis annual precipitation estimations

Return period (year)	Best distribution (GLO)
2	589.25
3	633.16
4	659.06
5	677.54
10	730.06
15	758.95
20	779.04
25	794.46
30	806.99
35	817.57
40	826.70
45	834.75
50	841.94
100	889.23
200	936.68
300	964.59
400	984.47
500	999.94
1000	1048.30

2.3. Runoff calculation

The potential amount of runoff from roofs is computed using the equation:

$$Q = RC \times R \times A, \quad (4)$$

where Q is the amount of water that runs off, RC is the runoff coefficient, R is the total rainfall (L/y), and A is the roof area or catchment area (m^2). For each building, we calculated the potential amount of water that can be collected for the return periods.

3. RESULTS

Modelling showed that the city of Niš will experience a steady growth in precipitations over the studied return periods, compared to the referent period 1946-2019.

Although the previous section presents annual precipitation estimations for return periods up to 1000 years, the illustrative assessment of potential runoff from roofs is presented for return periods of 2, 5, and 10 years. The analysis identifies four main functional types of buildings within the study area: administrative, educational, commercial, and residential. Their distribution is shown in Figure 2.

Fig. 2 Functional distribution.

Before calculating the average values the outliers are removed by applying the IQR (Interquartile Range) method. The IQR is the range between the first quartile (Q1) and the third quartile (Q3) of the data. Data points outside the range [Q1 – 1.5 * IQR, Q3 + 1.5 * IQR] are considered outliers.

The analysis indicates an increasing trend in average runoff from roofs across all sectors considering observed periods. The average runoff for the study area is 176762.7 L for the RP of 2 years and goes up to 215798.3 L for the RP of 10 years (Figure 3). Looking at the sectors individually, modelling shows noticeable differences. The sector of educational buildings shows the highest values, from an average of 440648.761 L for the RP of 2 years up to 537959.924 L for the RP of 10 years. A sector of administrative buildings is somewhat below the total average with 136249.97 L and 166338.9 L for the RP of 2 years and 10 years respectively. The administrative sector is followed by residential with 74914.06 L and 91457.79159 L for the return period of 2 and 10 years respectively, while the commercial sector shows the lowest runoff potential with 55237.9 L and 67436.4 L for the return period of 2 and 10 years respectively.

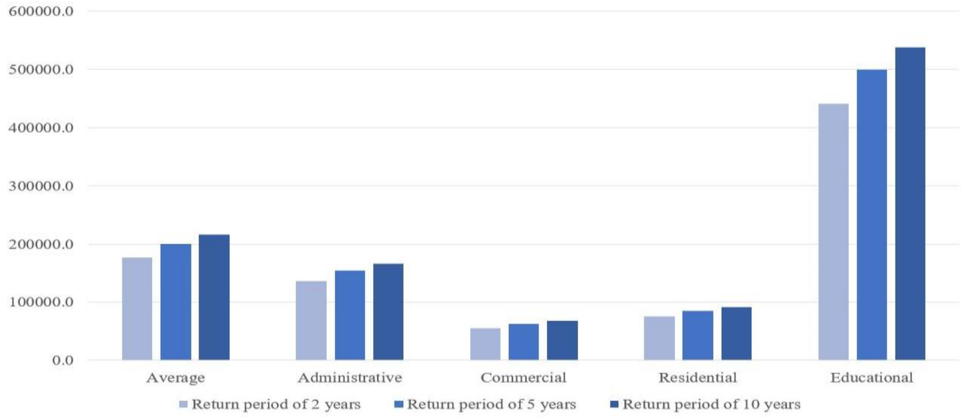

Fig. 3 Estimated average runoff from roofs according to functional categories.

On the other hand, when exploring individual buildings, the influence of multiple structural characteristics like roof type, total surface area and roof material on runoff potential is more prominent. As can be seen from Figure 4, available runoff from roofs widely differs from case-by-case. This is very apparent when extremes are considered.

4. Discussion

In line with the objective of this research - predicting potential runoff in the exemplary city area - the results of this GIS model contribute to the geospatial analysis for sustainable SWM and have the potential to be leveraged by planners, developers, urban advocacy groups, and the public. They indicate there is a substantial amount of roof area that has the potential to support water harvesting in the inner-city area. Given that technical water accounts for approximately 80% of total water consumption, the results indicate that there is a significant amount of runoff in the study area that could potentially be used as technical water.

However, some key factors necessary for precise calculation are complex to predict. Firstly, there are ongoing changes in functions in certain categories of objects. On the other hand, parts of the residential buildings are transformed into office spaces, restaurants, or apartments. Secondarily, the inner city is undergoing intense densification i.e. single-family houses are replaced by multi-family mid-rise residential buildings, thus the roof structure and materials are changing too. These shifts may significantly influence both catchment area characteristics and water consumption patterns. Thirdly, despite the steady increase in the amount of participation, the region has experienced extreme participation events in recent years, i.e., the distribution of participation has become more uneven, as observed by [7,37], which can lead to uncertainty in runoff reliability.

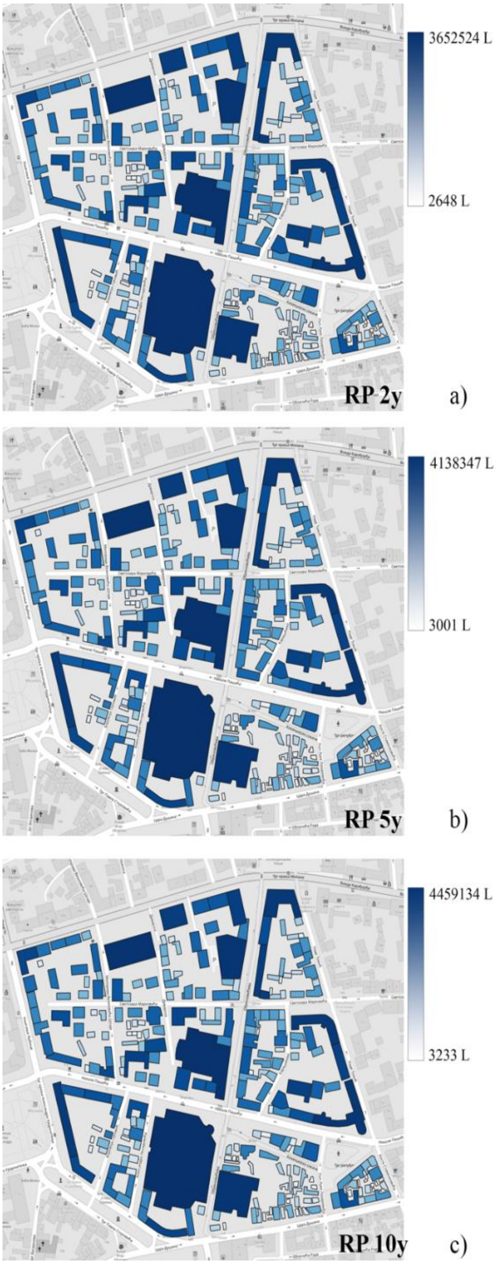

Fig. 4 Estimated runoff from roofs for the return period of 2 years, b) return period of 5 years, and c) return period of 10 years.

5. Concluding remarks

This is a baseline research for understanding the potential runoff from roofs in Niš. The presented methodology allows for fast estimation of potential runoff from the roof. The first goal of this GIS analysis is to raise awareness about the water harvesting potential and its benefits among the policy-makers, community and potential users. Furthermore, they inform both urban planning and design, and SWM practice affirming synergetic research towards addressing the highlighted challenges in the Development plan for the City of Niš related to stormwater management. To advance its capacity to inform in the decision-making process, future studies may include the following: 1) the analysis of the structural characteristics of the buildings and land availability for installation of storage tanks; the factors like storage tank size and overflow systems need to be detailed, in order to understand the full participation collection system capacity, 2) the estimation of the costs associated with system installation, maintenance, necessary water treatment equipment and pay off periods and 3) the assessment of the environmental impact of rainwater harvesting, considering factors like reduced stormwater runoff and potential benefits to local ecosystems.

Acknowledgement: *This work was supported by the Serbian Ministry of Science, Technological Development and Innovation through the Mathematical Institute of the Serbian Academy of Sciences and Arts.*

References

1. Kourtis, I. M., and Tsihrintzis, V. A. (2021). Adaptation of urban drainage networks to climate change: A review. Science of the Total Environment, 145431.
2. United Nations. (2019b). World Urbanization Prospects, the 2018 Revision. Retrieved from https://population.un.org/wup/Publications/Files/WUP2018-Report.pdf
3. Rosenberger, L., Leandro, J., Pauleit, S., and Erlwein, S. (2021). Sustainable stormwater management under the impact of climate change and urban densification. Journal of Hydrology, 596, 126137.
4. Berndtsson, R., Becker, P., Persson, A., Aspegren, H., Haghighatafshar, S., Jönsson, K.,... Tussupova, K. (2019). Drivers of changing urban flood risk: A framework for action. Journal of Environmental Management, 240, 47-56.
5. Yang, W., and Zhang, J. (2021). Assessing the performance of gray and green strategies for sustainable urban drainage system development: A multi-criteria decision-making analysis. Journal of Cleaner Production, 293, 126191.
6. Hadjikakou, M., Stanford, B. D., Wiedmann, T., Rowley, H. V., Kobayashi, Y., Ishii, S.,... Khan, S. J. (2019). A flexible framework for assessing the sustainability of alternative water supply options. Science of the Total Environment, 671, 1257-1268.
7. Haque, M. M., Rahman, A., and Samali, B. (2016). Evaluation of climate change impacts on rainwater harvesting. Journal of Cleaner Production, 137, 60-69.
8. Silva, A. S., and Ghisi, E. (2016). Uncertainty analysis of daily potable water demand on the performance evaluation of rainwater harvesting systems in residential buildings. Journal of Environmental Management, 180, 82-93.
9. Balian, E. H., Eggermont, H., and Le Roux, X. (2014). Nature-based solutions in a BiodivERsA context. In L-Outcomes of the strategic foresight workshop. Brussels, Belgium: BiodivERsA Report.
10. Doswald, N., and Osti, M. (2011). Ecosystem-based approaches to adaptation and mitigation – good practice examples and lessons learned in Europe. BfN-Skripten. Bonn, Germany: Bundesamt für Naturschutz.
11. Frantzeskaki, N. (2019). Seven lessons for planning nature-based solutions in cities. Environmental Science & Policy, 93, 101-111.
12. Brink, E., Aalders, T., Adam, D., Feller, R., Henselek, Y., Hoffmann, A., Ibe, K., Matthey-Doret, A., Meyer, M., Negrut, N. L., Rau, A.-L., Riewerts, B., von Schuckmann, L., Törnros, S., von Wirth, T., and Abson, D.

J. (2016). Cascades of green: A review of ecosystem-based adaptation in urban areas. Global Environmental Change, 36, 111-123.
13. Munang, R., Thiaw, I., Alverson, K., Liu, J., and Han, Z. (2013). Climate change and ecosystem-based adaptation: A new pragmatic approach to buffering climate change impacts. Current Opinion in Environmental Sustainability, 5(1), 67-71.
14. Benedict, M. A., and McMahon, E. T. (2006). Green infrastructure. Linking landscapes and communities. Washington, DC: Island Press.
15. Millennium Ecosystem Assessment (MEA). (2005). Ecosystems and human well-being: Synthesis. Millennium assessment report. Washington, DC: Island Press.
16. Zhang, S., Lin, Z., Zhang, S., and Ge, D. (2021). Stormwater retention and detention performance of green roofs with different substrates: Observational data and hydrological simulations. Journal of Environmental Management, 291, 112682.
17. She, L., Wei, M., and You, X. Y. (2021). Multi-objective layout optimization for sponge city by annealing algorithm and its environmental benefits analysis. Sustainable Cities and Society, 66, 102706.
18. Yang, Y., Li, J., Huang, Q., Xia, J., Li, J., Liu, D., and Tan, Q. (2021). Performance assessment of sponge city infrastructure on stormwater outflows using isochrone and SWMM models. Journal of Hydrology, 597, 126151.
19. Liu, W., Engel, B. A., and Feng, Q. (2021). Modelling the hydrological responses of green roofs under different substrate designs and rainfall characteristics using a simple water balance model. Journal of Hydrology, 602, 126786.
20. Cheng, Y., and Wang, R. (2018). A novel stormwater management system for urban roads in China based on local conditions. Sustainable Cities and Society, 39, 163-171.
21. Scholz, M. (2015). Sustainable drainage systems. MDPI
22. Stovin, V., Vesuviano, G., and Kasmin, H. (2012). The hydrological performance of a green roof test bed under UK climatic conditions. Journal of Hydrology, 414, 148-161.
23. Naserisafavi, N., Yaghoubi, E., and Sharma, A. K. (2021). Alternative water supply systems to achieve the net zero water use goal in high-density mixed-use buildings. Sustainable Cities and Society, 103414.
24. Amos, C. C., Rahman, A., and Gathenya, J. M. (2018). Economic analysis of rainwater harvesting systems comparing developing and developed countries: A case study of Australia and Kenya. Journal of Cleaner Production, 172, 196-207.
25. van Dijk, S., Lounsbury, A. W., Hoekstra, A., and Wang, R. (2020). Strategic design and finance of rainwater harvesting to cost-effectively meet large-scale urban water infrastructure needs. Water research, 184, 116063.
26. Lopes, V. A., Marques, G. F., Dornelles, F., and Medellin-Azuara, J. (2017). Performance of rainwater harvesting systems under scenarios of non-potable water demand and roof area typologies using a stochastic approach. Journal of Cleaner Production, 148, 304-313.
27. Spatial Plan of Republic of Serbia 2010-2013-2020.
28. Census. Census of Population, Households and Dwellings. Statistical Office of the Republic of Serbia, 2022.
29. Lancaster, B. (2006). Rainwater Harvesting for Drylands and Beyond: Guiding principles to welcome rain into your life and landscape (Vol. 1). Rainsource Press: Tucson, Arizona.
30. Liaw, C. H., and Tsai, Y. L. (2004). Optimum storage volume of rooftop rain water harvesting systems for domestic use. Journal of the American Water Resources Association, 40, 901e912.
31. Farreny, R. (2011). Roof selection for rainwater harvesting: Quantity and quality assessments in Spain. Water Research, 45, 324-3254.
32. Biswas, B. K., and Mandal, B. H. (2014). Construction and evaluation of rainwater harvesting system for domestic use in a remote and rural area of Khulna, Bangladesh. International Scholarly Research Notices, 751952.
33. Ward, S., Memon, F. A., and Butler, D. (2010). Harvested rainwater quality: the importance of appropriate design. Water Science and Technology, 61(7), 1707-1714.
34. Worm, J., and van Hattum, T. (2006). Rainwater harvesting for domestic use (Report No. 43). Agromisa Foundation.
35. Gocic, M., Velimirovic, L., Stankovic, M., and Trajkovic, S. (2021). Regional precipitation-frequency analysis in Serbia based on methods of L-Moment. Pure and Applied Geophysics, 178, 1499-1511.
36. Gocic, M., Velimirovic, L., Stankovic, M., and Trajkovic, S. (2021). Determining the best fitting distribution of annual precipitation data in Serbia using L-moments method. Earth Science Informatics, 14, 633-644.
37. Alim, M. A., Rahman, A., Tao, Z., Samali, B., Khan, M. M., and Shirin, S. (2020). Suitability of roof harvested rainwater for potential potable water production: A scoping review. Journal of Cleaner Production, 248, 119226.

PREDIKCIJA POTENCIJALA SKUPLJANJA KIŠNICE U NIŠU, PRIMENOM L-MOMENTA I GIS-A

Srbija, kao i mnoge druge zemlje, radi na upravljanju i zaštiti vodnih resursa, promovisanju održivih praksi i unapređenju infrastrukture. Međutim, ne postoji sistematsko zagovaranje za primenu održivih praksi upravljanja atmosferskim vodama (SVM) u urbanim sredinama u Srbiji. Kako se ističe Planom razvoja Grada Niša za period 2021-2027. u poslednjoj deceniji se povećava broj bujičnih poplava koje izazivaju infrastrukturne štete, pa se smanjenje rizika od poplava od spoljnih i unutrašnjih voda prepoznaje kao prioritet teritorijalnog razvoja i zaštite životne sredine. Kao doprinos razvoju SVM prakse, u ovom istraživanju, izvršeno je predviđanje potencijala kišnog oticanja sa krovova u gradu Nišu korišćenjem metode L-Momenta i GIS-a. Istraživanje je obuhvatilo 262 zgrada u centru grada. Rezultati ukazuju na trend povećanja prosečnog oticanja sa krova u svim sektorima.

Ključne reči: *L-Moment, GIS, podrška odlučivanju, održive prakse upravljanja atmosferskim vodama*

FACTA UNIVERSITATIS
Series: **Working and Living Environmental Protection** Vol. 21, Nº 1, 2024, pp. 71 - 76
https://doi.org/10.22190/FUWLEP240326006I

Review Paper

INTERNAL REMEDIATION MECHANISM OF EMPLOYEES DEFINED BY THE ACT ON CORPORATE DUE DILIGENCE OBLIGATIONS IN SUPPLY CHAINS IN GERMANY

UDC 331.45/.46:343.1:[366.1:658.8

Aleksandra Ilić Petković, Dejan Vasović

University of Niš, Faculty of Occupational Safety

ORCID iDs: Aleksandra Ilić Petković https://orcid.org/0000-0002-9831-722X
Dejan Vasović https://orcid.org/0000-0003-4043-8093

Abstract. *Modern working conditions continuously impose the need for efficiency and productivity of employees, but not at the expense of their occupational safety and health. One of the legal instruments that can be used to prevent potential injuries at work is the internal remediation mechanism. Until now, this legal institute has been available to employees and employers as a possibility. With the adoption of the Act on Corporate Due Diligence Obligations in Supply Chains in Germany, this became one of the legal obligations that apply not only to this country, but also to certain categories of employers and employees in Serbia. The paper analyzes the specific effects of the implementation of this act on the occupational safety and health system in Serbia, with special reference to the remediation mechanism institute.*

Key words: *internal remediation mechanism, Germany, Act on Due Diligence, occupational safety and health.*

1. INTRODUCTION

The fact that safe and efficient employees are the pillars of a company's productivity was recognized in literature and practice long ago. This is the key strategic goal of every country [1]. One of the most important factors in increasing the efficiency and productivity of employees is employers' ability to develop the work environment in which employees perceive the organization's goals as their own and take responsibility, without the need for constant supervision. In order for employers to achieve this goal, they are required to respect employees' needs and ensure their sense of safety, appreciation and respect at work.

Injuries at work are possible in every work organization. One of the modern legal institutes that represents a good preventive measure in the field of occupational safety

Received March 26, 2024 / Accepted April 24, 2024
Corresponding author: Aleksandra Ilić Petković
Faculty of Occupational Safety, Univesity of Niš, Čarnojevića 10a, 18000 Niš, Serbia
E-mail: aleksandra.ilic@znrfak.ni.ac.rs

and health is the internal remediation mechanism. There are also external complaint mechanisms that involve the inclusion of Labor inspection [2], judicial bodies [3], the Republic Agency for the Peaceful Settlement of Labor Disputes [4], and the Commissioner for the Protection of Equality [5]. Nonetheless, before employees are required to turn to one of these parties, there is a possibility to introduce an internal remediation mechanism for them to exercise their rights.

The introduction of such a mechanism into the legal system of Serbia does not represent a legal obligation, nor is it an obligation prescribed by the Labor Law, Law on Occupational Safety and Health, or another act. Therefore, the internal remediation mechanism is only a legal instrument available to employers as an opportunity to improve the occupational safety and health system. However, the adoption of the German Act on Corporate Due Diligence Obligations in Supply Chains made a difference in this practice.

This paper analyzes the impact of this law on employers and employees in Serbia by examining current scientific literature and relevant legal sources. Even though this is a legal act of another country, some of its provisions apply to individual subjects of the occupational safety and health system in Serbia. Therefore, our subject of interest are specific obligations of Serbian employers and employees pursuant to this act.

2. The Concept of Corporate Sustainability Due Diligence and Remediation Mechanism

In terms of dictionary definitions, due diligence represents the degree of care that is to be reasonably expected or that is legally required, especially of persons giving professional advice, as well as assessment and evaluation conducted with the prudent or necessary care. According to certain dictionaries, due diligence is: in legal terms, it is defined as the care that a reasonable person exercises to avoid harm to other persons or their property; in business terms, it is defined as research and analysis of a company or organization conducted in preparation for a business transaction [6].

The role of due diligence in international law can be viewed from two perspectives. [7]. Firstly, it is important to emphasize that, while due diligence may be a component of a primary rule of international law, this can only be determined by referring back to the relevant primary rule. There is no "general principle of due diligence" in international law, but this principle has to be implemented in some international legal acts. Secondly, states undertake what could be characterized as 'due diligence' activity, some elements of which may be a result of a legal requirement and some of which may not.

Considering these two facts, in 2022 the European Commission adopted a proposal for a Directive on corporate sustainability due diligence [8]. The aim of this Directive is to foster sustainable and responsible corporate behavior and to anchor human rights and environmental considerations in companies' operations and corporate governance. The new rules are to ensure that businesses address the adverse impacts of their actions, both within their value chains inside and outside Europe. They have numerous benefits for citizens, such as better protection of human rights (including labor rights), a healthier environment for present and future generations, increased trust in businesses, more transparency enabling informed choices, etc. Benefits for companies include better risk management and adaptability, better awareness of companies' negative environmental and human rights impacts, greater customer trust and employees' commitment, etc. Benefits for developing countries are better protection of human rights and the environment, sustainable investment, improved living conditions for people, etc. [9].

This Directive establishes a corporate due diligence duty. The core elements of this duty are identifying, bringing to an end, preventing, mitigating and accounting for negative human rights and environmental impacts in the company's own operations, their subsidiaries and their value chains. Managers are encouraged to contribute to sustainability and climate change mitigation goals.

The Directive also introduces duties for the managers of the EU companies covered. These duties include establishing and monitoring the implementation of the due diligence processes and integrating due diligence into the corporate strategy. In addition, when fulfilling their duty to act in the best interest of the company, managers need to consider the human rights, climate change, and environmental consequences of their decisions.

One of the legal institutes recognized by the proposal of the Directive is the internal remediation mechanism. Companies should provide the possibility for persons and organizations to submit complaints directly to them in case of legitimate concerns regarding actual or potential violations of human rights or negative effects on the environment.. Organizations that could submit such complaints include trade unions and other workers' associations representing individuals employed, as well as civil society organizations operating in areas connected to the value chain in question and possessing knowledge of a potential or actual adverse impact. Companies should establish a procedure for dealing with those complaints and inform workers, trade unions and other workers' representatives about such processes. Recourse to the complaints and remediation mechanism should not prevent the complainant from having recourse to judicial remedies. In accordance with international standards, complaints should be entitled to request the appropriate follow-up from the company regarding the complaint and to meet with the company's representatives at an appropriate level to discuss potential or actual severe adverse impacts that are the subject matter of the complaint. This access should not lead to unreasonable solicitations of companies [8].

3. ACT ON CORPORATE DUE DILIGENCE OBLIGATIONS IN SUPPLY CHAINS AND INTERNAL REMEDIATION MECHANISM

The implementation of the Act on Corporate Due Diligence Obligations in Supply Chains, adopted in Germany in 2021, commenced in 2023. It applies to German companies employing more than 3,000 people, and from 2024 to those employing 1,000 people [10]. On the basis of this act, German companies are required by this act to assume responsibility for the actions of their partners that endanger human rights and the environment, whether it is the acquisition of input components that German companies further process or the sale of their final products. Consequently, this act also applies to all Serbian companies that have business cooperation with German companies. It does not apply to exporters of finished products.

Pursuant to this act, German companies are required to establish processes for identifying potential risks to human rights and the environment within their supply chains, conduct their assessment, introduce preventive measures and steps to eliminate the identified risks, and submit reports on the completion of their tasks. These tasks will also involve the companies in the supply chain, which will inevitably have to participate in the entire process of identifying and eliminating risks. Those companies can also introduce some new procedures in their own business processes as a necessary step toward eliminating previously determined risks.

One of the legal institutes incorporated into the Act on Corporate Due Diligence Obligations in Supply Chains is the internal remediation mechanism [10]. Companies are expected to plan and create an internal remediation mechanism at all levels of operation, including companies that work as subcontractors, that is, those companies that are in their supply chain. The idea is to develop a company's internal remediation mechanism that will enable a better understanding of the risks or malpractice and timely react in order to eliminate harmful consequences.

Within the internal remediation mechanism, it is important to define the subject matter of the complaint, such as discrimination or abuse at work, non-compliance with occupational safety regulations, inadequate reaction in the event of an injury at work, unjustified denial of the right to annual leave, etc. Complaints can be signed, but anonymous complaints should also be allowed so as to protect the identity of the complainant. This should ensure the protection of complainants, their families or witnesses [11].

Complaints can be filed by individuals, groups or organizations, and the company is required to give an official response within the established period [11]. The remediation mechanism should be available to those who are applying for a job, employees, regardless of the type of contract, and third parties who are directly or indirectly related to the company (subcontractors, unions, subsidiaries of the company). The complaint should be submitted directly by the person whose right has been violated, or threatens to be violated, another person who is related to the complainant in a certain way (e.g. an heir in the event of the employee's death), a union representative if the complainant is a member of the union, a lawyer if they have the power of attorney. Complaints are filed against actions undertaken or not undertaken by the company, subsidiary companies or subcontractors that violate or endanger human rights. Complaints can be filed against the actions or oversights on the part of employees in the company, as well as against subsidiaries, subcontractors and other legal entities and their employees who are connected to the parent company in some manner. As can be seen, there is a very wide range of both the legal and physical entities that are eligible to receive complaints and the individuals that can be the target of a complaint.

It is important that the company defines the complete procedure, starting from the receipt of the complaint, up to the final decision. This means that the procedure for receiving a complaint, confirming receipt, registering a complaint, examining the complaint, and decision-making, should be defined in several stages. The procedure is expected to be fast and efficient, and the deadlines should be reasonable.

The purpose of such complaints and remediation mechanisms is that individuals, groups, or organizations connected with the company's activity can signal their dissatisfaction with a situation or a decision of the company. Such a procedure should provide an opportunity for the company to timely recognize potential risks and prevent a bad reputation on the market.

4. CONCLUSION

The idea of decent work, as opposed to precarious work, has received considerable attention in recent decades. One of the key components of decent work is occupational safety and health. The concept of due diligence is one of the instruments for achieving a high level of occupational safety and health. This concept describes the steps a company has to take in order to acknowledge, prevent and address adverse human rights impacts [6]. The concept of due diligence plays an important role in international human rights law in defining the scope of a state's obligations to prevent and respond to infringements of human rights by private actors within its territory or jurisdiction.

In international law, due diligence addresses supplying a standard of care against which malpractice can be assessed. It identifies the extent of states' responsibility, such as infringements of human rights, damage to foreign property and transboundary pollution. It imposes an external, 'objective' standard of conduct to take reasonable precautions to prevent or respond to certain types of harm specified by the rule in question [12].

Large companies have been increasingly implementing due diligence processes as they can provide some competitive advantage in the market. This also responds to the increasing market pressure on companies to act sustainably, which results in avoiding unwanted reputational risks vis-à-vis consumers and investors whose awareness of sustainability is growing [8]. However, these processes are based on voluntary standards and do not result in legal certainty for companies or victims in the event of harm.

Such policy and practice are introduced by adopting and implementing the German Act on Corporate Due Diligence Obligations in Supply Chains. However, the scope of application of this act is limited to companies that have their central administration, principal place of business, administrative headquarters or statutory seat in Germany and normally have at least 1,000 employees in Germany. Also, German companies are responsible for the activities carried out by their partners, with regard to threatening human rights and the environment, whether it is the acquisition of input components that German companies further process or the sale of their final products [10].

One of the important legal institutions within the concept of due diligence is the internal remediation mechanism. It represents a way to protect human rights, especially occupational safety and health. Regarding these procedures, several things should be taken into consideration.

Firstly, the creation of an internal remediation mechanism should be the task of a special expert team that will consider the needs of the company and the need to protect the human rights of all employees. The trade unions should be asked to provide their opinion in order to prevent employee resistance to the introduction of such mechanisms. When creating a complaint mechanism, it should be a multi-level process, that is, one complaint is expected to be reviewed at several levels within the company.

Then, the remediation mechanism is supposed to be developed within large companies that operate in particular fields and then be extended to subsidiary companies, subcontractors and all those companies that are in the supply chain. As internal remediation mechanisms are not identified in the Labor Law in Serbia, they are determined by some general act of the employer, e.g. labor regulations or collective agreement.

Finally, in order for the internal remediation mechanism to produce the intended effects, it is necessary that concerned parties are informed about it, trust it, and know how to use it. Therefore, all the information about the complaint process should be publicly available, procedures should be transparent and the e-mail addresses intended for complaints need to be provided on the website. Also, workers will be encouraged to use internal complaint mechanisms if there is a clear deadline for the implementation of the procedure, the procedures are simple and results are available.

Based on the above, it can be concluded that the adoption of the Act on Corporate Due Diligence Obligations in Supply Chains in Germany can motivate Serbian companies to meet the requirements that refer to human rights protection. The idea of introducing an internal remediation mechanism in case of suspected violation of some human rights in the company is a legal institute that represents a significant innovation in terms of improving occupational safety and environmental protection.

The protection of employee rights in Serbia does not end with the internal remediation mechanism. If the disputed issue is not successfully resolved by the internal complaint, external mechanisms are available to the employees. External mechanisms involve addressing the Labor inspection [2], the Republic Agency for the Peaceful Settlement of Labor Disputes [4], primary and higher courts [3], as well as the Commissioner for the Protection of Equality [5].

Acknowledgements: *The paper is the result of research funded by the Ministry of Education, Science and Technological Development of the Republic of Serbia. Contract No No 451-03-66/2024-03/ 200148.*

REFERENCES

1. Ilić Petković, A., Stratijev, M. (2023). OSH Strategic Directions in European and National Legislation. Proceedings of the 20th International Conference" Man and Working Environment" – SEMSIE 2023, Niš, pp. 133-136.
2. Labor inspection. Available at: https://www.minrzs.gov.rs/sr/struktura/organi-uprave-u-sastavu-ministarstva/inspektorat-za-rad. Accessed on: 1.2.2024.
3. The Law on Organization of Courts, "Official Gazette of the Republic of Serbia", No. 10/2023.
4. The Republic Agency for the Peaceful Settlement of Labor Disputes. Available at: https://www.ramrrs.gov.rs/sr-cyr. Accessed on: 1.3.2024.
5. The Law on Prohibition of Discrimination, "Official Gazette of the Republic of Serbia", No. 22/2009, 52/2021.
6. Bonnitcha, J., McCorquodale, R. (2017). The Concept of "Due Diligence" in the UN Guiding Principles on Business and Human Rights. European Journal of International Law, 28(3), 899–919.
7. McDonald, N. (2019). The Role of Due Diligence in International Law. International & Comparative Law, 68(4), 1041 – 1054.
8. Proposal for a Directive of the European Parliament and of the Council on Corporate Sustainability Due Diligence and amending Directive (EU) 2019/1937. Available at: https://commission.europa.eu/publications/proposal-directive-corporate-sustainability-due-diligence-and-annex_en. Accessed on: 9.1.2024.
9. EU Commission, Corporate Sustainability Due Diligence. Avalilable at: https://commission.europa.eu/business-economy-euro/doing-business-eu/corporate-sustainability-due-diligence_en. Accessed on: 1.2.2024.
10. Act on Corporate Due Diligence Obligations in Supply Chains. Available at: https://www.csr-in-deutschland.de/EN/Business-Human-Rights/Supply-Chain-Act/supply-chain-act.html. Accessed on: 6.12.2023.
11. International Labor Organization, (2023), Manual on Grievance Mechanisms, ILO, Geneva.
12. Hanquin, X. (2023). Transboundary Damage in International Law, Cambridge University Press, Cambridge.

INTERNI ŽALBENI MEHANIZAM ZAPOSLEHNIH PREMA NAMAČKOM ZAKONU O DUŽNOJ PAŽNJI U LANCIMA SNABDEVANJA

Savremeni uslovi rada sve više nameću potrebu za efikasnošću i produktivnošću zaposlenih, ali ne po cenu njihove bezbednosti i zdravlja na radu. Jedan od pravnih instrumenata kojima se mogu prevenirati potencijalne povrede na radu jeste interni žalbeni mehanizam. Ovaj pravni institut je do sada bio na raspolaganju zaposlenima i poslodavcima kao mogućnost. Ali, donošenjem Zakona o dužnoj pažnji u lancima snabdevanja u Nemačkoj, ovo je postala jedna od zakonskih obaveza koje se odnose, ne samo na ovu državu, već i na određene kategorije poslodavaca i zaposlenih u Srbiji. U radu se analiziraju konkretne reperkusije primene ovog zakona na sistem bezbednosti i zdravlja na radu u našoj državi, sa posebnim osvrtom na institut internog žalbenog mehanizma.

Ključne reči: *interni žalbeni mehanizam, Nemačka, Zakon o dužnoj pažnji, bezbednost i zdravlje na radu.*

CIP - Каталогизација у публикацији
Народна библиотека Србије, Београд

502/504

FACTA Universitatis. Series, Working and Living Environmental Protection / editor in chief Nenad Živković. - [Štampano izd.]. - Vol. 1, no. 1 (1996)- . - Niš : University of Niš, 1996- (Niš : Atlantis). - 24 cm

Dostupno i na:
http://casopisi.junis.ni.ac.rs/index.php/FUWorkLivEnvProt. - Tri puta godišnje. - Drugo izdanje na drugom medijumu: Facta Universitatis. Series: Working and Living Environmental Protection (Online) = ISSN 2406-0534
ISSN 0354-804X = Facta Universitatis. Series: Working and Living Environmental Protection
COBISS.SR-ID 72210956